Microbial evolution in changing environments

Peter L. Conlin

A dissertation
submitted in partial fulfillment of the
requirements for the degree of

Doctor of Philosophy

University of Washington

2018

Reading Committee:

Benjamin B. Kerr, Chair

Wenying Shou

Maitreya J. Dunham

Program Authorized to Offer Degree:
Biology

©Copyright 2018

Peter L. Conlin

University of Washington

Abstract

Microbial evolution in changing environments

Peter L. Conlin

Chair of the Supervisory Committee:
Professor Benjamin B. Kerr
Biology

Chapter 1. Compensatory mutations play a critical role in the evolution of drug resistance in microorganisms. Most directly, they serve to alleviate the fitness cost commonly associated with initial drug resistance mutations. Here we use experimental evolution to examine adaptation to the cost of rifampicin resistance in an antibiotic-free environment, and ask whether compensatory mutations that restore fitness back to ancestral levels could also be further increasing the level of drug tolerance in these resistant isolates. We suggest that the identity of the initial resistance conferring mutations may influence the relative frequency at which drug tolerance increases during compensatory evolution through epistatic interactions. *Chapter 2.* The evolutionary transition to multicellularity likely began with the formation of simple undifferentiated cellular groups. Such groups evolve readily in diverse lineages of extant unicellular taxa, suggesting that there are few genetic barriers to this first key step. In this chapter, we focus on how the transition to multicellularity may be stabilized against evolutionary reversion when environmental conditions change and tip the balance of selection back in favor of unicellularity. Using mathematical modeling, we show how multicellular adaptations can act as evolutionary "ratchets", limiting the potential for reversion to unicellularity. *Chapter 3.* Evolutionary transitions in individuality (ETIs) occur when

formerly autonomous organisms evolve to become parts of a new, 'higher-level' organism. Here we explore the key role that simple multicellular life cycles in facilitating this transition. Specifically, we use mathematical models to compute how canonical early life cycles vary in their ability to fix beneficial mutations via mathematical modeling. Building on our prevous work (Chapter 2), we show how life cycles that lack a persistent single-cell stage and develop clonally are far more likely to fix 'ratcheting' mutations that limit evolutionary reversion to the pre-ETI state. *Chapter 4.* Phenotypic plasticity is the ability of a single genotype to produce different phenotypes in response to changes in the environment. Theory suggests that the adaptive value of plasticity depends on the degree of environmental heterogeneity and the existence of environmental cues that provide reliable information about selective conditions. We tested this prediction using experimental evolution. We find that temporally varying selection can favor the evolution of phenotypic plasticity in experimental populations of yeast when selection is predictable but that plasticity is lost when selection in unpredictable. *Chapter 5.* Fitness trade-offs, while central to all of life history theory, are thought to take on a particularly important role during major evolutionary transitions such as the evolution of multicellularity. Specifically, trade-offs between survival and reproduction may drive increases in complexity and cellular differentiation. Here we used computer simulations of digital mulitcellular organisms to explore how trade-offs could promote the evolution of multicellular complexity. *Chapter 6.* In this chapter, we review how game theory can be a useful first step in modeling and understanding interactions among bacteria that produce and resist antibiotics. We introduce the basic features of evolutionary game theory and explore model microbial systems that correspond to some classical games. Each game discussed defines a different category of social interaction with different resulting population dynamics (exclusion, coexistence, bistability, cycling). We then explore how the framework can be extended to incorporate some of the complexity of natural microbial communities.

TABLE OF CONTENTS

LIST OF FIGURES

Figure Number Page

ACKNOWLEDGMENTS

Being a graduate student in the Department of Biology at the University of Washington has been an incredible experience both academically and personally. There are several people, without whom I would never have gotten here, that I'd like to thank for the many opportunities I was given to get involved in science: Christine Knight, Adam Houlihan, Joanne Chee-Sanford, Rhanor Gillette, Billie Swalla, Leonid Moroz, and Andrea Kohn. Thank you for your encouragement.

I want to thank the faculty, staff, and graduate students in the UW Biology department for supporting my education and helping me to be a better teacher, writer, speaker, and scientist. Specifically, I had the great luck to move in to a house full of biology graduate students in my first year of graduate school and ended up making life long friends. Elisha BH Vilhena, Daril Vilhena, Marie Clifford, Frazer Meacham, Stephanie Crofts, Max Maliska– thank you so much for your constant friendship and unwavering support.

I am also grateful for the wonderful community of researchers in the field of microbial experimental evolution and specifically the great friends I've made through the BEACON Center for the Study of Evolution in Action and the Gordon Research Conference on Microbial Population Biology. Some of these people have also become incredible collaborators. Josephine Chandler, William Ratcliff, Eric Libby, Matthew Herron– thank you all so much for what you've done to help me improve my science and further my career.

I want to thank my lab for being the nicest, silliest, most brilliant, and caring people I've ever had the opportunity to work with. I especially would like to thank the many undergraduate students who played major roles in my research projects (from conception

to execution): Samuel Reed, Joseph Marcus, Riane Young, Chase O'Neil, Caroline Miller, Elsha Eggink, and Homma Khosroyani. I'm so incredibly proud of your work and all of the great things you've gone on to do since leaving the our lab.

And to my advisor, Ben. Thank you for being an amazing role model, mentor, and friend to me for 7 years now. Thank you for leading by example and for always taking the time to talk with me even when you have literally hundreds of other obligations. Those conversations with you have been the defining moments of my graduate career. It has been a great inspiration and an honor to be a part of your lab.

DEDICATION

to my parents

Chapter 1

PLEIOTROPIC EFFECTS OF COMPENSATORY EVOLUTION IN RIFAMPICIN RESISTANT *ESCHERICHIA COLI*

Peter L. Conlin[1,*] Chase M. O'Neil[1] Benjamin Kerr[1]

[1]Department of Biology and BEACON Center for the Study of Evolution in Action, University of Washington, Seattle, WA 98195, United States of America

∗ **corresponding author, email: pconlin2@uw.edu**

Keywords: antibiotic resistance | compensatory mutation | epistasis | pleiotropy | evolution

Abstract

Compensatory mutations play a critical role in the evolution of drug resistance in microorganisms. Most directly, they serve to alleviate the fitness cost commonly associated with initial drug resistance mutations. When compensatory mutations are deleterious in the absence of the initial resistance mutation, they also make drug resistance more stable by making reversion selectively disadvantageous. The fitness effects of compensatory mutations have been extensively studied, but more recent work has begun to highlight the possible role of compensatory mutations in the evolution of increased drug resistance. We hypothesized that compensatory mutations could lead to changes in the level of drug resistance due to strong pleiotropic effects, especially in cases where second-site mutations occur within the same gene as the original resistance conferring mutation. We tested this hypothesis using a highly replicated evolution experiment in which 30 replicate populations of 20 strains of *Escherichia coli* with varying levels of rifampicin resistance were evolved for 100 generations in the absence of antibiotics. We present data suggesting that antibiotic resistance can increase even in the absence of antibiotics. Furthermore, we explore the effect of the identity of initial resistance mutation on the observed outcomes.

Introduction

Mutations conferring antibiotic resistance in bacteria often impose a fitness cost in the absence of selecting drugs (Andersson and Levin 1999; Andersson and Hughes 2010; MacLean and Vogwill 2014; Melnyk et al. 2015). Removal of the selecting drug should therefore favor reversion back to sensitivity. Contrary to this expectation, experimental studies have found that resistance is often stably maintained in populations of drug resistant microorganisms even in the absence of antibiotics (Schrag et al. 1997; Björkman et al. 1998, 2000; Levin et al. 2000; Reynolds 2000; Maisnier-Patin and Andersson 2004; Gifford and MacLean 2013). This occurs when bacteria acquire second-site mutations that

ameliorate the cost of resistance, called compensatory mutations.

Compensatory mutations are thought to play a critical role in the evolution of drug resistance. By partially, or completely, restoring the fitness of drug resistant bacteria back to ancestral levels, compensatory mutations may effectively mitigate the selective pressure against resistance in the absence of drug exposure. Additionally, compensatory mutations are often deleterious or neutral in the absence of the initial resistance mutation (Schrag et al. 1997; Maisnier-Patin et al. 2002), a phenomenon known as genetic epistasis (Weinreich et al. 2005). In the case of reciprocal sign epistasis, where each mutation is deleterious in the wild-type background but beneficial in the presence of the other mutation, the fixation of a compensatory mutation may prevent direct reversion to sensitivity as either single-step mutation will be selectively disadvantageous (Tanaka and Valckenborgh 2011). Theoretical studies have found that compensatory mutations can promote the emergence and spread of epidemics (Handel et al. 2006) and suggest that compensatory mutations could be one of the primary reasons that costly antibiotic resistance persists even after drugs have stop being used (Zur Wiesch et al. 2010). (But see MacLean and Vogwill (2014) for a discussion of why compensatory adaptation may be less effective in natural populations.)

In some cases, compensation can occur between two individually costly resistance mutations (Hall and MacLean 2011), resulting in a genotype with both increased fitness and increased resistance. Mutations that concomitantly increase fitness and drug resistance are of obvious concern because they could create a situation of cost-free, high-level drug resistance (which may be very difficult to reverse due to sign epistatic interactions between the mutations). Meftahi et al (2015) specifically suggest that such a mutation may have contributed to the successful transmission of a multidrug-resistant strain of *Mycobacterium tuberculosis* that caused a disease outbreak in northern Tunisia. In the laboratory, this phenomenon has been observed between pairs of mutations conferring resistance to rifampicin (Hall and MacLean 2011; Brandis et al. 2012) and among sets of 2 to 4 alleles conferring resistance to fluoroquinolones (Lindgren et al. 2005; Rozen et al. 2007;

Marcusson et al. 2009). However, beyond the aforementioned studies, changes in drug tolerance after compensatory evolution has occurred are not widely reported. This led us to ask whether resistance increases following compensation are simply rare or if their occurrence could be explained by some biological factor.

We hypothesized that different drug resistance alleles may differ in their likelihood of acquiring compensatory mutations that improve their level of drug resistance due to epistatic interactions between mutations. Most laboratory studies of compensation examine the evolution of a small number of spontaneously generated drug-resistant mutants or engineer specific combinations of naturally occurring resistance alleles. We chose to examine this hypothesis using the evolution of rifampicin resistance in *Escherichia coli* as our model system. The drug rifampicin, an important front-line drug used to treat tuberculosis, binds to the β-subunit of the bacterial DNA-directed RNA polymerase and inhibits transcription (Campbell et al. 2001). Mutations conferring resistance to rifampicin occur primarily in the *rpoB* gene (Jin and Gross 1988; Reynolds 2000). Our goal in this work is to estimate the frequency of compensatory mutations that raise drug resistance and to determine the extent to which this frequency of occurrence is contingent upon genetic background. To address these issues, we evolved 30 replicate populations of 20 *E. coli* strains carrying different *rpoB* alleles for 100 generations in the absence of rifampicin. We found that MIC increases in the absence of antibiotic selection are relatively common, occurring in 108/600 of our evolved populations. Here we report on the identification of putative compensatory mutations and their effects on rifampicin resistance.

Methods

Isolation of mutant strains

Escherichia coli B (REL606) was used as our ancestral strain. Rifampicin-resistant strains, derived from this REL606 ancestor, were isolated by plating 200µl of an overnight culture

grown in lysogeny broth (LB) onto LB agar containing 50µg/ml rifampicin. From each plate that had colonies, a single representative colony was inoculated into 5ml of LB medium and shaken at 205 r.p.m. overnight at 37°C. Then 1ml of the culture was mixed with 160µl of 80% glycerol and stored at -80°C for later sequencing and phenotypic characterization. In total, 14 unique spontaneous mutant genotypes were isolated by plating. All mutations were non-synonymous. We refer to these strains as "single mutants" because the opportunity for double mutations to arise during the isolation of strains by plating on selective media is thought to be low (Kassen and Bataillon 2006). However, we cannot rule out the possibility that some of our strains have mutations elsewhere in the genome. An additional 5 non-synonymous single mutant genotypes, previously constructed in our lab using allelic replacement (Link et al. 1997; Lindsey et al. 2013), were also included for a total of 19 unique mutant alleles (Table 1).

Experimental evolution

30 replicate populations of each genotype were initiated in 96-well flat-bottom microtiter plates by a 1:100,000 dilution (1,000 cells per well) from overnight cultures grown in a 1% minimal glucose (MG) medium. Bacterial cultures were propagated in 96-well flat-bottom microtiter plates via daily 1:40 dilutions into 200µl of fresh MG media using a pin replicator that transfers 5µl of culture / well for a total of 20 days (100 generations). Each growth cycle lasted 24h, during which time the microtiter plates were incubated and shaken at 405 r.p.m. in an orbital microtiter plate shaker at 37°C. At the end of the evolution experiment, 32µl of 80% glycerol was added to each well of the microtiter plate and whole populations were stored at -80ºC.

Growth rate assays

We used maximum growth rate (V_{max}) in MG media in the absence of rifampicin as a proxy for bacterial fitness. Although several other factors can influence bacterial fitness (Vasi et

Table 1.1: **Strains of *Escherichia coli* and associated *rpoB* mutations.**

Isolate	Nucleotide change	Codon change	Amino acid change	Mutated region	Strain origin
Ancestor	–	–	–	–	–
Rif^R -1	g436t	GTT→TTT	V146F	N-term	This study
Rif^R -2	a443t	CAG→CTG	Q148L	N-term	This study
Rif^R -3	c1527a	AGC→AGA	S509R	rpoB (I)	This study
Rif^R -4	t1534c	TCT→CCT	S512P	rpoB (I)	This study
Rif^R -5	c1535t	TCT→TTT	S512F	rpoB (I)	This study
Rif^R -6	a1538c	CAG→CCG	Q513P	rpoB (I)	This study
Rif^R -7	c1576t	CAC→TAC	H526Y	rpoB (I)	This study
Rif^R -8	a1577t	CAC→CTC	H526L	rpoB (I)	This study
Rif^R -9	g1586a	CGT→CAT	R529H	rpoB (I)	This study
Rif^R -10	c1592t	TCC→TTC	S531F	rpoB (I)	This study
Rif^R -11	t1598c	CTC→CCC	L533P	rpoB (I)	This study
Rif^R -12	a1714t	ATC→TTC	I572F	rpoB (II)	This study
Rif^R -13	t1715g	ATC→AGC	I572S	rpoB (II)	This study
Rif^R -14	c1721t	TCT→TTT	S574F	rpoB (II)	This study
Rif^R -e1	g428a	CGT→CAT	R143H	N-term	Lindsey et al (2013)
Rif^R -e2	t437a	GTT→GAT	V146D	N-term	Lindsey et al (2013)
Rif^R -e3	t1532g	CTG→CGG	L511R	rpoB (I)	Lindsey et al (2013)
Rif^R -e4	g1546a	GAC→AAC	D516N	rpoB (I)	Lindsey et al (2013)
Rif^R -e5	a1685c	GAA→GCA	E562A	rpoB (II)	Lindsey et al (2013)

al. 1994; Wiser and Lenski 2015), we found a positive correlation between bacterial growth rate and competitive fitness in our *rpoB* single mutants (Spearman's rank correlation test; $\rho = 0.654$, $p = 0.003$; Fig. S1). Briefly, bacteria were grown in 96-well microtiter plates in MG medium for 20 hours at 37ºC in a Molecular Devices VersaMax plate reader. Optical density (OD450) was measured every 20 seconds. Raw data was exported as a text file. Maximum growth rate (V_{max}) was calculated from kinetic plate reader data using the grofit package in R (Kahm et al. 2010). A spline smoothing factor of 0.85 was chosen on the basis of visual inspection of fitted curves to avoid problems with over-estimation of V_{max} that arose when OD450 data was noisy. See Supplemental Materials for further details and example V_{max} calculations (Fig. S2).

Minimum inhibitory concentration (MIC) assays

Changes in rifampicin resistance after evolution were gauged using a minimum inhibitory concentration (MIC) assay using the broth micro-dilution method (Wiegand et al. 2008). Briefly, evolved populations were revived from the -80ºC freezer in 96-well microtiter plates and grown overnight in minimal glucose media. Bacterial populations were then diluted 1:1600 to achieve a bacterial inoculum of 5×10^5 colony forming units (cfu) ml^{-1} and exposed to increasing concentrations of rifampicin using 2-fold dilutions in MG media. Microtiter plates were then incubated for 20 hours under standard growth conditions (405 r.p.m. in an orbital microtiter plate shaker at 37°C). Finally, OD650 was measured as a proxy for growth for using a Molecular Devices VersaMax plate reader. The MIC of a population was determined as the lowest drug concentration that caused a greater than 50% decrease in OD650 relative to the maximal OD650 achieved by that genotype. We note the difference in wavelength used for MIC assays (OD650 instead of OD450, used for growth assays). The absorbance spectrum of the drug rifampicin has a peak at 474nm (Dabbs 1987). Thus, this change was necessary in order to measure absorbance of bacterial cultures at very high concentrations of rifampicin without interference.

Sequencing

PCR amplification of the *rpoB* gene was performed using the primers described in Reynolds (2000). After confirmation of successful amplification via gel electrophoresis, the PCR product was purified using the ExoI/SAP (shrimp alkaline phosphatase) method. Purified products were sent for sequencing (GeneWiz) and analyzed with ClustalX (version 2.1).

Statistical analyses

All plotting and statistical analyses were performed using the R software environment (R Core Team 2018).

Results and discussion

Characterization of rpoB single mutants

We characterized each of the 14 unique spontaneous mutant genotypes and the 5 previously engineered *rpoB* mutants by measuring minimum inhibitory concentration (MIC) in rifampicin and maximum growth rate, V_{max}, in the absence of the drug (Fig. 1). In keeping with previous studies of *rpoB* single mutants, we found that most rifampicin resistance mutations are costly (Reynolds 2000; Gagneux et al. 2006): only three *rpoB* mutant genotypes (R143H, L511R, and S574F) had growth rates comparable to the ancestor while the rest had growth rate costs ranging from 3-40% that of the ancestor. Additionally, we found no strong relationship between MIC and the cost of resistance for *rpoB* mutants with an MIC greater than that of the ancestor (Spearman's rank correlation test; ρ = -0.276, p = 0.284). Note that two of the engineered single mutants were excluded from this analysis because they showed no significant increase in MIC relative to the ancestor.

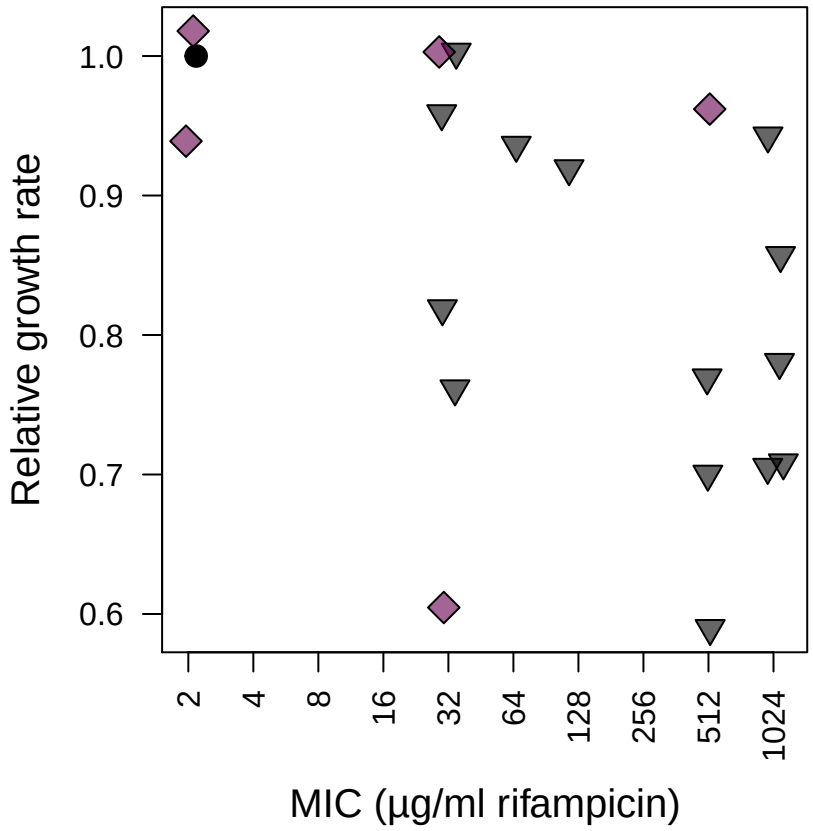

Figure 1.1: **Phenotypic characterization of *rpoB* single mutant isolates.** Strains exhibited considerable variation in relative growth rate and minimum inhibitory concentration (MIC). Strains with different origins are denoted using different symbols and colors. The rifampicin sensitive ancestor is represented by a black circle, spontaneous mutants as grey triangles, engineered single mutants as purple diamonds. Points have been jittered slightly along the x-axis to improve readability.

Growth rates of evolved populations

We measured the maximal growth rates of all 600 evolved populations and their respective single mutant ancestors in MG media in the absence of the drug rifampicin to check for evidence of compensation. Growth rates for all evolved populations and single mutant strains are reported here in relative terms, as the maximal growth rate achieved relative to the mean maximal growth rate of 6 replicate wells of the wild type ancestor REL606 grown in the same microtiter plate. Four *rpoB* genotypes (V146F, Q513R, H526Y and L533P) showed significant improvements in growth rate relative to their single mutant ancestors (Fig. 2; significant improvements indicated by background shading). The remaining strains showed no significant changes in growth rate. In Supplemental Materials we examine the effect of varying the smoothing parameter used to fit the bacterial growth curves (Fig. S3).

The lack of observable growth rate improvement for several evolved populations was somewhat unexpected, especially in those that had initially low growth rates relative to the wild-type ancestor (such as strains R529H, S531F, and I572F). However, we find that the overall growth rate improvements are proportional to the initial cost of resistance (Spearman's rank correlation test; $\rho = 0.696$, $p < 0.001$), consistent with the findings of a previous study of *E. coli rpoB* mutants adapting to the fitness costs of resistance in a drug-free medium (Barrick et al. 2010). Thus, it is likely that some populations experienced an insufficient number of generations for beneficial mutations to rise to high-enough frequencies to substantially affect the population growth rate. Despite the lack of evidence that growth rate compensation had occurred in many of our populations, we reasoned that fitness improving mutations should still be present in the evolved populations, albeit at low frequencies.

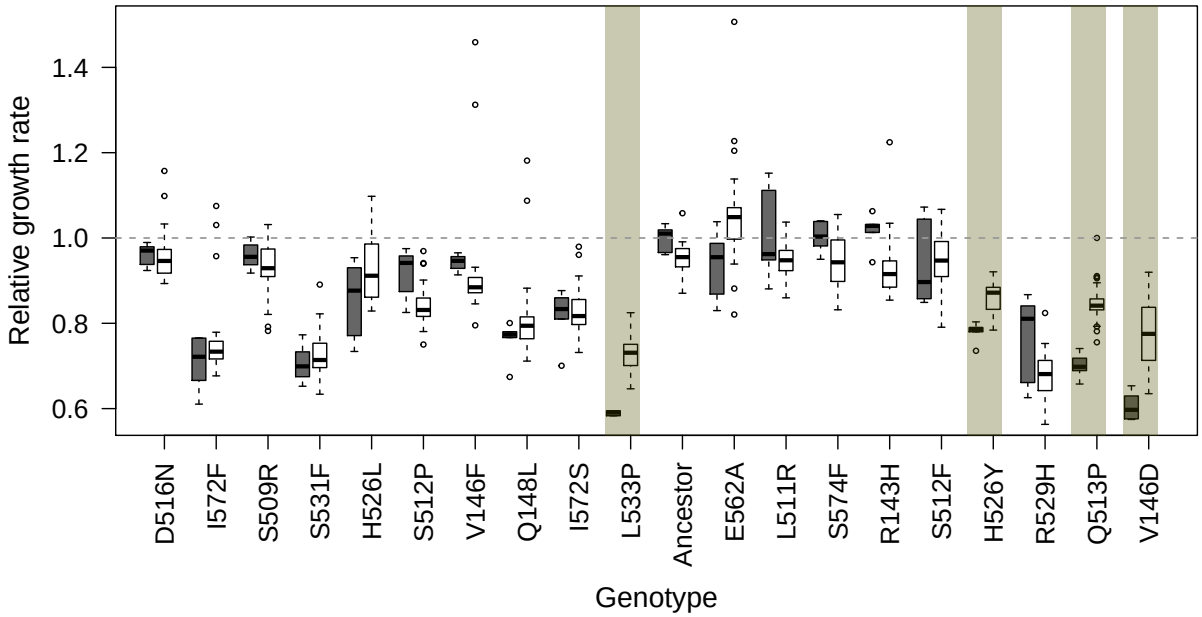

Figure 1.2: **Relative growth rates of replicate populations after 100 generations of evolution.** Bacteria were revived from freezer in 96-well microtiter plates and grown overnight in minimal glucose media before being transferred with a 1:40 dilution to fresh media for the growth assay. Maximal growth rates were extracted for each well using the spline fitting function from the grofit package in R. Evolved populations are shown in white (n=1 for each of the 30 populations), single mutant ancestors in grey (n=6 per genotype). Measurements of evolved populations and their corresponding single mutant ancestor were performed on the same day and in the same microtiter plate. Strains that exhibit a significant change in growth rate relative to their respective single mutant ancestor are indicated by background shading. Significant differences were determined using a Welch Two Sample t-test ($p < 0.00238$ after Bonferroni correction).

Increases in minimum inhibitory concentration

We measured the minimum inhibitory concentration (MIC) of all 600 evolved populations using 2–fold dilutions of rifampicin. All MIC assays were performed in triplicate using 3 separate microtiter plates for which well-position had been reassigned by row to limit the potential for spatial biases (Blomberg 2011). Each of the three replicate MIC assays represents an independent sampling from the evolved population. A population was said to show an increase in MIC only if the same population grew at a rifampicin concentration beyond that of its single mutant ancestor's MIC in two of three replicates. Using this approach, we determined that any mutations conferring an increase in rifampicin resistance must be present at a frequency greater than 1:286,000 cells ($3.5 \times 10^{-}6$) in order to be detected by our MIC assay (see Supplemental Materials for details; Fig. S4).

In total, 108/600 (18%) evolved populations exhibited an increase in MIC while 6/600 (1%) evolved populations exhibited a decrease. In most cases, populations that exhibited an elevated MIC increased by 2-fold, but in some cases MIC increased by as much as 16 to 32-fold. The largest decrease in MIC we observed was 2-fold lower than the single mutant ancestor. The MIC shifts exhibit a markedly non-random distribution (Pearson's Chi-squared test; $X^2 = 483.92$, df = 19, $p < 0.001$) with 102/108 (94%) increases falling on the background of only 4/20 (20%) genotypes tested. This is consistent with the hypothesis that different genotypes may differ in their likelihood of acquiring compensatory mutations that improve their level of drug resistance due to epistasis. We examined the effect of varying the threshold used to distinguish growth from non-growth in our spectrophotometer data and found no significant differences in our qualitative results. See supplemental materials for detailed analyses of MIC data using different thresholds (Fig. S5).

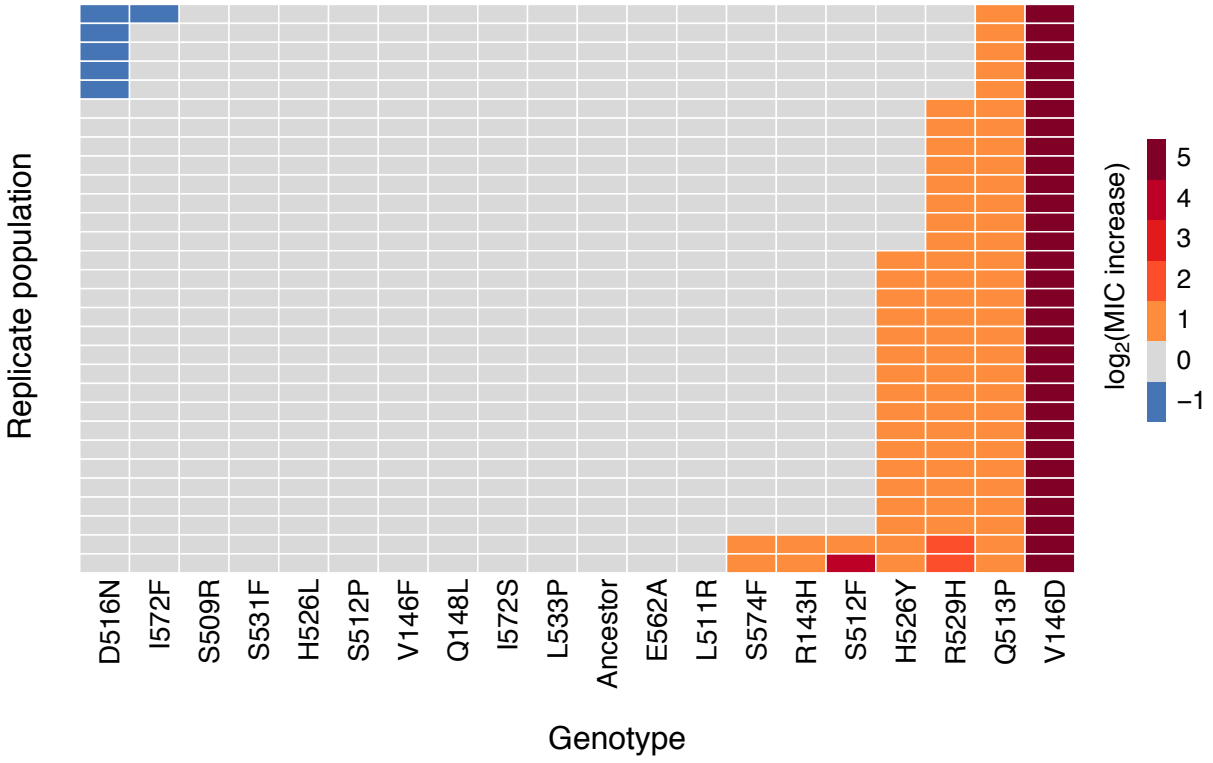

Figure 1.3: **Changes in MIC after 100 generations of evolution.** Bacteria were revived from freezer in 96-well microtiter plates and grown overnight in minimal glucose media. Each MIC assay was initiated with a 1:1600 dilution from revived overnight cultures. A population is said to show an increase in MIC only if the same population grows beyond its previously identified MIC in two of three replicate MIC assays. Each column shows the change in MIC for all 30 replicate populations of each genotype. Changes in MIC are indicated by the color of the cell as indicated by the scale bar on the right-hand side of the plot.

Correlation between MIC increase and growth rate compensation

We hypothesized that MIC increases could occur as a pleiotropic effect of selection for growth compensatory mutations in rifampicin resistant *E. coli*. The results of our MIC and growth assays generally support this hypothesis; three of the four genotypes that exhibited significant growth improvements also exhibit MIC increases in the majority of evolved replicate populations and there is a weak but significant correlation between MIC shifts and change in growth rate (Fig. 4; Spearman's rank correlation test; $\rho = 0.281$, $p < 0.001$). However, there are a few notable exceptions to this rule. In the case of *rpoB* R529H, we found that 25/30 populations exhibited MIC increases without detectable growth rate increases. This suggests that a significantly detectable increase in growth rate is not necessary for an MIC shift in our study. However, we note that although we use maximal growth rate as a convenient proxy for bacterial fitness due to the large number of populations, growth assays are typically successful in identifying fitness differences >5% (Andersson and Hughes 2010). Therefore, it is possible that we would identify significant differences in fitness if we were to instead measure relative fitness directly using pairwise competitions (Lenski et al. 1991). In the case of *rpoB* L533P, we found that evolved populations had a significant improvement in growth rate but there was no change in MIC. Thus, a significantly detectable increase in growth rate is not sufficient for MIC shift.

rpoB mutations as adaptation to growth in minimal glucose media

Mutations in *rpoB* are known to confer fitness benefits in certain laboratory culture environments. Specifically, increases in rifampicin resistance in the absence of antibiotic exposure have been found under starvation conditions in aging bacterial colonies (Wrande et al. 2008; Katz and Hershberg 2013), during adaptation to thermal stress (Rodríguez-Verdugo et al. 2013), and during adaptation to growth in minimal glucose media (Knöppel et al. 2017). The latter case is particularly relevant to our study since we used a very similar growth medium for our evolution experiment. Briefly, Knöppel et al.

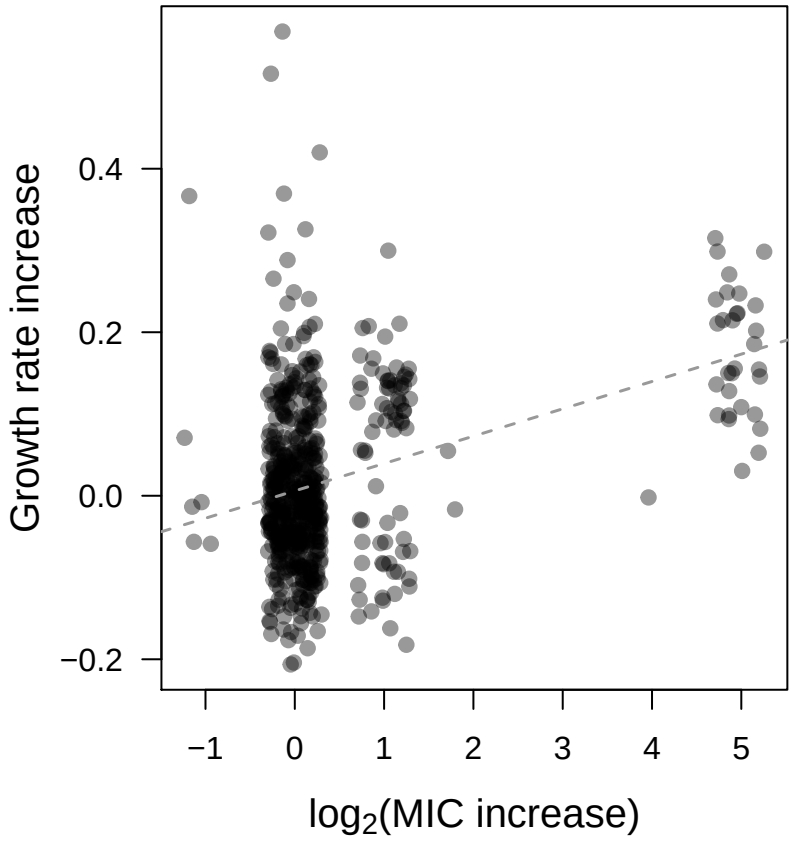

Figure 1.4: **Shifts in MIC exhibit a weak correlation with changes in growth rate.** The difference in maximum growth rate for each evolved population relative to its single mutant ancestor is plotted on the y-axis; difference in MIC value on the x-axis. Points have been jittered along the x-axis to improve readability. The grey dashed line is a linear best fit with all 600 populations treated as independent data points.

(2017) evolved 8 replicate populations of an initially drug sensitive *E. coli* K-12 strain for 500 generations in M9 minimal glucose media and found 1/8 populations where rifampicin resistance had increased. Although we cannot rule out the possibility that adaptation to growth in minimal media played a role here, the fact that we observe such a strong effect of initial resistance mutation and no MIC increases on the background of our initially drug sensitive ancestor suggest that minimal media adaptation is unlikely to be the cause of the MIC increases seen in our study. We also observe MIC increases in a higher percentage of evolved populations and in fewer generations (e.g., 18% in 100 generations compared to 12.5% in 500 generations); providing further evidence that initial resistance mutations were important to our findings.

Limitations of this study

In a study similar to ours, Brandis et al. (2012) explored growth compensation in ten replicate populations of *Salmonella enterica* harboring the rifampicin resistance mutation *rpoB* R529C. After 60 generations of growth in the absence of antibiotic selection, they found evidence of one compensatory mutation that increased MIC (*rpoB* D516G) as well as one that caused an MIC decrease (*rpoB* P564S). These results suggest that increases and decreases in rifampicin resistance associated with compensatory mutations could be equally common (at least for this particular *rpoB* mutation and this strain of *S. enterica*), yet we observe MIC decreases extremely rarely. The most probable cause of this discrepancy can be traced back to our choice to perform MIC assays using evolved populations rather than clones. A whole population MIC assay is unlikely to detect alleles with decreased rifampicin resistance because even a small subpopulation of more resistant bacteria will grow to high density, effectively masking the presence of more sensitive genotypes. The choice to perform whole population MIC assays was made to facilitate the screening of hundreds of populations in parallel. However, as a consequence, we are likely missing many instances of MIC decrease.

A second limitation of our study is that we have not elucidated the underlying causes of the MIC increases or the influence of genetic background. We hypothesized that different resistance mutations might differ in their likelihood of acquiring compensatory mutations that improve their level of drug resistance due to epistatic interactions. While our results are consistent with this hypothesis, a formal test of epistasis would require that we do the following for putative compensatory mutations arising on different genetic backgrounds: (i) identify the secondary mutation responsible for compensation and (ii) construct the relevant single and double mutants to assess their individual and combined effects on MIC and growth rate.

Conclusion

While the historical emphasis has been on the fitness effects of compensation, a growing number of studies have reported the existence of compensatory mutations that also significantly increase the level of drug resistance (Lindgren et al. 2005; Rozen et al. 2007; Marcusson et al. 2009; Hall and MacLean 2011; Brandis et al. 2012; Meftahi et al. 2015). Fitness improvements have also been documented between sets of alleles conferring resistance to different antibiotics (Trindade et al. 2009; Ward et al. 2009; Silva et al. 2011; Borrell et al. 2013). However, existing studies have largely focused on interactions among small sets of resistance mutations, making it hard to determine how common these pleiotropic resistance increases might be in populations harboring large amounts of genetic variation. We chose to investigate this phenomenon by evolving 20 strains of rifampicin resistant *Escherichia coli* carrying different *rpoB* alleles in the absence of antibiotics for 100 generations. We found that increases in drug resistance occur quite commonly in the absence of antibiotic selection, but that MIC increases occur disproportionately on certain genetic backgrounds. Significant growth improvement was correlated with an increase in MIC, but the dependency on genetic background cannot be explained by overall growth improvement alone.

Rather than being rare exceptions to the rule, we speculate that increases in MIC due to compensatory mutations may be fairly common, especially in cases where second-site mutations occur within the same gene as the original resistance conferring mutation. In the case of rifampicin resistance, for example, resistance is typically achieved by structural modification of the β-subunit of the bacterial DNA-directed RNA polymerase, encoded by the *rpoB* gene (Campbell et al. 2001). Thus, it is reasonable to expect that a second-site mutation in the same protein coding gene where the initial resistance mutation occurred (*rpoB*) could impact the level of drug resistance by causing further structural changes to the protein. Intragenic compensatory mutations may also be among the most likely to exhibit idiosyncratic effects due to the identity of the initial resistance mutation because compensatory mutations have been found to cluster around the site of their associated deleterious mutation (Davis et al. 2009). Hopefully further studies of compensatory mutations and their pleiotropic effects on resistance will clarify this point.

Author contributions

All authors participated in the design of the evolution experiment; PLC and CMO performed the evolution experiment; PLC measured bacterial growth rates and MICs, performed the data analyses, and wrote the first draft of the manuscript.

Acknowledgements

The authors thank B. Connelly for help with the analysis of bacterial growth rates and L. Zaman for many helpful discussions about the relationship between bacterial growth rate and minimum inhibitory concentration. Furthermore, we would like to thank the members of the Kerr lab for their thoughtful comments on this project. This work was supported by the National Science Foundation under Cooperative Agreement Number DBI-0939454 and UW Royalty Research Fund Award (A74107). PLC was supported by a National Science

Foundation Graduate Research Fellowship under Grant Number DGE-1256082 and funds made available by the UW Biology department.

References

Andersson, D. I., and D. Hughes. 2010. Antibiotic resistance and its cost: Is it possible to reverse resistance? Nature Reviews Microbiology 8:260–271.

Andersson, D. I., and B. R. Levin. 1999. The biological cost of antibiotic resistance. Current Opinion in Microbiology 2:489–493.

Barrick, J. E., M. R. Kauth, C. C. Strelioff, and R. E. Lenski. 2010. *Escherichia coli rpoB* mutants have increased evolvability in proportion to their fitness defects. Molecular Biology and Evolution 27:1338–1347.

Björkman, J., D. Hughes, and D. I. Andersson. 1998. Virulence of antibiotic-resistant *Salmonella typhimurium*. Proceedings of the National Academy of Sciences of the United States of America 95:3949–3953.

Björkman, J., I. Nagaev, O. G. Berg, D. Hughes, and D. I. Andersson. 2000. Effects of environment on compensatory mutations to ameliorate costs of antibiotic resistance. Science 287:1479–1482.

Blomberg, A. 2011. Measuring growth rate in high-throughput growth phenotyping. Current Opinion in Biotechnology 22:94–102.

Borrell, S., Y. Teo, F. Giardina, E. M. Streicher, M. Klopper, J. Feldmann, B. Müller, et al. 2013. Epistasis between antibiotic resistance mutations drives the evolution of extensively drug-resistant tuberculosis. Evolution, Medicine and Public Health 2013:65–74.

Brandis, G., M. Wrande, L. Liljas, and D. Hughes. 2012. Fitness-compensatory mutations in rifampicin-resistant RNA polymerase. Molecular Microbiology 85:142–151.

Campbell, E. A., N. Korzheva, A. Mustaev, K. Murakami, S. Nair, A. Goldfarb, and S. A.

Darst. 2001. Structural mechanism for rifampicin inhibition of bacterial RNA polymerase. Cell 104:901–12.

Dabbs, E. R. 1987. Rifampicin inactivation by *Rhodococcus* and *Mycobacterium* species. FEMS Microbiology Letters 44:395–399.

Davis, B. H., A. F. Y. Poon, and M. C. Whitlock. 2009. Compensatory mutations are repeatable and clustered within proteins. Proceedings of the Royal Society B 276:1823–7.

Gagneux, S., C. D. Long, P. M. Small, T. Van, G. K. Schoolnik, and B. J. M. Bohannan. 2006. The competitive cost of antibiotic resistance in *Mycobacterium tuberculosis*. Science 312:1944–1946.

Gifford, D. R., and R. C. MacLean. 2013. Evolutionary reversals of antibiotic resistance in experimental populations of *Pseudomonas aeruginosa*. Evolution 67:2973–81.

Hall, A. R., and R. C. MacLean. 2011. Epistasis buffers the fitness effects of rifampicin-resistance mutations in *Pseudomonas aeruginosa*. Evolution 65:2370–9.

Handel, A., R. R. Regoes, and R. Antia. 2006. The role of compensatory mutations in the emergence of drug resistance. PLOS Computational Biology 2:1262–1270.

Jin, D. J., and C. A. Gross. 1988. Mapping and sequencing of mutations in the *Escherichia coli rpoB* gene that lead to rifampicin resistance. Journal of Molecular Biology 202:45–58.

Kahm, M., G. Hasenbrink, Lichtenberg-Fraté, J. Ludwig, and M. Kschisco. 2010. grofit: Fitting biological growth curves with R. Journal of Statistical Software 33:1–21.

Kassen, R., and T. Bataillon. 2006. Distribution of fitness effects among beneficial mutations before selection in experimental populations of bacteria. Nature Genetics 38:484–488.

Katz, S., and R. Hershberg. 2013. Elevated mutagenesis does not explain the increased frequency of antibiotic resistant mutants in starved aging colonies. PLOS Genetics 9:e1003968.

Knöppel, A., J. Näsvall, and D. I. Andersson. 2017. Evolution of antibiotic resistance without antibiotic exposure. Antimicrobial Agents and Chemotherapy 61:1–5.

Lenski, R. E., M. R. Rose, S. C. Simpson, and S. C. Tadler. 1991. Long-term experimental evolution in *Escherichia coli*. I. Adaptation and divergence during 2,000 generations. The American Naturalist 138:1315–1341.

Levin, B., V. Perrot, and N. Walker. 2000. Compensatory mutations, antibiotic resistance and the population genetics of adaptive evolution in bacteria. Genetics 154:985–997.

Lindgren, P. K., L. L. Marcusson, N. Frimodt-møller, D. Hughes, and D. Sandvang. 2005. Biological cost of single and multiple norfloxacin resistance mutations in *Escherichia coli* implicated in urinary tract infections. Antimicrobial Agents and Chemotherapy 49:2343–2351.

Lindsey, H. A., J. Gallie, S. Taylor, and B. Kerr. 2013. Evolutionary rescue from extinction is contingent on a lower rate of environmental change. Nature 494:463–467.

Link, A. J., D. Phillips, and G. M. Church. 1997. Methods for generating precise deletions and insertions in the genome of wild-type *Escherichia coli*: Application to open reading frame characterization. Journal of Bacteriology 179:6228–6237.

MacLean, R. C., and T. Vogwill. 2014. Limits to compensatory adaptation and the persistence of antibiotic resistance in pathogenic bacteria. Evolution, Medicine and Public Health 2015:4–12.

Maisnier-Patin, S., and D. I. Andersson. 2004. Adaptation to the deleterious effects of antimicrobial drug resistance mutations by compensatory evolution. Research in Microbiology 155:360–9.

Maisnier-Patin, S., O. G. Berg, L. Liljas, and D. I. Andersson. 2002. Compensatory adaptation to the deleterious effect of antibiotic resistance in *Salmonella typhimurium*. Molecular Microbiology 46:355–366.

Marcusson, L. L., N. Frimodt-Møller, and D. Hughes. 2009. Interplay in the selection of fluoroquinolone resistance and bacterial fitness. PLOS Pathogens 5:e1000541.

Meftahi, N., A. Namouchi, B. Mhenni, G. Brandis, D. Hughes, and H. Mardassi. 2015. Evidence for the critical role of a secondary site *rpoB* mutation in the compensatory evolution and successful transmission of an MDR tuberculosis outbreak strain. Journal of Antimicrobial Chemotherapy 71:1–9.

Melnyk, A. H., A. Wong, and R. Kassen. 2015. The fitness costs of antibiotic resistance mutations. Evolutionary Applications 8:273–283.

R Core Team. 2018. R: A language and environment for statistical computing. R Foundation for Statistical Computing, Vienna, Austria.

Reynolds, M. G. 2000. Compensatory evolution in rifampin-resistant *Escherichia coli*. Genetics 156:1471–81.

Rodríguez-Verdugo, A., B. S. Gaut, and O. Tenaillon. 2013. Evolution of *Escherichia coli* rifampicin resistance in an antibiotic-free environment during thermal stress. BMC Evolutionary Biology 13:50.

Rozen, D. E., L. McGee, B. R. Levin, and K. P. Klugman. 2007. Fitness costs of fluoroquinolone resistance in *Streptococcus pneumoniae*. Antimicrobial Agents and Chemotherapy 51:412–416.

Schrag, S. J., V. Perrot, and B. R. Levin. 1997. Adaptation to the fitness costs of antibiotic resistance in *Escherichia coli*. Proceedings of the Royal Society B 264:1287–1291.

Silva, R. F., S. C. M. Mendonça, L. M. CarvalhoLuí, A. M. Reis, I. Gordo, S. Trindade, and F. Dionisio. 2011. Pervasive sign epistasis between conjugative plasmids and drug-resistance chromosomal mutations. PLOS Genetics 7:e1002181.

Tanaka, M. M., and F. Valckenborgh. 2011. Escaping an evolutionary lobster trap: Drug resistance and compensatory mutation in a fluctuating environment. Evolution 65:1376–87.

Trindade, S., A. Sousa, K. B. Xavier, F. Dionisio, M. G. Ferreira, and I. Gordo. 2009. Positive epistasis drives the acquisition of multidrug resistance. PLoS genetics 5:e1000578.

Vasi, F., M. Travisano, and R. E. Lenski. 1994. Long-term experimental evolution in *Escherichia coli*. II . Changes in life-history traits during adaptation to a seasonal environment. American Naturalist 144:432–456.

Ward, H., G. G. Perron, and R. C. MacLean. 2009. The cost of multiple drug resistance in *Pseudomonas aeruginosa*. Journal of Evolutionary Biology 22:997–1003.

Weinreich, D. M., R. A. Watson, and L. Chao. 2005. Perspective: Sign epistasis and genetic constraint on evolutionary trajectories. Evolution 59:1165–1174.

Wiegand, I., K. Hilpert, and R. E. W. Hancock. 2008. Agar and broth dilution methods to determine the minimal inhibitory concentration (MIC) of antimicrobial substances. Nature Protocols 3:163–75.

Wiser, M. J., and R. E. Lenski. 2015. A comparison of methods to measure fitness in *Escherichia coli*. PLOS ONE 10:e0126210.

Wrande, M., J. R. Roth, and D. Hughes. 2008. Accumulation of mutants in "aging" bacterial colonies is due to growth under selection, not stress-induced mutagenesis. Proceedings of the National Academy of Sciences of the United States of America 105:11863–11868.

Zur Wiesch, P. S., J. Engelstädter, and S. Bonhoeffer. 2010. Compensation of fitness costs and reversibility of antibiotic resistance mutations. Antimicrobial Agents and Chemotherapy 54:2085–2095.

Chapter 2

STABILIZING MULTICELLULARITY THROUGH RATCHETING

Eric Libby[1,*,+] Peter L. Conlin[2,+] Ben Kerr[2] William C. Ratcliff[3]

[1]**Santa Fe Institute, Santa Fe, NM 87501, United States of America**

[2]**Department of Biology and BEACON Center for the Study of Evolution in Action, University of Washington, Seattle, WA 98195, United States of America**

[3]**Department of Biology, Georgia Institute of Technology, Atlanta, GA 30332, United States of America**

∗ **corresponding author, email: elibby@santafe.edu**

[+] **EL & PC share first authorship**

Keywords: multicellularity | ratcheting | major transition | evolution | stability

Abstract

The evolutionary transition to multicellularity likely began with the formation of simple undifferentiated cellular groups. Such groups evolve readily in diverse lineages of extant unicellular taxa, suggesting that there are few genetic barriers to this first key step. This may act as a double-edged sword: labile transitions between uni- and multicellular states may facilitate the evolution of simple multicellularity, but reversion to a unicellular state may inhibit the evolution of increased complexity. In this paper, we examine how multicellular adaptations can act as evolutionary "ratchets", limiting the potential for reversion to unicellularity. We consider a nascent multicellular lineage growing in an environment that varies between favoring multicellularity and favoring unicellularity. The first type of ratcheting mutations increase cell-level fitness in a multicellular context but are costly in a single-celled context, reducing the fitness of revertants. The second type of ratcheting mutations directly decrease the probability that a mutation will result in reversion (either as a pleiotropic consequence or via direct modification of switch rates). We show that both types of ratcheting mutations act to stabilize the multicellular state. We also identify synergistic effects between the two types of ratcheting mutations in which the presence of one creates the selective conditions favoring the other. Ratcheting mutations may play a key role in diverse evolutionary transitions in individuality, sustaining selection on the new higher-level organism by constraining evolutionary reversion.

Introduction

Complex life has evolved through a series of events in which organisms evolve to become specialized parts of new, "higher-level" organisms [12]. These events have come to be known as major transitions in evolution [2], or evolutionary transitions in individuality [3], and include the origin of cells from groups of interacting replicators, the origin of eukaryotes from mutualistic prokaryotes, the evolution of multicellular organisms from unicellular ancestors, and

the evolution of eusocial "superorganisms" from solitary individual multicellular organisms. The hierarchical nature of life, with genes nested within cells nested within multicellular organisms nested within societies, is a historical signature of these repeated evolutionary transitions in individuality.

Here, we focus on the evolution of multicellular organisms from unicellular ancestors. Multicellular organisms are a ubiquitous part of our environment. As Kirk (2005)[44] rightly observed, "…if all multicellular eukaryotes suddenly vanished from Earth, our planet would appear as barren as Mars." Despite the profound challenges involved in making the transition, multicellularity has evolved at least 25 times in taxonomically and ecologically diverse microbial lineages [56]. Filamentous cyanobacteria are the first lineage known to evolve multicellularity on Earth, dating between 2.25 and 2.45 billion years ago [6]. Centimeter-scale macrofossils of putative multicellular organisms composed of cells growing in radially-organized sheets have also been recovered from a period of elevated oxygen 2.1 billion years ago [7], though little is known about their biology. The red algae *Bangiomorpha* is the first known multicellular eukaryote, making this transition approximately 1.2 billion years ago [63]. Within the last billion years, there have been numerous transitions to multicellularity across lineages spanning the deepest divergences within eukaryotes [9, 10, 11] and within archaea [12].

The fact that multicellularity has independently arisen so many times in diverse lineages suggests that the selective conditions favoring this transition must be rather common [56]. Theoretical and experimental works support this hypothesis, and indeed the formation of simple clusters of cells (the first step in the transition) can be adaptive under a number of distinct ecological scenarios [13]. For example: clusters may provide protection from predation [14, 15, 16], protection from environmental stress [17], or improved utilization of diffusible nutrients [18, 19, 20]. Experimental studies have also demonstrated that (under the right selective conditions) simple undifferentiated multicellularity evolves readily in diverse species [16, 21, 32, 23, 24]; suggesting that the genetic changes necessary to achieve simple

undifferentiated multicellularity are few.

Two independent experiments observed the evolution of multicellularity in the budding yeast, *Saccharomyces cerevisiae* [32, 23, 19]. Both found that a loss of function mutation in the transcription factor *ACE2* was enough to produce simple undifferentiated multicellularity [23, 19]. In *Pseudomonas fluorescens*, another model organism for studying the evolution of multicellularity, switching between multicellular "wrinkly spreader" (WS) and unicellular "smooth morph" (SM) states can be achieved readily by mutations in a small number of loci that affect the production of an extracellular glue [26, 27, 28].

The evolutionary lability of multicellularity seen in experimental systems raises an interesting issue: *if simple multicellularity is so easy to achieve, shouldn't it also be easy to lose?* Reversion to unicellularity may therefore represent a significant threat to the long-term stability of multicellularity, particularly when its benefits are environmentally dependent (e.g., when predators are present). Experiments with microbes have also highlighted costs of multicellularity. In a study where selection for rapid sedimentation in liquid media promoted the evolution of multicellularity in yeast, Ratcliff et al (2012) [32] found that multicellularity was associated with 10% reduced fitness in the absence of settling selection, likely due to slower growth rates caused by diffusional limitation [29]. In addition, Rainey and Rainey (2003) [27] found that the WS genotype suffered a 20% fitness cost relative to the ancestral SM genotype under conditions that did not require colonization of the air-liquid interface. Similar results have been found in natural systems. For example, the green alga *Desmodesmus subspicatus* facultatively forms multicellular colonies when it senses chemical cues released by its predator *Daphnia*, increasing fitness during predation, but in the absence of predation the unicellular phenotype displaces multicelled phenotypes [30]. This suggests that there would be strong selection for unicellular revertants from nascent multicellular organisms if the environment were to shift in such a way that groups of cells were no longer favored. How then is multicellularity stabilized in the face of this threat?

Questions of the evolutionary stability of major transitions have long been considered of

key importance [2]. Historically, evolutionary conflict between lower and higher levels of selection have been regarded as the largest threat to nascent higher-level entities [12, 52, 32]. During the transition to multicellularity, for example, the focus has been on explaining why selection among competing cell lineages within a single multicellular entity does not disrupt the integrity of the group. Indeed, multicellular organisms are rife with the potential for such conflict, which in animals manifests as cancer [33]. Several mechanisms that limit within-organism variation, and thus limit the potential for conflict among lower level units, have evolved in multicellular organisms such as the early sequestration of the germ line [12] and the evolution of a single-cell bottleneck during development [34, 17, 18]. Other conflict minimizing strategies, such as greenbeard genes [17, 37] and policing [38, 39], have evolved in cooperative groups that lack clonal development such as social amoebae and myxobacteria.

In this paper, we focus on how the transition to multicellularity may be stabilized against evolutionary reversion when environmental conditions change and tip the balance of selection back in favor of unicellularity. Solving this problem is necessary for the long-term success of a major transition. There are two ways that evolutionary change can limit the potential effects of reversion. The first solution we consider is for mutations that are adaptive in the multicellular context to be disadvantageous in the single-celled context. This could make reversion less beneficial and maintain selection for group cohesiveness even when the environment favors unicellularity [40, 41]. Here, we refer to the accumulation of mutations that have this effect as a "ratcheting" process (and traits that have this property may be referred to as "ratcheting" traits). Similarly, multicellularity can be stabilized if unicellularity simply becomes less accessible by mutation. This could happen via deletion of a gene essential for unicellularity or if the genetic architecture evolves in such a way that it increases the number of mutations needed to return to the unicellular state. As these processes also limit the potential effects of reversion, they can also be considered as a form of ratcheting. To delineate between the two processes we label the accumulation of traits with different fitness characteristics in uni- and multicellular contexts as "type 1 ratcheting" and the reduction in

the switch rate between uni- and multicellular states as "type 2 ratcheting".

Here, we examine both types of ratcheting and their potential to stabilize multicellularity in environments that fluctuate between selecting for uni- and multicellular states. Through the use of mathematical models we show that both forms of ratcheting can be effective on their own under certain conditions. Furthermore, when both types of ratcheting are permitted there are synergistic effects that increase the stability of multicellularity.

Model

We consider the evolutionary dynamics of a population of genotypes with the capacity to switch between unicellular/independent (I) cell types and cells that exist as part of multicellular/group states (G cells). While there are many modes by which multicellular groups grow and reproduce, we choose a more general, cell-level approach. We do not explicitly model a particular multicellular form or group structure. Rather, we consider the population dynamics of I and G cells where the benefit (or cost) of being multicellular manifests in the fitness values of G cells. So in an environment that favors multicellularity the G cells have higher fitness than the I cells. This approach eliminates the need to track which G cells belong to which multicellular organisms.

If there were only one environmental state then either multicellular or unicellular cell types would have a selective advantage and drive the other extinct. Instead, we assume that there is an environment that fluctuates between two states: E_G and E_I. The E_I state favors unicellular I cells and the E_G environmental state favors multicellular G cells. When exposed to either environmental state, cells reproduce until they reach a certain number, N, the carrying capacity ($N = 10^5$ in this paper). Each reproductive event is chosen randomly from the current population based on the fitness values of cells. So, if there is an I cell with fitness k_i and two G cells with fitness k_g then the probability that the I cell would reproduce next would be $\frac{k_i}{k_i+2k_g}$. The manner in which we simulate population expansion is based on the Gillespie algorithm [42] and permits simulation of large populations with different fitness

values and rare, stochastic events such as mutations. After the population reaches carrying capacity, it experiences a bottleneck whereby a fraction of individuals (10^2 in this paper) are chosen randomly from the population to seed growth in the next round/environmental state. Thus populations experience cycles of expansion to 10^5 and contraction to 10^2.

As populations expand, reproductive events allow for chance mutations that change the fitness value of cells. At the start the fitness values are shown in Table 1, where c is a cost of being maladapted ($c > 0$). With each reproduction there is a fixed probability p_{f} (10^{-3}

Table 2.1: Initial fitness values

type	E_G	E_I
I	1-c	1
G	1	1-c

in this paper) that a cell will gain a mutation that improves its fitness. For simplicity, we ignore deleterious mutations and consider only beneficial mutations. The maximum fitness benefit of a mutation, Δs, is sampled from an exponential distribution with $\lambda = 35$ [43]. This is assigned to I cells in E_I and G cells in E_G. In addition, we assume that there is a correlation for fitness gaining mutations such that a cell also gains a fraction of this benefit in the environment to which it is not well-suited. We use a fraction of $\frac{1}{5}$ throughout this paper. Thus, as a result of a single mutation the following fitness values can be obtained in I or G cells. (Table 2).

Table 2.2: Fitness values after a beneficial mutation

type	E_G	E_I
I	1-c+$\frac{1}{5}$ Δs	1+Δs
G	1+Δs	1-c +$\frac{1}{5}$ Δs

At reproduction, there is also a chance that a cell can switch types between I and G cell types. This occurs randomly with probability p_s and is the same for both I to G and G to I cell switching. We also assume that this probability is fixed and independent of other evolved traits including fitness increasing mutations– later we relax part of this assumption and allow p_s to evolve. If we assume that the I and G cell switch is independent of fitness-affecting mutations, it implies that the responsible mechanisms reside at different loci and have no epistatic interactions with the fitness-affecting mutations.

As a consequence of allowing the cell types to switch, we must track four fitness values: the E_G and E_I fitness for the current cell type and the E_G and E_I fitness for the opposite cell type should a switch occur. This permits the possibility that a fitness-affecting mutation in the current cell type may also affect the fitness values of the opposite cell type which would only manifest following a switch. We consider two possibilities: coupled, contrasting fitness effects (ratcheting) or uncoupled, independent fitness effects (non-ratcheting). In the ratcheting case, a beneficial mutation in one cell type has deleterious pleiotropic effects in the opposite cell type (see Table 3).

Table 2.3: Fitness values after a beneficial mutation with ratcheting

current type	E_G	E_I	opposite type	E_G	E_I
I	1-c+$\frac{1}{5}$ Δs	1+Δs	G	1- Δs	1-c-Δs
G	1+Δs	1-c +$\frac{1}{5}$ Δs	I	1-c- Δs	1-Δs

Results: Ratcheting type 1

The first type of ratcheting is when the accumulation of fitness-affecting traits in the multi-cellular context, i.e. as a G cell, have corresponding negative consequences in the I cell form. Without ratcheting, as G cells improve in fitness in environment E_G there are no effects for

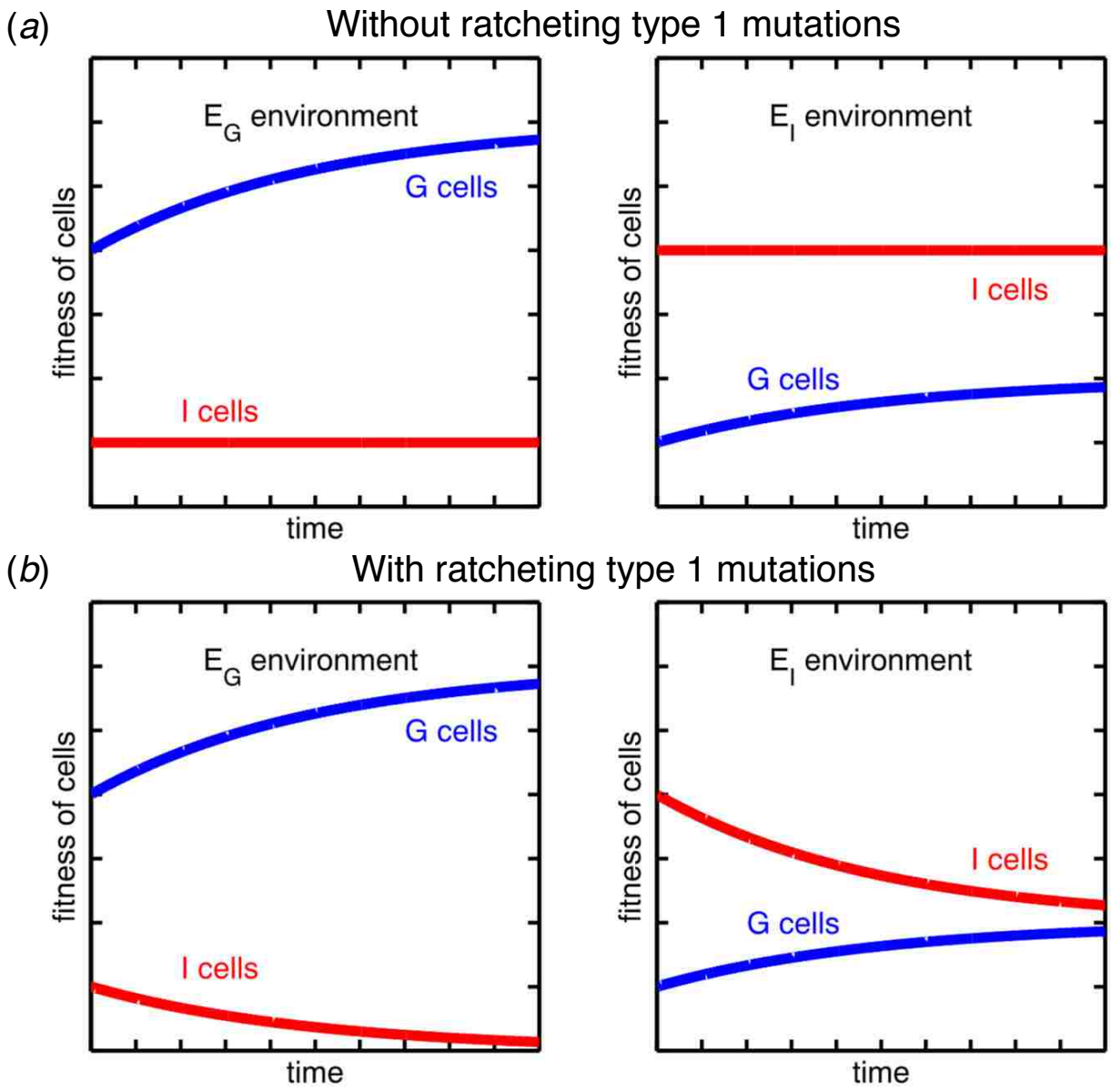

Figure 2.1: **Schematic showing the effects of evolution in an E_G environment on the fitness of I and G cells in environments E_G and E_I.** (a) Evolution of G cells in an E_G environment leads to increased fitness in both E_G and E_I environments, though the effect is smaller in E_I. These fitness changes have no consequences on the fitness of I cells in either environment. (b) The addition of ratcheting effects couples increases in G cell fitness with decreases in I cell fitness in both E_I and E_G. Ultimately, the effect is that the relative advantage of I cells (derived from G cells by mutation) in E_I is significantly decreased while the relative advantage of G cells in E_G is increased.

the I cells (see (a) in Figure 1). When compared to systems that evolve with ratcheting traits (see (b) in Figure 1), there are two key differences: 1. the selective benefit of being a G cell in an E_G environment increases and 2. the selective cost of being a G cell in an E_I environment decreases. As a result of the first effect, G cells progressively outcompete unicellular types driving them from the population. The second effect acts to stabilize the multicellular form because it reduces the fitness benefit of being unicellular in an E_I environment. Should the environment switch from an E_G state to an E_I state, it will take longer for unicellular I cells to overtake a population of multicellular G cells.

To observe the stabilizing effect of ratcheting traits, we simulated the evolution of populations grown in an E_G environment for different periods of time that were then switched to an E_I environment. We then determined the time it took for the I cell types to occupy 99% of the population (see Figure 2). The longer populations were exposed to the E_G environment, the more ratcheting traits they accumulated and the longer it took for I cells to reach numerical dominance. Populations that spent too little time in E_G did not accumulate enough ratcheting traits to stabilize the multicellular form. Since the strength of ratcheting depends on the remaining fitness gap between G and I cells in E_I, it depends on factors that influence this– such as the distribution of fitness effects for beneficial mutations and the initial fitness difference between types. If there is a larger initial gap in fitnesses between I and G cells and mutations tend to confer little advantage then it takes longer to reduce the fitness gap by a meaningful amount. In our model, if we increase the initial fitness difference from .1 to .5 then we find that the time frame and population size examined here are not enough to show a difference between evolution with and without ratcheting traits (data not shown). Inversely, an increase in the carrying capacity or the bottleneck size affords more opportunity to gain ratcheting mutations and have them fix in a population.

A more extreme form of ratcheting can occur if I cells lose fitness in E_I until G cells are fitter (see Figure 3). In this case, once a sufficient number of mutations have occurred there is no longer a selective advantage to producing I cells in any environment. Even if G cells

were to revert to unicellular I cells, they would be quickly outcompeted. While this type of ratcheting might seem unlikely, it may be quite common. For example, the evolution of mutualistic interdependence among cells, a common trait in complex multicellular organisms, may result in extremely steep costs of reversion in which single cells lack the capacity to survive autonomously.

Results: Ratcheting type 2

Another way that organisms can become ratcheted in a multicellular form is if the switch from G cells to I cells becomes less accessible by mutation, or if a switch is no longer possible. Such a decrease in switch rate could arise as a pleiotropic consequence of mutations that are adaptive in the multicellular context, analogous to the type 1 ratcheting case. Alternatively, when growing and evolving in an E_G environment (where G cells have a fitness advantage), it could be independently advantageous to lower the rate of switching back to I cells– assuming that this trait is evolvable. To demonstrate this latter possibility, we consider a simple model with discrete time steps (see Eqn 2.1). During each time step, G cells reproduce and with probability p produce I cells. Also during the time step, a smaller fraction of I cells reproduce– the c term is the reproductive cost for being an I cell in an E_G environment. For simplicity we do not permit I cells to switch back into G cells– this removes higher order terms that include the unlikely event that a cell switches between G and I forms upon every reproduction.

$$\begin{aligned} G_{t+1} &= G_t + (1-p)G_t \\ I_{t+1} &= I_t + (1-c)I_t + (p)G_t \end{aligned} \tag{2.1}$$

The total population of cells at time t can be solved analytically (see Eqn. 2.2).

$$I_t + G_t = (2-c)^t I_0 + \frac{p(2-c)^t - c(2-p)^t}{p-c} G_0 \tag{2.2}$$

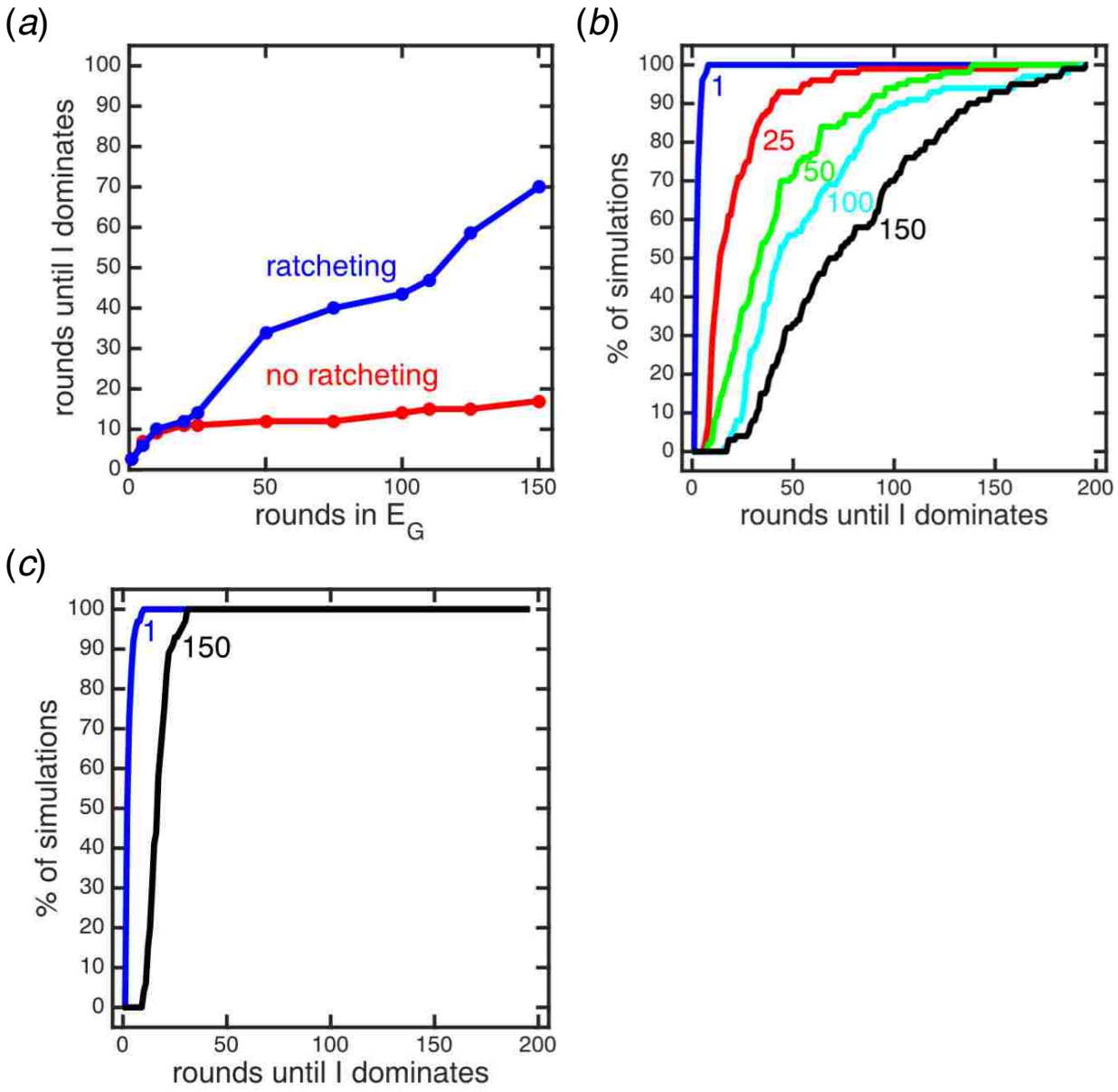

Figure 2.2: **Ratcheting type 1 increases the stability of multicellularity.** (a) The duration of G cells in an E_I environment is shown as a function of the duration of growth in the E_G environment. Each point is the median of 100 simulations. If type 1 ratcheting mutations do not occur (red) then the duration in E_G has only a small effect on the stability of multicellularity by removing all pre-existing I cells from the population. In contrast, if ratcheting type 1 mutations occur (blue) there is a much larger increase in the stability of the multicellular form. Increased duration of growth in E_G leads to increased accumulation of ratcheting traits and greater multicellular stability. (b) An empirical cumulative distribution function plot shows the effect of the duration of growth in E_G on the variation in the persistence of multicellularity when ratcheting mutations occur. Depending on the magnitude and number of ratcheting mutations that fix in the population, the stability of multicellularity can be 3-5 times greater than the median. (c) For comparison, a similar plot is shown when there are no ratcheting mutations.

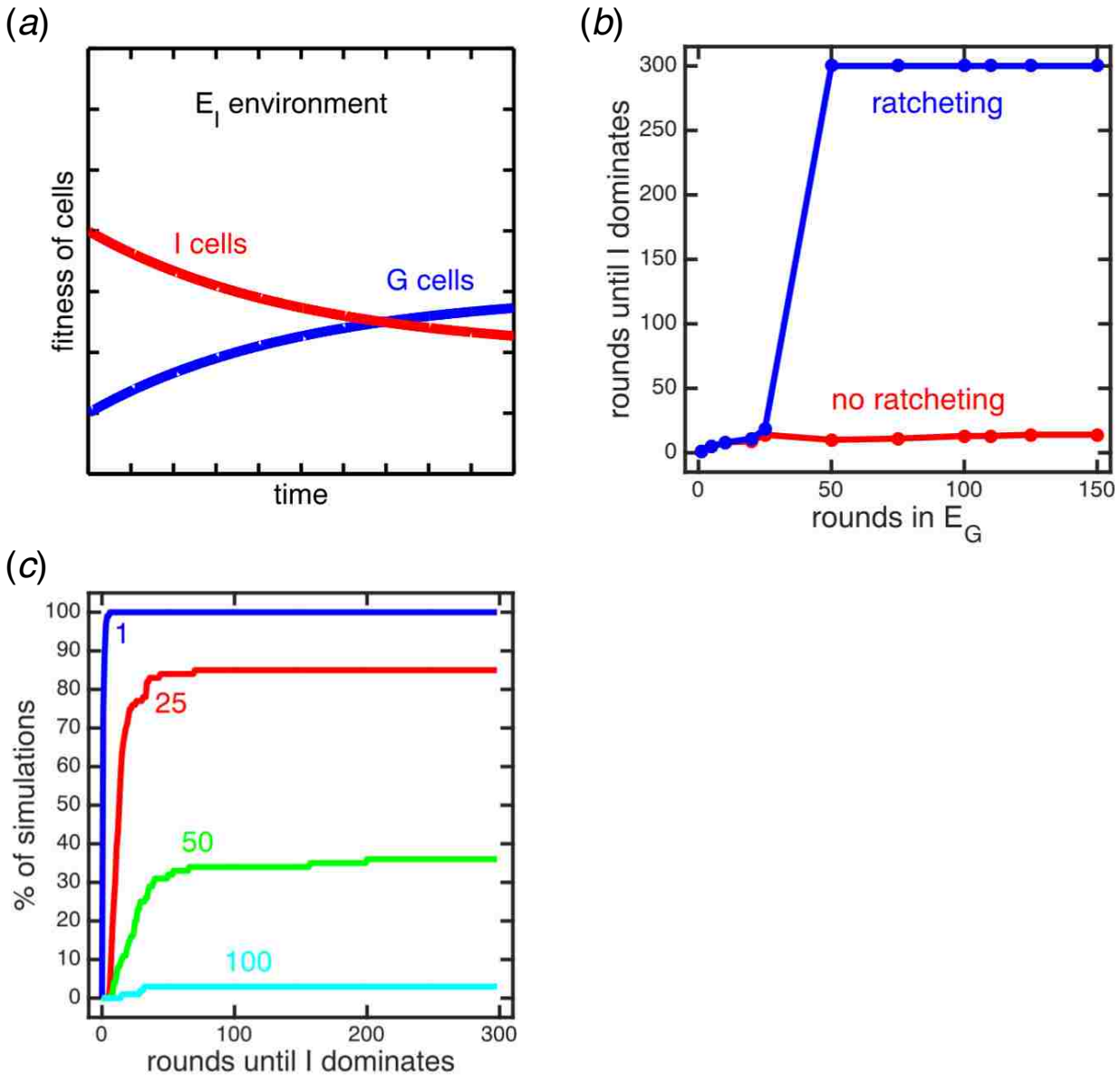

Figure 2.3: **The case when I cells become less fit than G cells in the E_I environment.** (a) As a result of G cells evolving in an E_G environment, the evolution of ratcheting traits drive the fitness of I cells in E_I below G cells. (b) The consequence of this is that once such mutations fix, there is no selective benefit for G cells to revert back to I cells even when grown in an E_I environment. The time it takes for I cells to occupy 99% of the population is shown by the blue curve. Each point is the median of 100 simulations. Simulations were run for only 300 rounds so a value of 300 means that G cells are still dominant for the entire duration of the simulation. For comparison, the red curve shows the case without type 1 ratcheting mutations. (c) An empirical cumulative distribution function plot shows the variation in the stability of multicellularity for different durations of growth in E_G. The value of each curve at 300 shows the percentage of simulations in which I cells eventually dominated the population. Those that do not reach 100 correspond to simulations in which G cells remained dominant.

Whenever $c > 0$, i.e. there is a cost to being an I cell and Eqn. 2.2 is a decreasing function over the range $p \in [0, 1]$. The rate of population growth is at a maximum when $p = 0$, i.e. when G cells stop switching to I cells (this is readily apparent for the extreme case of $c = 2$ where Eqn. 2.2 reduces to $I_t + G_t = 2(2-p)^{t-1}G_0$). Thus, with prolonged growth in the E_G environment, it is advantageous for multicellular cells to decrease the rate of switching to unicellular types. We can see this in our simulation model with prolonged growth in the E_G environment assuming cells can switch bidirectionally between G and I types. The average population switch rate from G to I (and vice versa) decreases with time when grown in the same environment (see Figure 4). Cells initially switch with probability $p = .1$ and evolve to switch a hundred fold less frequently, at $p = .001$. In theory populations could do better to switch less often than $p = .001$ but the relative benefit is much smaller compared to the difference between $p = .1$ and $p = .001$ and a population size of 10^5, i.e. the benefit of slower switching declines as p approaches 0.

Results: Combining types

Each type of ratcheting has particular conditions that make it more successful. The type 1 form of ratcheting relies on the accumulation of mutations that lower the fitness gap between G and I cells in the E_I environment. As a consequence, the effectiveness of this type of ratcheting depends on the distribution of mutations and the initial gap in fitnesses that must be overcome. If there is a small fitness gap and beneficial mutations are common then type 1 ratcheting can quickly decrease the benefit of being unicellular in the E_I environment. This, in turn, improves the evolutionary stability of the multicellular form should the environment switch from E_G to E_I. If, instead, there is a large fitness gap and beneficial mutations of sizable effect are rare then type 1 ratcheting may not be effective without prolonged time or opportunity to gain mutations in the E_G environment. While large fitness gaps between I and G cells may limit the effectiveness of type 1 ratcheting, they are conducive to type 2 ratcheting. A large fitness gap imposes a significant cost on producing the maladapted

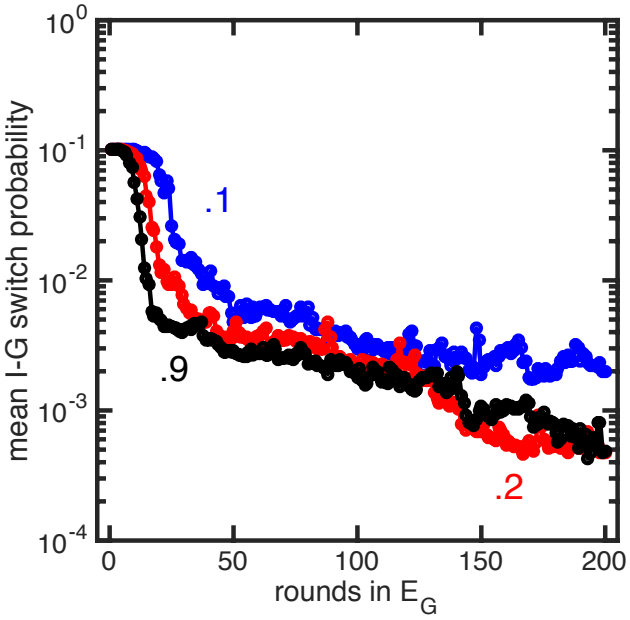

Figure 2.4: **Selection for lower probability of switching.** The probability of switching between I and G cells is shown as a function of the number of rounds grown in E_G. Each curve is the median of 10 evolved simulations and colors correspond to different c values– fitness differences between I and G cells– such that blue is $c = .1$, red is $c = .2$, and black is $c = .9$. All populations evolve lower probabilities of switching, starting at $p = 10^{-1}$ and evolving close to $p = 10^{-3}$ which is the same value as the probability that a mutation changes the probability of switching.

phenotypes in the wrong environment and can generate selection to reduce the switch rate. In contrast, smaller fitness gaps reduce the selective pressure– which is the opposite case for type 1 ratcheting. Thus, because the two types of ratcheting are suited to different conditions, we expect that in a single selective environment one type of ratcheting will be more effective and, therefore, more likely to occur than the other.

Although the types of ratcheting are better suited to different environmental conditions, there can be a synergistic effect such that one type of ratcheting changes the selective conditions to promote the other type of ratcheting. We consider a fluctuating environment that cycles between E_G and E_I after a fixed period of growth in each: n_g reproductive generations in E_G and n_i reproductive generations in E_I. Eqn. 2.3 shows the population dynamics for growth in both environments with fitness differences c_g and c_i between G and I cells $(c_g, c_i \geq 0)$ in E_G and E_I environmental states, respectively.

$$\begin{pmatrix} (1-c_i)(1-p)+1 & p \\ (1-c_i)p & 1+(1-p) \end{pmatrix}^{n_i} \begin{pmatrix} 1+(1-p) & (1-c_g)p \\ p & (1-c_g)(1-p)+1 \end{pmatrix}^{n_g} \begin{pmatrix} G_t \\ I_t \end{pmatrix} = \begin{pmatrix} G_{t+n_g+n_i} \\ I_{t+n_g+n_i} \end{pmatrix} \tag{2.3}$$

If the two periods are equal, $n_i = n_g$ and the benefit of being I in E_I is the same as being G in E_G $(c_g = c_i)$, then a non-zero, switch rate, p, maximizes growth of the collective I and G cells (see blue curve in Figure 5). The exact value of the optimal switch rate depends on the particular duration in each environmental state– the longer the duration the slower the switch rate that maximizes growth. When $n_i, n_g = 10$ there is selection for a high switch rate, close to $p \approx 0.2$, between I and G cells. In such a case, evolution of the switch rate would not generate type 2 ratcheting. If, however, a G cell were to gain a type 1 ratcheting mutation that creates an asymmetry in fitness such that $c_g > c_i$ then the benefit of being G in E_G would be greater than the benefit of being I in E_I. This fitness asymmetry creates selective pressure to lower the switch rate. Figure 5 shows that larger fitness asymmetries result in stronger selection against high rates of switching. Thus, the acquisition of type 1 ratcheting mutations can create the selective conditions that drive the evolution of type 2

ratcheting.

Alternatively type 2 ratcheting can increase the probability of gaining type 1 ratcheting mutations. A key factor for the effectiveness of type 1 ratcheting is the time it takes to gain a mutation that can decrease the fitness gap between G and I cells in E_I. Increasing the number of G cell reproductive events can improve the odds of finding such a mutation– especially if the fitness gap is large. To this end, type 2 ratcheting can help by decreasing the switch rate between G and I cells and thereby giving G cells more reproductive opportunities to obtain a useful type 1 ratcheting mutation. If the fitness gap to overcome is c then the chances of getting a beneficial mutation of c or higher within n reproductive events and a mutation rate of m is $1 - (1 - e^{\lambda c})^{nm}$, where λ is the rate parameter for the distribution of beneficial mutations. As the fitness gap increases, the usefulness of decreasing the switch rate, i.e. type 2 ratcheting, increases (see Figure 6). Indeed, type 2 ratcheting can improve the odds of finding a beneficial mutation to overcome $c = .5$ by a factor of 2.4 and $c = .75$ by a factor of 3.

Discussion

A confluence of evidence suggests that simple multicellularity is relatively easy to evolve, but it is also susceptible to loss due to reversion when environmental conditions change. The simple model presented here illustrates two possible solutions to the problem of reversion (referred to here as ratcheting type 1 and type 2). In ratcheting type 1, we explore the evolution of traits that increase fitness in the multicellular context and decrease fitness in the unicellular context. As expected, with more time spent in an environment that favors multicellularity (E_G) there is fixation of a greater number of ratcheting type 1 mutations. Accumulation of these mutations decreases the selective advantage of a multicellular (G) to unicellular (I) reversion mutation should the environment switch to favor unicellularity (E_I). This makes it more difficult for unicellularity to re-invade and increases the chances that the multicellular form can survive until the environment switches back to favor multicellularity

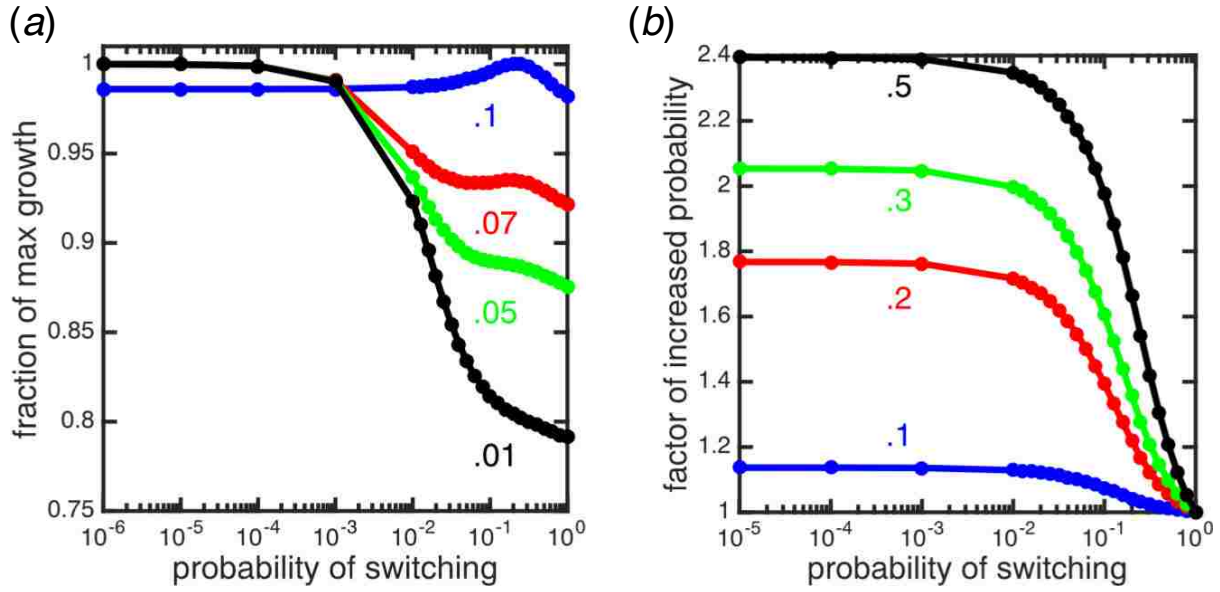

Figure 2.5: **Combining ratcheting types.** (a) Type 1 ratcheting can promote type 2 ratcheting. The fraction of maximal growth rate, as determined by the largest eigenvalues of Eqn. 2.3, is shown as a function of the switch rate p for different values of c_i (c_g is fixed at .1). The blue curve shows that when $c_g = c_i = .1$ the optimal switch rate is $p \approx 0.5$. When $c_g > c_i$, as a consequence of ratcheting type 1 mutations, then the optimal switch rate is $p < 10^{-6}$. The red ($c_i = .07$), green ($c_i = .05$), and black ($c_i = .01$) curves show that as the fitness asymmetry increases there is stronger selection against switching frequently. (b) Type 2 ratcheting can promote type 1 ratcheting. The probability of finding a beneficial mutation to overcome a fitness gap of c is shown as a function of the switch rate p for different values of c. Each curve represents a different fitness gap (blue is $c = .1$, red is $c = .2$, green is $c = .3$, and black is $c = .5$) and is scaled by the probability of finding a beneficial mutation when $p = 1$, i.e. the worst case scenario. Thus, the vertical axis shows the factor of improvement when switching is lowered from $p = 1$. The chance of finding a beneficial mutation to overcome c increases as the switch rate is lowered, which can result from type 2 ratcheting.

again. In ratcheting type 2, the reversion probability itself can evolve. With more time spent in the E_G environment, there is a selective benefit to decreasing the switch rate– reducing the likelihood of a a G to I reversion mutation. Although the conditions that select for each type of ratcheting are different, we found that one type of ratcheting can alter conditions to promote the other type of ratcheting and increase the stability of the multicellular state.

This work highlights the types of traits that stabilize a major evolutionary transition against reversion to a previous form/lower level. In the case of multicellularity, these traits increase fitness in the multicellular context and decrease it in the unicellular context. We speculate that traits with such an effect could be common during the early stages of a major transition because the only requirement is that they be disadvantageous outside of a multicellular context. A putative example of a trait with a ratcheting effect has been identified in a yeast model of multicellularity where selection for rapid settling in liquid media resulted in the evolution of multicellular clusters [32]. In independent replicate populations, researchers have repeatedly observed the evolution of elevated rates of apoptosis– a trait which is presumably maladaptive in the unicellular context. Mathematical modeling suggests that elevated rates of apoptosis may benefit cells in large multicellular clusters by decreasing cluster size [44]. Smaller clusters face less volumetric and nutrient flow limitations and allow populations to grow faster. In the volvocine green algae, a model system for the evolution of multicellularity with species that range from unicellular to large multicellular spherical colonies, it has been suggested that changes in the regulation of growth or in the number of successive (palintomic) cell divisions that cells undergo could be early targets for adaptation to a primitive multicellular life cycle [40, 45]. If the optimal regulation of these traits for small colonial forms differs from that of the unicellular form, these traits could also behave as evolutionary ratchets. However, the distribution of ratcheting mutations is an empirical question that can only be addressed with more data. Ideally, future experimental work could assess the fitness effects of candidate ratcheting traits by performing controlled pairwise competitions where the presence of the trait of interest is manipulated in both the

multicellular and unicellular context.

While ratcheting traits may act to stabilize some forms of multicellularity, there are other forms in which ratcheting traits would be detrimental. In this paper, we have been assuming that once organisms make the transition to multicellularity they no longer require a persistent unicellular form. Yet, some multicellular life cycles require alternation between unicellular and multicellular life stages [30]. For instance, the slime mold *Dictyostelium discoideum* regularly switches between free-living unicellular amoeba and multicellular slugs. The multicellular form acts as a type of stress response that is triggered when resources are depleted. It allows *D. discoideum* to find new environments with abundant resources. However, *D. discoideum* cannot reap any benefits without reverting back to the unicellular form because colonization only takes place as spores that generate free-living amoeba. As a consequence of this mutual reliance on types, ratcheting into either form would be detrimental to *D. discoideum* and other organisms that rely on plasticity. It is interesting to consider whether organisms that rely on plasticity to shift between uni- and multicellular forms have different evolutionary trajectories than those that break the plasticity to stabilize the multicellular state.

Discussions of a major transition in evolution are rarely without mention of a shift in the level of selection. Often times this distinction is made in terms of MLS1 and MLS2 theory [47]: with MLS1 being used to describe the early stages of the transition where the fitness of the group is a function of the fitness of its component parts and MLS2 applying to cases where group fitness can no longer be defined in terms of its component parts. The latter typically signifies that a successful transition has been made [48, 49] and that groups themselves now exist as Darwinian individuals (that is, they exhibit variation, heredity, and differences in reproductive success [50]). One aspect of our modeling approach that has interesting implications is that we did not explicitly model multicellular groups or their reproduction. As such, the fitness of groups only acts indirectly in our model via the fitness of G cells, without assigning G cells to particular multicellular groups. This suggests that

the stabilizing effects we observe due to the accumulation of ratcheting traits could apply during the early (MLS1) as well as the late (MLS2) stages of a major evolutionary transition. However, we do not provide a mechanistic explanation for how and why such traits would be favored by natural selection.

An important limitation to our modeling approach is the lack of specificity in considering the multicellular form. We adopted a general model in which unicellular I and multicellular G cells compete in the same niche and the success of multicellularity is defined by the fitness and frequency of G cells without regard to how they interact with the environment or each other. Yet, the benefits of multicellularity are often derived from the spatial structure of the multicellular group. For example, multicellular yeast are capable of growing at low density in media containing the sugar sucrose, which they break down extracellularly into monosaccharides (glucose and fructose) that can be easily imported into the cell. Without the benefit of group metabolism generating high concentrations of consumable sugars, solitary cells are unable to grow [19, 23]. Not only can the spatial structure imposed by a group of cells underlie the benefit of multicellularity, it can influence the evolution of novel traits [44, 19, 51] and may play a role in determining the likelihood of reversion. Structures that impose reproductive division of labor or physical barriers to cells abandoning groups may inhibit reversion and stabilize multicellularity. In contrast, more flexible spatial structures such as the wrinkly mats in the *P. fluorescens* experimental system permit frequent reversions to unicellularity [26, 27, 28]. Although the specific reasons that multicellular groups benefit in the E_G environment will depend on the details of the system under study, our models do not consider the causal link between multicellular form and fitness. Instead, we identify general conditions under which mutations limiting evolutionary reversion to unicellularity can evolve.

In this paper, we explore how adaptations that limit the potential effects of evolutionary reversion may stabilize nascent major evolutionary transitions. Using the evolution of multicellularity from unicellular ancestors as an example, we allowed for two types of mutations

to occur in our model: mutations that are beneficial in the multicellular context but deleterious in the unicellular context and mutations that affect the rate at which cells switch from the multicellular to the unicellular state. The evolution of these "ratcheting" traits may also play a key role in facilitating the evolution of increased complexity. By limiting the rate that unicellular revertants are produced (type 2) and the benefit of reversion (type 1), ratcheting mutations ensure that selection has sufficient time to act in the higher-level context, allowing lineages in the early stages of a major evolutionary transition opportunities to evolve increased complexity (i.e., functional integration, division of labor, etc.) via the gradual accumulation of novel traits that improve fitness in this higher-level context. By stabilizing the earliest steps in an evolutionary transition in individuality, ratcheting traits may provide a simple and robust stepping stone on the path towards increased biological complexity.

Data accessibility

Sample computer code is provided as supplementary material. Additional data and code are available upon request.

Competing interests

We have no competing interests.

Author contributions

EL, WR, PC, & BK conceived of the study and designed the research agenda. EL conducted the modeling and analyzed the data. All authors helped draft the manuscript and gave final approval for publication.

Acknowledgments

The authors thank Ricard Solé and Eörs Szathmáry for organizing the working group and theme issue on "The major synthetic evolutionary transitions".

Funding

This work was supported by NASA Exobiology Award #NNX15AR33G and the National Science Foundation under Cooperative Agreement Number DBI-0939454. PLC was supported by a National Science Foundation Graduate Research Fellowship under Grant Number DGE-1256082.

BIBLIOGRAPHY

[1] Buss LW. 1987 *The evolution of individuality.* Princeton, N.J. : Princeton University Press.

[2] Smith JM & Szathmary E. 1995 *The major transitions in evolution.* Oxford, UK: Oxford University Press.

[3] Michod RE & Roze D. 1999 Cooperation and conflict in the evolution of individuality. III. Transitions in the unit of fitness. In *Mathematical and Computational Biology: Computational Morphogenesis, Hierarchical Complexity, and Digital Evolution* (ed. CL Nehaniv (Ed.), pp. 47-92. Providence, Rhode Island: American Mathematical Society.

[4] Kirk DL. 2005 A twelve-step program for evolving multicellularity and a division of labor. *BioEssays* **27**, 299–310.

[5] Grosberg RK & Strathmann RR. 2007 The evolution of multicellularity: A minor major transition? *Annual Review of Ecology, Evolution, and Systematics* **38**, 621–654.

[6] Schirrmeister BE, Anisimova M, Antonelli A, & Bagheri HC. 2011 Evolution of cyanobacterial morphotypes: Taxa required for improved phylogenomic approaches. *Communicative & Integrative Biology* **4(4)**, 424–427.

[7] El Albani A, Bengtson S, Canfield D. E, Bekker A, Macchiarelli R, et al.. 2010 Large colonial organisms with coordinated growth in oxygenated environments 2.1 Gyr ago. *Nature* **466**: 100–104.

[8] Butterfield NJ. 2000 Bangiomorpha pubescens n. gen., n. sp.: implications for the evolution of sex, multicellularity, and the Mesoproterozoic/ Neoproterozoic radiation of eukaryotes. *Paleobiology* **26**: 386–404.

[9] King N. 2004 The unicellular ancestry of animal development. *Developmental cell* **7**: 313–325.

[10] Bonner JT. 1998 The origins of multicellularity. *Integrative Biology: Issues, News, and Reviews* **1**: 27–36.

[11] Herron MD, Hackett JD, Aylward FO & Michod RE. 2009 Triassic origin and early radiation of multicellular volvocine algae. *Proc Natl Acad Sci USA* **106**: 3254–3258.

[12] Galagan JE, Nusbaum C, Roy A, Endrizzi MG, Macdonald P, Fitzhugh W et al.. The genome of M. acetivorans reveals extensive metabolic and physiological diversity. Genome Res. 2002; 12:532-42.

[13] Bonner JT. 2001 *First Signals: The Evolution of Multicellular Development.* Princeton, N.J. : Princeton University Press.

[14] Stanley SM. 1973 An ecological theory for the sudden origin of multicellular life in the late Precambrian. *Proc Natl Acad Sci USA* **70**: 1486–1489.

[15] Kessin RH, Gundersen GG, Zaydfudim V, Grimson M. 1996 How cellular slime molds evade nematodes. *Proc Natl Acad Sci USA* **93**: 4857–4861.

[16] Boraas M, Seale D, Boxhorn J. 1998 Phagotrophy by a flagellate selects for colonial prey: a possible origin of multicellularity. *Evol Ecol* **12**: 153–164.

[17] Smukalla S, Caldara M, Pochet N, Beauvais A, Guadagnini S, Yan C, Vinces MD, Jansen A, Prevost MC, Latgé J-P, Fink GR, Foster KR & Verstrepen KJ. 2008 FLO1 Is a Variable Green Beard Gene that Drives Biofilm-like Cooperation in Budding Yeast. *Cell* **135**: 726–737.

[18] Pfeiffer T & Bonhoeffer S. 2003 An evolutionary scenario for the transition to undifferentiated multicellularity. *Proc Natl Acad Sci USA* **100**: 1095–1098.

[19] Koschwanez JH, Foster KR & Murray A. 2011 Sucrose Utilization in Budding Yeast as a Model for the Origin of Undifferentiated Multicellularity. *PLoS Biol* **9(8)**: e1001122.

[20] Biernaskie JM & West SA. 2015 Cooperation, clumping and the evolution of multicellularity. *Proc Biol Sci.* **282(1813)**: 20151075.

[21] Becks L, Ellner SP, Jones LE & Hairston Jr. NG. 2010. Reduction of adaptive genetic diversity radically alters eco-evolutionary community dynamics.*Ecol. Lett.* **13**: 989–997.

[22] Ratcliff WC, Denison RF, Borrello M & Travisano M. 2012 Experimental evolution of multicellularity *Proc Natl Acad Sci USA* **109**: 1595–1600.

[23] Koschwanez JH, Foster KR & Murray A. 2013 Improved use of a public good selects for the evolution of undifferentiated multicellularity. *eLife* **2**:e00367.

[24] Ratcliff WC, Herron M, Howell K, Pentz J, Rosenzweig F & Travisano M. 2013 Experimental evolution of an alternating uni- and multicellular life cycle in Chlamydomonas reinhardtii. *Nature Communications* **4**: 2742.

[25] Ratcliff WC, Fankhauser JF, Rogers D, Greig D & Travisano M. 2015 Origins of multicellular evolvability in snowflake yeast. *Nature Communications* **6**: 6102.

[26] Spiers AJ, Kahn SG, Bohannon J, Travisano M, Rainey PB. 2002 Adaptive divergence in experimental populations of Pseudomonas fluorescens. I. Genetic and phenotypic bases of wrinkly spreader fitness. *Genetics* **161(1)**:33–46.

[27] Rainey PB, Rainey K. 2003 Evolution of cooperation and conflict in experimental bacterial populations. *Nature* **425(4)**: 72–74.

[28] McDonald MJ, Gehrig SM, Meintjes PL, Zhang XX, Rainey PB. 2009 Adaptive divergence in experimental populations of Pseudomonas fluorescens. IV. Genetic constraints guide evolutionary trajectories in a parallel adaptive radiation. *Genetics* **183(3)**:1041–1053.

[29] Lavrentovich MO, Koschwanez JH, Nelson DR. 2013 Nutrient shielding in clusters of cells. *Phys Rev E Stat Nonlin Soft Matter Phys.* **87(6)**: 062703.

[30] Yokota K & Sterner RW. 2011. Trade-offs limiting the evolution of coloniality: ecological displacement rates used to measure small costs. *Proc. Biol. Sci.* **278**: 458–463.

[31] Simpson C. 2011. How many levels are there? How insights from evolutionary transitions in individuality help measure the hierarchical complexity of life. In, *The Major Transitions in Evolution Revisited*, Brett Calcott & Kim Sterelny eds. MIT Press.

[32] Michod RE. 1996 Cooperation and conflict in the evolution of individuality. II. Conflict mediation. *Proc Biol Sci.* **263(1372)**:813–22.

[33] Nunney L. 1999 Lineage selection and the evolution of multistage carcinogenesis. *Proc.R. Sci. London Ser B* **266**: 493–498.

[34] Kondrashov AS. 1994. Mutation load under vegetative reproduction and cytoplasmic inheritance *Genetics* **137**: 311–318.

[35] Grosberg RK & Strathmann RR. 1998 One cell, two cell, red cell, blue cell: the persistence of a unicellular stage in multicellular life histories. *Trends Ecol. Evol.* **13**: 112–116.

[36] Roze D & Michod RE. 2001 Mutation, multilevel selection, and the evolution of propagule size during the origin of multicellularity. *Am. Nat.* **158**: 638–654.

[37] Queller DC, Ponte E, Bozzaro S & Strassmann JE. 2003 Single gene greenbeard effects in the social amoeba Dictyostelium discoideum. *Science* **299**: 105–106.

[38] Khare A, Santorelli LA, Strassmann JE, Queller DC, Kuspa A & Shaulsky G. 2009 Cheater-resistance is not futile. *Nature* **461**: 980–982.

[39] Manhes P & Velicer GJ. 2011 Experimental evolution of selfish policing in social bacteria. *Proc. Natl Acad. Sci. USA* **108**: 8357–8362.

[40] Shelton DE & Michod RE. 2014 Group Selection and Group Adaptation During a Major Evolutionary Transition: Insights from the Evolution of Multicellularity in the Volvocine Algae. *Biological Theory* **9 (4)**:452–469.

[41] Libby E & Ratcliff WC. 2014 Ratcheting the evolution of multicellularity. *Science* **346(6208)**: 426–427.

[42] Gillespie DT (1977) Exact stochastic simulation of coupled chemical reactions. *J Phys Chem* **81**: 2340–2361.

[43] Gerrish PJ & Lenski RE. 1998 The fate of competing beneficial mutations in an asexual population. *Genetica* **102/103(0)**: 127–144.

[44] Libby E, Ratcliff WC, Travisano M & Kerr B. 2014 Geometry shapes evolution of early multicellularity. *PLoS Computational Biology* **10(9)**: e1003803, 1–12.

[45] Maliet O, Shelton DE, & Michod RE. 2015 A model for the origin of group reproduction during the evolutionary transition to multicellularity. *Biology Letters* **11**: 20150157.

[46] Libby E & Rainey PB. 2013 A conceptual framework for the evolutionary origins of multicellularity. *Phys Biol.* **10(3)**: 035001.

[47] Damuth J & Heisler IL. 1988 Alternative formulations of multilevel selection. *Biol. Philos.* **3**: 407–430.

[48] Okasha S. 2005 Multilevel Selection and the Major Transitions in Evolution. *Philosophy of Science* **72**: 1013–1025.

[49] Michod RE & Nedelcu AM. 2003 On the reorganization of fitness during evolutionary transitions in individuality. *Integr. Comp. Biol.* **43**: 64–73.

[50] Godfrey-Smith P. 2009 *Darwinian Populations and Natural Selection.* Oxford Univ. Press, New York.

[51] Conlin PL & Ratcliff WC. 2016 Trade-offs Drive the Evolution of Increased Complexity in Nascent Multicellular Digital Organisms. In, *Multicellularity: Origins and Evolution*, Karl Niklas & Stuart Newman eds. MIT Press.

Chapter 3

NASCENT LIFE CYCLES AND THE EMERGENCE OF HIGHER-LEVEL INDIVIDUALITY

William C. Ratcliff[1,*] Matthew Herron[1] Peter L. Conlin[2] Eric Libby[3]

[1]Department of Biology, Georgia Institute of Technology, Atlanta, GA 30332, United States of America

[2]Department of Biology and BEACON Center for the Study of Evolution in Action, University of Washington, Seattle, WA 98195, United States of America

[3]Santa Fe Institute, Santa Fe, NM 87501, United States of America

∗ **corresponding author, email: will.ratcliff@biology.gatech.edu**

Keywords: multicellularity | life cycles | major transition | evolution | ratcheting

Abstract

Evolutionary transitions in individuality (ETIs) occur when formerly autonomous organisms evolve to become parts of a new, 'higher-level' organism. One of the first major hurdles that must be overcome during an ETI is the emergence of Darwinian evolvability in the higher-level entity (e.g. a multicellular group), and the loss of Darwinian autonomy in the lower-level unit (e.g. individual cells). Here we examine how simple higher-level life cycles are a key innovation during an ETI, allowing this transfer of fitness to occur 'for free'. Specifically, we show how novel life cycles can arise and lead to the origin of higher-level individuals by i) mitigating conflicts between levels of selection, ii) engendering the expression of heritable higher-level traits, and iii) allowing selection to efficiently act on these emergent higher-level traits. Further, we compute how canonical early life cycles vary in their ability to fix beneficial mutations via mathematical modeling. Life cycles that lack a persistent lower-level stage and develop clonally are far more likely to fix 'ratcheting' mutations that limit evolutionary reversion to the pre-ETI state. By stabilizing the fragile first steps of an evolutionary transition in individuality, nascent higher-level life cycles may play a crucial role in the origin of complex life.

Introduction

Few biological phenomena have created more scope for evolutionary innovation than the creation of new 'levels of selection', and the resulting rise of new types of biological individuals. All known organisms that populate Earth today are the result of at least one such Evolutionary Transition in Individuality (ETI [1, 2]). Notable ETIs include the origin of membrane-bounded protocells encapsulating chemical replicators, the aggregation of genetic replicators into chromosomes, the domain-spanning symbiotic origins of eukaryotic cells, the origin of multicellular organisms from unicellular ancestors, and the evolution of colonial 'super-organisms' from solitary multicellular organisms [2]. Like layers to an onion, Earth's

organisms maintain the signature of their multi-level evolutionary history.

Despite the profound differences in these evolutionary transitions, they appear to proceed in an analogous manner. Extant individuals (e.g. single-celled organisms) first form a new unit of selection—this typically occurs through tight spatial coupling between cooperating individuals in a collective (e.g. a cluster of cells). Increased complexity subsequently arises as the result of adaptation taking place in collective-level traits, not in the traits of the lower-level individuals [2]. Such a shift in evolutionary process would appear to be susceptible to evolutionary conflict, with contrasting Darwinian dynamics playing out at the lower- and higher-levels. Indeed, lower-level units would appear to have numerous advantages, including a shorter generation time, a larger population size, and greater trait heritability. This rationale will sound familiar to many evolutionary biologists, as it forms the core of the argument made against group selection since the 1960s [3, 4].

Unfortunately for ETIs, it gets worse. Perhaps the largest obstacle they must overcome is an organizational asymmetry. Lower-level units tend to be fully-fledged organisms that have long been evolving as the primary unit of selection, gaining adaptations that enhance fitness at their organismal level. In fact, some philosophers consider this to be a defining feature of biological individuality [5, 6], though it is important to remember that not all traits that are beneficial at level X are the result of selection acting at level X [7]—they may have arisen through non-adaptive means. In the terminology of Godfrey-Smith, 'Darwinian individuals' are the members of populations that are capable of adaptive evolution, i.e. those that possess heritable variation in traits that affect fitness [5, 8]. Their long history as Darwinian individuals gives lower-level units ample opportunity to evolve traits that make them more effective Darwinian individuals (e.g. by increasing robustness [9, 10] and evolvability [11], or by mitigating conflicts between levels of selection [2, 12, 13]), while novel collectives have no such advantage. Thus, during an ETI, novel collectives face a daunting challenge: they must overcome these systemic biases in favor of lower-level adaptation in order for the higher-level unit to be the 'dominant' Darwinian individual. Interestingly, it appears very difficult to

fully remove the potential for Darwinian individuality from an entity that once had it: cells in multicellular organisms readily mutate and grow in an unchecked manner, causing cancer [14], non-functional mitochondria take over yeast cells when given the opportunity [15], and 'selfish' genetic elements reproduce at the rest of the genome's expense [16]. Still, in each case, the balance of selection, and corresponding adaptation, is clearly on the higher-level individual.

In this paper, we examine how nascent life cycles arise and drive the origin of new biological individuals. We examine how critical elements of the life cycle necessary to satisfy the Darwinian algorithm arise 'for free' as a side effect of physical interactions among particles within the collective. Specifically, we focus on how collectives gain the capacity to act as Darwinian individuals: that is, how heritable collective-level traits emerge from particle-level traits, and how key elements of the life cycle potentiate collective-level evolvability. We examine the role of life cycles in collective-level adaptation by modeling the spread of beneficial mutations across various life cycles. Finally, we examine how mutations that epistatically increase collective-level fitness while reducing the fitness of particles can de-Darwinize lower-level units, reinforcing the ETI. Taken together, we demonstrate that biological consortia readily form, grow, and reproduce in a manner that catalyzes the emergence of higher-level individuals, facilitate selection for beneficial mutations at this new biological level, and can fix mutations that stabilize the ETI by stripping lower level units of their evolutionary autonomy.

Life cycles

For conceptual and empirical simplicity, we will focus on the transition from uni- to multicellularity, but our arguments should apply to other ETIs that occur through an analogous process of multilevel selection (e.g. symbiosis or the evolution of super-organisms). Life cycles in well-established multicellular organisms (e.g. plants and animals) describe the process through which individuals grow and reproduce. Similarly, we may describe the process

through which any multicellular collective forms, grows and reproduces as its 'life cycle', even if the collective is not organismal (e.g. a bacterial biofilm).

One of the most important consequences of nascent life cycles is the extent to which they partition cellular variation among groups [17]. Life cycles that reduce within-group genetic diversity and increase between-group diversity help establish the collective as a Darwinian individual in a number of key ways (Box 1). While there are many routes through which microbial collectives form and reproduce, there are two key elements that affect within-group genetic diversity: 1) Is growth clonal, or do growing collectives merge or incorporate cells from other lineages? 2) How genetically diverse are propagules? The latter depends both on propagule size (smaller propagules are less diverse) [18] and on the physical structure of cells within collectives. Multicellular clusters that develop clonally via branching (such as filamentous bacteria or snowflake yeast) spatially partition genetic variation, so even multicellular propagules generated by fragmentation tend to have low genetic diversity [19].

Box 1. The importance of limiting within-collective variation.

"We designate something as an organism, not because it is n *steps up on the ladder of life, but because it is a consolidated unit of design, the focal point where lines of adaptation converge. It is where history has conspired to make between-unit selection efficacious and within-unit selection impotent."* -David Queller, 1997 [20]

Life cycles that strongly partition genetic variation (e.g. through clonal development and a unicellular bottleneck in ontogeny) help make among-collective selection efficacious through three key steps: 1) *Limiting the potential for evolutionary conflict between levels of selection.* Within-collective cellular evolution cannot occur if there are no heritable differences among those cells for selection to act on. 2) *Facilitating the emergence of heritable multicellular traits.* When the cells in a collective are genetically identical, selection

on multicellular traits may correspond directly with genes affecting those multicellular traits. Within-collective genetic diversity should lower the heritability of multicellular traits if the genetic composition of collectives changes across generations (the logic here is identical to why epistatic variation does not contribute to standard measures of narrow sense heritability). 3) *Increasing among-collective variation, accelerating collective-level adaptation.* As long as cellular genotypes produce heritable multicellular phenotypes, then the variance of collective-level traits in the population will be maximized when each group is formed by a single genotype. Applying Fisher's fundamental theorem [21], this accelerates collective-level adaptation. Taken together, life cycles that limit within-group genetic diversity should produce more effective Darwinian individuals.

Extant microbes display an extensive variety of nascent multicellular life cycles. While a comprehensive review is beyond the scope of this paper, we will examine several representative examples (Figure 1). Perhaps the most ubiquitous multicellular collectives formed by microbes are biofilms. There are many ways to form a biofilm [22, 23], but in general, they require the production of adhesive polymers. When biofilms grow by aggregation and reproduce via multicellular propagules (Figure 1), it is difficult for selection to act on biofilm-level traits, as this growth form leaves them susceptible to within-group genetic conflict and reduces the heritability of collective-level traits [19, 24]. One notable exception is that of *Pseudomonas fluorescens* 'wrinkly spreaders'. In free-swimming *Pseudomonas*, mutations cause the bacteria to begin producing a cell-cell adhesive [25]. This wrinkly spreader mutant then forms a multicellular mat at the air-water interface through clonal division, and produces unicellular propagules when mutations cease production of the cellular adhesive. In principle, this life cycle includes single-cell bottlenecks at each life stage transition (dictated by the mutational steps that alternate between unicellular and multicellular growth), and experimental work shows that it is capable of multicellular adaptation [26]. Although initially unstable, due to a reliance on *de novo* mutations to complete the multicellular life

cycle, the formation of such a 'proto-life cycle' may set the stage for developmental control which could arise via an epigenetic mechanism that enables switching between multicellular and unicellular states [26, 27, 28, 29, 30, 31].

Experimentally-evolved 'snowflake' yeast have an obligately multicellular life cycle, caused by a loss-of-function mutation at the gene *ACE2* [19]. As a result, daughter cells remain attached to mother cells after mitosis, forming a fractal-like branched growth form. Propagules are produced whenever a cell-cell connection is severed. Despite the rarity of unicellular propagules [32], the physical structure of snowflake yeast introduces regular genetic bottlenecks, as every cell in a propagule is clonally derived from the cell at its base (Figure 1) [19]. Simple multicellular traits, such as cluster size, are highly heritable ($H^2 = 0.84$) [19], and snowflake yeast readily respond to multicellular selection [32, 33].

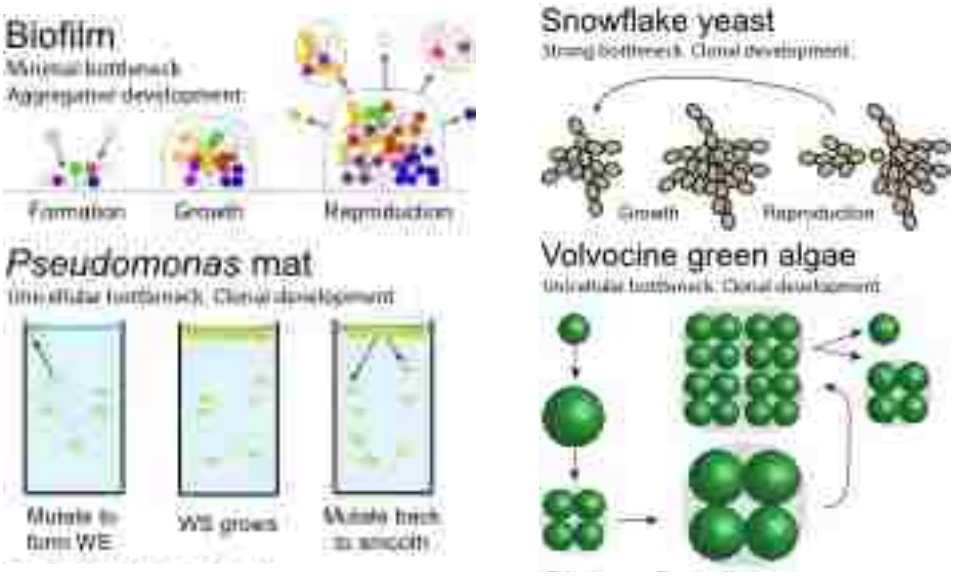

Figure 3.1: **Nascent microbial multicellular life cycles in extant microrganisms.**

The volvocine green algae and their unicellular relatives possess a cell cycle that has decoupled growth and reproduction. Individual cells grow, sometimes many times larger than their starting size, then rapidly divide to produce 2, 4, or 8 daughter cells [34]. In unicellular

Chlamydomonas, daughter cells can remain attached after division, forming multicellular palmelloids [35]. Regardless of whether these collectives disperse via unicells or small clusters of cells, each dispersing unit experiences a unicellular genetic bottleneck (Figure 1).

The transition to a multicellular life cycle in the volvocine algae appears to have occurred primarily through the co-option of existing genes rather than through the origin of *de novo* genes [36, 37]. Genomic comparisons among unicellular *C. reinhardtii*, undifferentiated *Gonium pectorale*, and germ/soma differentiated *V. carteri* show that few genes are uniquely shared between *G. pectorale* and *V. carteri*, i.e. that few genes are specific to the multicellular members of the clade [36]. Direct experimental evidence of the importance of co-option comes from a complementation experiment: replacement of the cell cycle regulator *mat3*, a retinoblastoma homolog, with the *G. pectorale* version of the gene causes *C. reinhardtii* to form colonies of 2–16 cells [36]. Thus a change to the coding sequence of a cell cycle regulator is sufficient to cause a shift to a multicellular life cycle.

Choanoflagellates are a group of unicellular and colony-forming aquatic eukaryotes. They have generated intense interest among evolutionary biologists because they are the closest known living unicellular relatives of animals [38]. Some species possess extensive developmental plasticity, switching between unicellular and multicellular growth ([39]). Multicellular rosettes typically develop from unicells via clonal reproduction [40], but these bottlenecks are not strict, as rosettes can generate additional rosettes via multicellular propagules [39].

While genetic conflict is rightfully seen as a major impediment to ETIs, the above examples demonstrate that diverse microbes readily form collectives with little within-group genetic diversity. In the case of small, relatively short-lived collectives such as these, clonal development and regular genetic bottlenecks should be sufficient to maintain this low diversity state, largely immunizing them from within-collective genetic conflict. Conflict, of course, is not the only issue ETIs face: in the next section, we examine how heritable multicellular traits emerge from the properties of cells.

Origin of higher-level traits: volvocine algae as a case study

Individuals have traits, and adaptive phenotypic change results from selection on those traits. The outcome of an ETI is a new kind of individual, which has traits that did not exist before the transition. Selection on these novel traits results in adaptations at the new, higher level, but where do the new traits come from?

A *Volvox* colony (or spheroid), for example, has a diameter, a behavioral response to light, and an anterior-posterior polarity. A *Volvox* cell, and for that matter a *Chlamydomonas* cell, has these traits as well, but in each case the colony-level trait is not the cell-level trait. In the most recent unicellular ancestor of *Volvox*, these traits were defined at the cell level, but in *Volvox* we can define them at both the cell level and the colony level. Somehow, during the transition from a unicellular to a multicellular life cycle, the colony-level traits came into existence. How did these new traits arise, and how are their values determined?

The initial transition to a multicellular life cycle necessarily begins with some mechanism of keeping (or bringing) cells together [41, 42]. In the volvocine algae, this was accomplished through modifications to the cell wall that resulted in the formation of an extracellular matrix [43, 44]. The resulting colonies may have been similar to those of the modern *Basichlamys* [45], in which four *Chlamydomonas*-like cells are held together by a common extracellular matrix.

By forming simple multicellular structures, the ancestors of *Basichlamys* acquired traits that are defined at the colony level, such as colony diameter and number of cells. In McShea's [46] terminology, they underwent an increase in hierarchical object complexity, adding an additional hierarchical level (the colony) while retaining all those nested within it (the cell and lower levels). The new, colony-level traits could conceivably affect fitness and vary in heritable ways, thus meeting Lewontin's criteria for adaptive evolution [8]. Colony diameter is meaningless in the context of unicells. Although unicells have a cell number, they have no heritable variation in cell number. The formation of multicellular structures automatically

generates new traits that are potentially capable of adaptive evolution.

In both cases, these traits are simple functions of cell-level traits. Colony cell number (N) is determined by the number of rounds of cell division (n) each cell undergoes to form a daughter colony: $N = 2^n$. The colony-level trait N potentially meets Lewontin's criteria for adaptive evolution, but it is completely and uniquely determined by the cell-level trait n. Genetic variation in n generates genetic variation in N, which is potentially subject to selection, for example if small N colonies reproduce more quickly than large N colonies.

Colony diameter (D) is also potentially subject to selection, for example, if a gape-limited predator preferentially consumes colonies smaller than a threshold diameter. For a spheroidal colony such as *Eudorina*, D is a function of n, cell volume (v), and the volume of extracellular matrix produced by each cell (e): $D = 2\sqrt[3]{\frac{n(v+e)}{4\pi}}$. Genetic variation in n, v, and/or e generates genetic variation in D. The colony-level trait D is completely determined by the cell-level traits, but different combinations of n, v, and e values can generate the same value of D.

Colony diameter and cell number are colony-level traits that come into existence as a necessary consequence of the transition to a multicellular life cycle. Although they are simple functions of cell-level traits, neither is defined at the cell level. Rather, they emerge from the properties of the cells. These colony-level traits have the potential to meet Lewontin's criteria for evolution by natural selection at the colony level, and we can expect that selection **on** the colony-level traits will drive adaptive change **in** the colony-level traits (provided there is genetic variation).

The functions relating colony diameter and cell number to cell-level traits are among the simplest such functions possible. We now consider a colony-level trait whose relationship to cell-level traits is more complicated and more difficult to define. In the volvocine family Volvocaceae, which includes *Volvox* and a number of smaller spheroidal genera, the process of embryogenesis includes a complete inversion of the developing daughter colony. After cell division, the flagella of the cells are oriented toward the inside of the colony, a situation not

conducive to efficient motility. Over the course of an hour or so, the embryos turn themselves inside-out, moving the flagella to the outside surface of the colony.

Although the details of the inversion process vary among Volvocaceaean species, the fundamentals are similar. Inversion involves a combination of changes in cell shape and movements of the cytoplasmic bridges that connect cells during embryogenesis [47]. Cells elongate to become spindle-shaped, and the cytoplasmic bridges migrate to the narrow ends of the cells, causing local changes in the curvature of the cell sheet. These changes propagate through the embryo in a spatially and temporally coordinated wave, eventually reversing the curvature of the entire cell sheet and inverting the embryo.

How this process is coordinated is not known; cells could be responding to mechanical signals (*e.g.* stresses from local curvature) [48] or to chemical signals transmitted through the cytoplasmic bridges. Regardless, inversion is driven by cell-level developmental processes, possibly influenced by plastic responses to local environmental cues. In principle, the colony-level process of inversion could be described as a function of cell-level traits, with arguments possibly including the degree of cell elongation, the number of cytoplasmic connections formed by each cell, and the shapes of reaction norms describing cellular responses to mechanical or chemical signals. The likely complexity of such a function does not change the fact that the colony-level process of inversion is entirely controlled by cell-level traits.

The analogous functions underlying many colony-level traits will be even more complex and even inscrutable. They may include signaling, positional information, feedbacks, and more complicated cell-cell interactions. However, their obscurity and complexity do not imply their nonexistence. Traits of multicellular organisms must emerge from the traits of their cells; there is no other source.

Heritability of higher-level traits

Predicting the magnitude of a response to selection requires estimates of both the strength of selection and the heritability of the trait under selection. This relationship is expressed

in the breeder's equation of quantitative genetics: $R = h^2S$, where R is the response to selection (the difference between mean trait value before and after selection), h^2 is the narrow-sense heritability, and S is the selection differential. Narrow-sense heritability is the ratio of additive genetic variance to total phenotypic variance [49], i.e. $Var(A)/Var(P)$. In addition to additive genetic variance, the denominator may include environmental effects and the effects of dominance, epistasis (interactions among genes), genotype by environment interactions, maternal effects, etc.

For asexual reproduction, the appropriate expression uses broad-sense heritability H^2, [49]: $R = H^2S$. Broad-sense heritability is the ratio of total genetic variance to total phenotypic variance: $Var(G)/Var(P)$. In this case genetic effects that are not additive (dominance, epistasis, etc.) are included in the numerator. Because these effects persist in subsequent generations in asexual reproduction, broad-sense heritability, rather than narrow-sense heritability, correctly predicts the response to selection in this case.

Both forms of the breeder's equation succinctly capture the basic insight that heritability is just as important as the strength of selection in predicting the magnitude of a response to selection. This is important for any process that involves multilevel selection. Regardless of the strength of selection on a collective-level trait, no adaptive response is possible unless there is heritable variation in the collective-level trait.

Since colony-level traits are functions of cell-level traits, the heritability of colony-level traits can, in principle, be related to that of cell-level traits. For complex functions, estimating this relationship may be intractable, but for simple functions it can be calculated. Herron and Ratcliff derived an analytical solution for the relationship between cell-level and collective-level heritability for traits for which the colony-level trait is a linear function of the cell-level traits [50]. Under reasonable assumptions, the heritability of a collective-level trait is never less than that of the cell-level trait to which it is linearly related. This asymmetry is driven by an advantage groups have over cells: emergent group-level traits depend on the sum of constituent cell phenotypes, which cancels out (by averaging) much of the

heritability-lowering effects of cellular phenotypic noise. For more complicated functions relating cell-level to colony-level traits, collective-level heritability is higher under most (but not all) conditions [50].

A crucial assumption underlying these models is that the development of collectives is clonal, i.e. that particles reproduce asexually within a collective. This roughly corresponds to Queller's 'fraternal' major transitions (Tarnita's 'staying together'), in which collectives consist of genetically similar (or identical) particles [20, 42, 51], and it characterizes most multicellular organisms. Land plants, animals, multicellular fungi, red algae, Ulvophyte and Chlorophyte green algae, and brown algae develop clonally.

Clonal development ensures that within-collective genetic variability is low; the only source of such variability is *de novo* mutations during development. For a particular trait, especially for small collectives (as are likely early in a transition), it will usually be zero. Nevertheless, phenotypic variability among particles within a collective is inevitable, as stochastic and micro-environmental effects will influence particle phenotypes (both sources of non-genetic variation are treated as 'environmental' components in quantitative genetics models). As long as phenotypic variability is randomly distributed around the genetic mean, though, collectives benefit from an averaging effect, which reduces their non-heritable phenotypic variation relative to the particles that comprise them [50].

Although collective-level heritability has sometimes been considered a hurdle that must be overcome during an ETI [1, 52], these results show that it comes 'for free' when development is clonal [50]. Heritability of collective-level traits does not have to 'arise' during the transition to a multicellular life cycle (given clonal development)—it must necessarily exist if the underlying cell-level traits are heritable. This is likely true for other 'fraternal' transitions as well.

Next, we quantitatively examine how nascent multicellular life cycles affect the ability for evolutionary innovation. Specifically, we examine the spread of beneficial mutations across three canonical simple multicellular life cycles and consider the implications of key

differences.

The spread of a beneficial mutation across different life cycles

The structure of a life cycle may affect its capacity to harness beneficial mutations. To explore this idea we introduce a modeling framework that enables direct comparison of the fixation dynamics of beneficial mutations within different nascent multicellular life cycles (see Figure 3.2). In each life cycle, we assume that a mutation arises in a single group during the group stage of a multicellular life cycle. For life cycles that alternate between group and single cell stages, we assume that the mutation occurs right at the end of the group stage so that it begins at some low frequency x_0 within the single cell population. For the life cycle that forgoes a unicellular stage, we assume that, for comparison, the mutation occurs in a group of size N at relative frequency x_0. In each case, we compute the relative frequency of the mutation in the group's lineage over the course of many life cycles.

The beneficial aspect of a mutation can potentially occur at two levels: cell and group. At the cell level, a beneficial mutation may increase the frequency of the mutant in a population of single cells or within the group depending on the structure of the life cycle. At the group level, the mutation may improve the ability for the group to leave offspring. To explore these different aspects and potential interactions between them, we use two parameters: s_c and s_g that correspond to the fitness benefit conferred to cells and groups. In the following sections we determine how a beneficial mutation spreads in three canonical multicellular life cycles.

Model: Aggregative life cycle

To compute the spreading dynamics of a beneficial mutation in the aggregative life cycle, we split the life cycle into three phases: 1) growth as single cells, 2) formation of aggregates, and 3) survival of aggregates followed by the release of single cells.

During the unicellular phase, cells reproduce, causing the population to expand. We

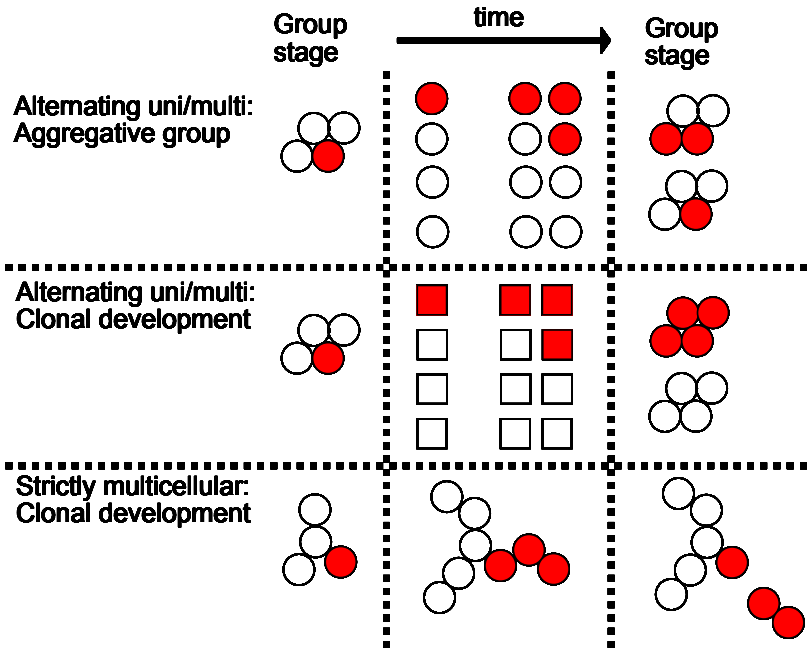

Figure 3.2: **Schematics of canonical early microbial multicellular life cycles.** We depict three multicellular life cycles in which groups of cells replicate. The top two life cycles alternate between unicellular and multicellular stages. The primary difference between them is how they form groups. In the aggregative group life cycle, cells form groups through random binding similar to flocculating yeast. The groups eventually dissociate, releasing cells so as return to the unicellular phase. In the clonal development alternating life cycle, groups are formed from single cells, similar to the formation of wrinkly mats by smooth cells in the *Pseudomonas fluorescens* experimental system [25]. Groups release single cells, usually through a phenotypic switch, indicated by the box and circle shaped cells. Finally, there is the strictly multicellular life cycle in which there is no unicellular phase. Cells reproduce within groups and groups eventually split into smaller groups, similar to snowflake yeast [32].

assume that if there is a benefit during this phase, i.e. $s_c > 0$, then the relative frequency of the mutants should increase in the population. So if the mutants start at a certain proportion, x_0, in the population then they will increase to x_1 by the end of this first phase where $x_1 > x_0$. The new proportion will depend on many factors including x_0, s_c, and the population growth structure. For simplicity, we assume that the new proportion x_1 is a simple function of x_0 and s_c, called $f_c(x_0, s_c)$, where $f_c(x_0, s_c) = (1 + s_c)x_0/(1 + s_c x_0)$. This form of $f_c(x_0, s_c)$ follows from a simple model of an exponentially growing population; Eqn.3.1 shows the derivation of $f_c(x, s_c)$ where λ is the growth rate of non-mutant single cells and we assume that $e^{s_c t} = (1 + s_c)$. We use the assumption that $e^{s_c t} = (1 + s_c)$ so that the relative frequency of the mutant compared to the non-mutants increases by $1 + s_c$. Choosing this time enables us to more easily compare between s_c and s_g. We could choose a different time but would then need to rescale s_g so that their effects would be comparable.

$$\frac{x_0 e^{(\lambda+s_c)t}}{x_0 e^{(\lambda+s_c)t} + (1 - x_0)e^{\lambda t}} = \frac{x_0 e^{s_c t}}{x_0 e^{s_c t} + (1 - x_0)} = \frac{x_0(1 + s_c)}{x_0(1 + s_c) + (1 - x_0)} = \frac{(1 + s_c)x_0}{(1 + s_c x_0)} \qquad (3.1)$$

After the single cell growth phase, there is an aggregation phase. We assume that cells randomly aggregate to form groups of size N. If we assume that the populations of mutants and non-mutants are very large, then the binomial distribution approximates the distribution of aggregates with different proportions of mutants. Thus, a group with proportion $x = i/N$ of mutants has probability $\binom{N}{i} x_1^i (1 - x_1)^{N-i}$ of forming, which we denote as $p(x; N, x_1)$ for $x \in [0/N, 1/N, \ldots, N/N]$ and 0 otherwise.

In the last phase, aggregates compete for survival so as to release single cells and complete the life cycle. For simplicity, we assume that cells do not reproduce while in the aggregate phase. If the mutation confers a fitness benefit to the group, i.e. $s_g > 0$, then this benefit increases the ability of the group to release single cells, either via increased fecundity or increased survival. We do not need to specify the precise mechanism by which the mutation confers a benefit. Instead, we only need a measure of fitness that can be used to translate the distribution of groups with different proportions of mutants $p(x; N, x_1)$ into a scalar

corresponding to the population proportion of single-celled mutants, x_0. To this end, we define a group fitness function $f_g(x)$ that assumes the fitness of groups only depends on the frequency of the mutant within the group and groups with higher proportions of mutants are fitter. We assign a group that only contains mutants, $x = 1$, with fitness $f_g(1) = 1 + s_g$ while a group that has no mutants, $x = 0$, with fitness $f_g(0) = 1$. For intermediate proportions we consider a simple linear fitness function: $f_g(x) = 1 + s_g x$. The new population proportion of the mutant following this final phase is simply: $\frac{\int_0^1 x f_g(x) p(x;N,x_1)\partial x}{\int_0^1 f_g(x) p(x;N,x_1)\partial x}$ where the denominator is a normalization term.

Eqn. 3.2 shows the combined effect on the population proportion of the mutant ($x_0 \rightarrow x_0'$) after the three phases of the life cycle.

$$x_0' = \frac{\int_0^1 x f_g(x) p(x; N, f_c(x_0, s_c))\partial x}{\int_0^1 f_g(x) p(x; N, f_c(x_0, s_c))\partial x} \tag{3.2}$$

Model: Alternating life cycle (clonal development)

We can determine the spreading dynamics of a beneficial mutation in the alternating life cycle with clonal development by using a similar approach as before with the aggregative life cycle. Again, we split the life cycle into three phases: 1) growth as single cells, 2) formation of groups, and 3) survival of groups so as to release single cells. The approaches for phases 1 and 3 are the same as with the aggregative life style. The main difference is in the second phase where groups are formed.

In the aggregative life cycle, groups form randomly such that different types of chimeras are possible. In the case with clonal development, all groups grow from a single cell. This means that there are no chimeric groups and there are only two possibilities: groups with $x = 0$ and groups with $x = 1$. The proportion of groups with $x = 1$ and $x = 0$ is the same as the proportion of mutant and non-mutant cells in the population, respectively. As before, we use the function p to characterize the distribution of groups. We omit the parameter N

for group size since it has no effect in the context of this life cycle. The result is $p(x; x_1)$ where $p(1; x_1) = x_1$, $p(0; x_1) = 1 - x_1$, and $p(x; x_1) = 0$ for $0 < x < 1$. We note that although there is growth during the group stage we assume that the function f_g, as described in the aggregative life cycle, adequately encapsulates the combined process of growth in the group stage and selection on groups in the alternating life cycle with clonal development.

Model: Strictly multicellular life cycle

In the strictly multicellular life cycle there is no unicellular phase. Instead groups of cells grow and reproduce via fission. Nonetheless, we can adopt a similar approach to that used to model the two alternating life cycles. Again, we break the life cycle into three phases analogous to the other life cycles: 1. growth within the group, 2. group fission, and 3. group survival.

In the previous life cycles, we were able to model the spreading dynamics of a beneficial mutation via x_0, the proportion of mutants in the general population. However, in the strictly multicellular life cycle cells are always members of groups and their distribution across groups may be important to the spreading dynamics. Thus, we use $P(x)$ to track the relative frequency of groups with different proportions of mutants, e.g. $P(0)$ is the proportion of groups with no mutants. If the groups are the same size then we can relate the proportion of mutants across all cells to the distribution across groups through $x_0 = \int_0^1 xP(x)\partial x$.

The actual structure of the group plays a key role in determining the spread of a beneficial mutation in the same way that population structure does in the other models. It is outside the scope of this paper, however, to consider the gamut of group morphologies. So for simplicity, we will only consider the simplest (and one of the earliest-evolving, within the cyanobacteria) life cycles: a linear cellular filament. Cells are each connected in linear chains and all cells can reproduce. Eventually filaments fragment into smaller filaments and thereby complete the life cycle (see Figure 3.3). For simplicity, we assume that a beneficial mutation occurs at a terminal cell in a group of size N. As a consequence, all new mutant cells will be

connected to each other and only the original mutant will be connected to a wild type cell.

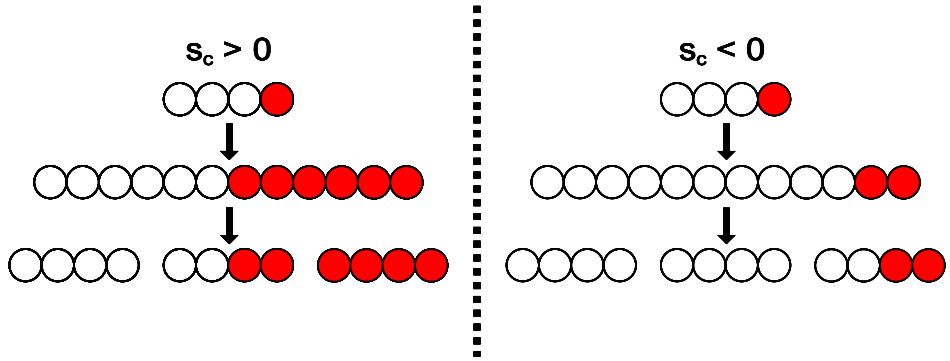

Figure 3.3: **Filament reproduction.** Filaments reproduce through binary fission. The mutant (red) increases in relative frequency within the filament when $s_c > 0$ and decreases when $s_c < 0$. In either case, because the mutant increases in absolute numbers this can lead to offspring filaments with high proportions of mutants.

The manner in which cells grow within the filament makes it difficult to apply both the same form of $f_c(x, s_c)$ from Eqn.3.1 and its underlying theoretical framework. Since mutant and non-mutant cells reproduce at different rates, if all groups reproduce via fission after some fixed time then the filaments will be of different lengths. Moreover, depending on the choices for parameters, the length of one type of filament (either mutant or non-mutant) would perpetually increase or decrease. To circumvent this issue, we consider two cases: one that uses the same form as $f_c(x, s_c)$ as in the other models and one that uses the same underlying theoretical model. For the first case, we assume that the fragments all grow to reach the same size prior to fragmentation, at which point they all reproduce simultaneously. During the growth phase of the filaments, the proportion of mutants in a group increases according to $f_c(x, s_c)$ from Eqn.3.1. While this model is directly comparable to the other life cycles, it invokes a mechanism other than simple exponential growth. For the second case, we assume that the cells are all growing exponentially and filaments reproduce whenever they reach a size N—this will occur at different times for mutant and non-mutant filaments.

The different time scales for the life cycles of non-mutants and mutants means that group reproduction will not be synchronous and so the methodology must be modified. As a result the spreading dynamics are not directly comparable to the two alternating life cycles. The mutation can still fix in the population even when $s_c < 0$ but the analysis is more involved and thus considered in the Supplementary material.

Following growth within filaments, there is a second phase of the life cycle in which groups reproduce through fission. We assume that the filament breaks evenly such that all new filaments are the same size. So if the filament splits into k smaller filaments, then every $1/k^{\text{th}}$ segment of the large filament is a group offspring. This process results in three possible types of offspring depending on the proportions and the number of offspring: homogeneous with all non-mutant cells, homogeneous with all mutant cells, and one possible heterogeneous filament. If the mutant makes up proportion x_1 of a large filament then the number of homogeneous mutant offspring filaments are $\lfloor kx_1 \rfloor$ (or `floor(`kx_1`)`, which returns the largest preceding integer to kx_1). Similarly the number of homogeneous non-mutant filaments is $\lfloor k(1-x_1) \rfloor$. If x_1 cannot be divided evenly by $1/k$ then there is a heterogeneous filament that contains proportion $(kx_1 - \lfloor kx_1 \rfloor)/(kx_1 - \lfloor kx_1 \rfloor + k(1-x_1) - \lfloor k(1-x_1) \rfloor)$ which we label $\hat{x}_{x_1}$. We define a distribution function $p_G(x; x_1, k)$ that describes the fraction of group offspring with mutant proportion x produced by a group with mutant proportion x_1. Eqn. 3.3 shows the possible values of $p_G(x; x_1, k)$. We use a subscript G to denote that this p function is different in character from the previous ones. Here, p_G describes the distribution of types of groups following fission from a single type of group, while the previous p functions described the distribution of types of groups in the population.

$$p_G(x; x_1, k) \begin{cases} \lfloor kx_1 \rfloor / k, & \text{for } x = 1 \\ \lfloor k(1-x_1) \rfloor / k, & \text{for } x = 0 \\ 1/k, & \text{for } x = \hat{x_{x_1}} \\ 0, & \text{otherwise} \end{cases} \tag{3.3}$$

The third and last phase of the life cycle has groups with different distributions of mutants competing for survival and reproduction. We can apply the same functional form, $f_g(x)$, as used earlier in the other life cycles. The effect of the life cycle on the distribution of groups is shown in Eqn. 3.4. The primary difference in form from Eqn. 3.2 is a consequence of the shift in focus from x_0 to $P(x)$.

$$\begin{aligned} P'(x) &= \frac{\int_0^1 f_g(x) p_G(x; f_c(\widetilde{x}, s_c), k)) P(\widetilde{x}) \partial \widetilde{x}}{\int_0^1 \int_0^1 f_g(x) p_G(x; f_c(\widetilde{x}, s_c), k)) P(\widetilde{x}) \partial \widetilde{x} \partial x} \\ x'_0 &= \frac{\int_0^1 x \int_0^1 f_g(x) p_G(x; f_c(\widetilde{x}, s_c), k)) P(\widetilde{x}) \partial \widetilde{x} \partial x}{\int_0^1 \int_0^1 f_g(x) p_G(x; f_c(\widetilde{x}, s_c), k)) P(\widetilde{x}) \partial \widetilde{x} \partial x} \end{aligned} \tag{3.4}$$

Comparison of spreading dynamics

With our modeling framework, we can now directly compare the spread of mutations in different life cycles. Figure 3.4 shows the spreading dynamics for mutations with different values of $s_c, s_g > 0$ (see Figure S3 for a broader set of parameter sweeps). In all cases, the mutation spreads the fastest in the alternating life cycle with clonal development. Between the other two life cycles, the mutation spreads faster in the aggregative life cycle in 3 of the 4 cases corresponding to $s_c \geq s_g$. One reason the mutation spreads slowest in the strictly multicellular life cycle is the manner of the s_c fitness benefit. The s_c benefit manifests such that the mutant has a competitive advantage to the wild type. This is important in life cycles with a unicellular phase because the different cell types are in direct competition as single cells. In the strictly multicellular life cycle, the cell types are only in direct competition within heterogeneous groups. Since heterogeneous groups (filaments) make up a small proportion of the population, the s_c advantage is effectively masked. Interestingly, the heterogeneity of groups explains why the mutation spreads slower in the aggregative life cycle than the alternating clonal life cycle. The heterogeneity of aggregative groups dilutes the s_g benefit of the mutation and inhibits its spread.

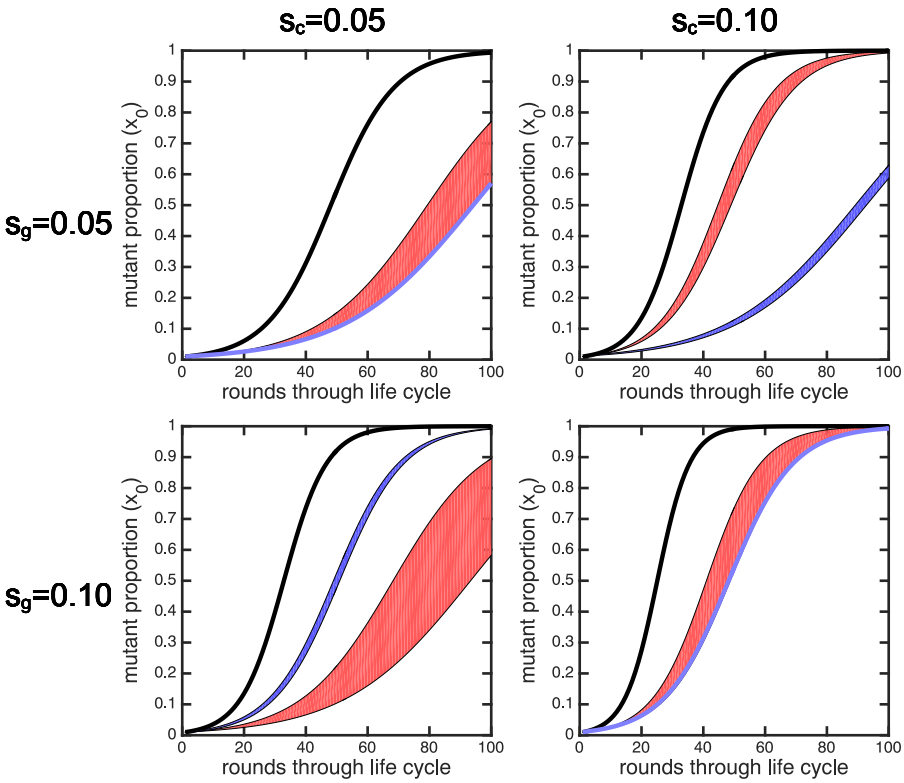

Figure 3.4: **Spreading dynamics of mutations beneficial to both cells and groups in different life cycles.** The plots show the proportion of the mutation in a population as a function of the number of rounds through different life cycles for different values of $s_c > 0$ and $s_g > 0$. The aggregative life cycles are shown in the red area (spanning $N = 5$ to $N = 100$), the alternating clonal life cycle is in black, and the strictly multicellular life cycles are in the blue area (spanning $k = 2$ to $k = 50$). In all cases the mutation spreads fastest in the alternating clonal life cycle. When $s_g \leq s_c$ the mutation spreads faster in the aggregative life cycle than the strictly multicellular life cycle.

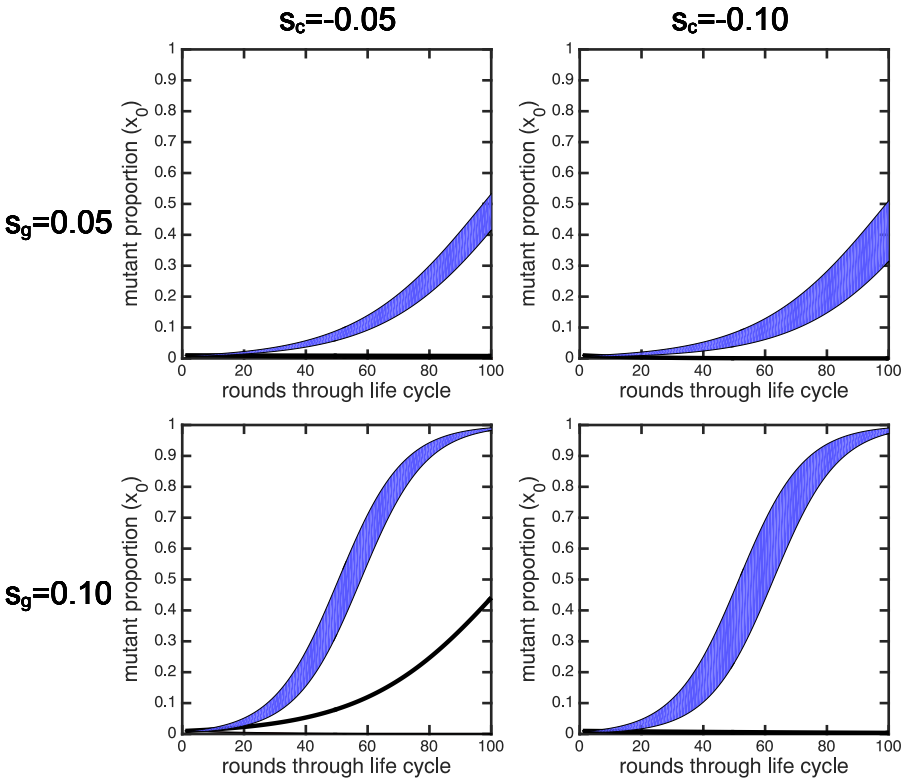

Figure 3.5: **Spreading dynamics of mutations beneficial for groups but deleterious for cells in different life cycles.** The plots show the proportion of the mutation in a population as a function of the number of rounds through different life cycles for different values of $s_c < 0$ and $s_g > 0$. The coloring is the same as in Fig. 3.4. In all cases the mutation spreads fastest in the strictly multicellular life cycle. It does not spread in the aggregative life cycle and only spreads in the alternating clonal life cycle when $s_g > -s_c$.

If we compare the spread of a mutation that has opposite group-level and cell-level effects, i.e. $s_g > 0, s_c < 0$, then we find different spreading dynamics. These mutations spread fastest in the strictly multicellular life cycle (Figure 3.5; see Figure S4 for a broader set of parameter sweeps). This is a result of the same phenomenon that made $s_c > 0$ mutations spread more slowly: this life cycle is shielded from the effects of cell-level fitness, which in this case is negative. As a result, mutations that improve group-level fitness can spread even when they are costly to the fitness of individuals cells. This mutation is generally prevented from spreading when the life cycle includes a unicellular stage: it never spreads in the aggregative life cycle and did so only in the clonal life cycle when $s_g > -s_c$, $s_g > 0$. While the $s_g > -s_c$ mutation should confer a net benefit, selection could only act on it in the clonal life cycle where group-level fitness benefits were not shared with non-mutant competitors cells.

The evolutionary stability of multicellularity

Mutations where $s_c < 0$ and $s_g > 0$ are of particular interest because they may act to increase the stability of the multicellular collective and facilitate the evolution of increased multicellular complexity [53, 54]. The reason for this can be seen by imagining the fitness effect of such a mutation if that genotype were to revert to a purely unicellular lifestyle (this is similar to the 'counterfactual fitness' approach developed by Shelton and Michod [53]). With the group context eliminated, competition occurs in a way analogous to phase 1 of the aggregative life cycle with a global population of cells multiplying according to Eqn.1. In such a scenario, the beneficial effects of s_g never manifest and mutant cells with $s_c < 0$ would be expected to be driven extinct. This differs from the case of uniformly beneficial mutations (where $s_c, s_g > 0$) because even if a genotype were to revert back to unicellularity it would have fitness higher than its ancestor.

Libby et al. (2016) previously studied the effect of mutations that are beneficial in the multicellular context but deleterious in the unicellular context, which they referred to as "ratcheting" mutations, in populations of genotypes that could switch between unicellular

and multicellular states [55]. They found that longer periods of time spent in an environment favoring multicellularity led to the fixation of more ratcheting mutations; this made it more difficult for groups to revert to unicellularity even when environmental conditions favored single cells. Furthermore, the fixation of ratcheting mutations was shown to favor lower rates of switching between multicellular and unicellular states. Which suggests that ratcheting mutations can promote further commitment to the multicellular lifestyle. However, this study did not consider alternating multicellular life cycles, and the deleterious consequences of the ratcheting mutations did not manifest unless a mutation caused reversion back to unicellularity.

Here we find that the spreading dynamics of ratcheting mutations ($s_c < 0$ and $s_g > 0$) vary dramatically depending on the details of the multicellular life cycle. Strictly multicellular life cycles are able to fix ratcheting mutations for some value of k under all conditions tested in which $s_g > 0$ (Figures S2 and S4). Alternating clonal life cycles can also fix ratcheting mutations, but only under restrictive conditions (where $s_g > -s_c$ and $s_g > 0$). Clonality appears to be essential for the spread of ratcheting mutations, as we did not observe their spread in the aggregative life cycle under any of the conditions tested. However, we note the possibility that mutations exhibiting magnitude epistasis (where $s_c, s_g \geq 0$ and $s_g >> s_c$) could also behave in a ratchet-like manner, although this would not result in cells that are maladapted in the unicellular phase. Collectively, our modeling suggests that ratcheting mutations fix most easily in clonally-developing life cycles that do not exhibit a persistent unicellular phase, which is consistent with the observation that all lineages that have evolved complex multicellularity (e.g. metazoans, plants, brown algae, and large multicellular fungi) possess this life cycle [62].

Summary / concluding remarks

One of the most astonishing facts about life on Earth is the remarkable fluidity of biological individuality: life, since its inception more than 3.5 billion years ago, has experimented

endlessly with novel collaborations, some of which have resulted in new kinds of organism and paved the way for transformative adaptive radiations. These Evolutionary Transitions in Individuality (ETIs) have been surprisingly common, occurring repeatedly in diverse lineages [2]. In this paper, we examine how simple, emergent life cycles can provide a critical scaffold supporting an ETI during its fragile beginning.

At least in principle, ETIs would appear to be exceptionally restrictive. During an ETI, novel collectives must form and become the focal point of adaptation while not being undone by adaptations occurring among lower-level units. This is challenging, because lower-level units should possess numerous evolutionary advantages (i.e. larger population size, shorter generation time, direct expression of traits that are heritable, and prior adaptations that enhance evolvability). Using the transition to multicellularity as a model to explore ETIs in general, we find that the structure of nascent multicellular life cycles can mitigate these factors.

Life cycles that restrict within-group genetic variation through frequent cellular bottlenecks and clonal development evolve readily in diverse taxa (e.g. Figure 1), in some cases (*e.g., Pseudomonas* [25], snowflake yeast [19], and unicellular relatives of volvocine algae [36]) through a single mutation. These life cycles limit the potential for within-group evolution and facilitate the emergence of heritable multicellular traits (Box 1). As a result, selection shifts to the higher level, efficiently acting on mutations that increase multicellular fitness, even if these mutations reduce single-cell fitness (Figure 5) and can restrict the lineage's ability to revert back to strict unicellularity. Given sufficient time, the accumulation of 'ratcheting' mutations can erode cellular autonomy and transform cells into mere parts of the multicellular individual. Taken together, it appears trivially easy for unicellular organisms to form multicellular collectives that grow and reproduce in a manner that is ideal for spurring an ETI.

We are not the first to note that multicelluarity appears to evolve readily—Grosberg and Strathmann (2007) labeled it a 'minor major transition' [56], but our life-cycle focused results

provide additional insight into how and why multicellularity has evolved so many times. Our argument also extends beyond multicellularity, applying to any ETI that evolves through the creation of a new level of selection. The same features that make a multicellular life cycle efficacious at spurring an ETI (Box 1) apply to the origins of cells, super-organisms, and novel organisms emerging from symbiosis. For example, monogamy is ancestral to eusocial hymenopterans [57], super-organismal siphonophores are composed of clonal individual animals [58], and the symbiotic origins of cellular plastids occurs readily when symbionts are vertically transmitted [59] (a process facilitated by a uniparental bottleneck at fertilization [60]). While much less is known about the origin of cells, when particle movement between cells is limited and sub-cellular replicators reproduce mainly through protocellular fission, this simple life cycle efficiently allows for selection to act on cell-level fitness [61], minimizing within-cell conflict, improving cell-level heritability, and promoting cell-level adaptation. In each case, the life cycle involves a strong ontogenetic bottleneck (or, in the case of symbiosis and protocells, a mechanism that ensures partner fidelity across multiple generations) that limits the potential for within-collective conflict and increases the heritability of collective-level traits.

Observations of extant multicellular organisms are consistent with the idea that clonal development and unicellular bottlenecks facilitate the evolution of complex multicellularity. All extant clades that have evolved complex multicellularity (in the sense of Knoll [62]) develop clonally and have strong genetic bottlenecks, though not necessarily every generation. Unfortunately, this hypothesis is difficult to test. Modern life cycles cannot be assumed to represent ancestral life cycles, and most origins of multicellular life are ancient, with little or no fossil evidence that illuminates the first steps in the transition. However, an increased focus on small, soft-bodied, ancient fossils provides reason for optimism that this situation will improve. Some such fossils are sufficiently abundant that they can be arranged into a developmental series. For example, the large number of fossils of the red alga *Bangiomorpha* preserved at different developmental stages allows a nearly complete re–construction of their

ontogeny [63]. Our results suggest a prediction: if clonal development and single-celled bottlenecks are prerequisites for complex multicellularity, we should expect that future fossil discoveries will show that the ancestors of complex multicellular groups had these traits.

The evolution of complex life on Earth provides us with a model for how complexity might evolve elsewhere in the Universe. Taking Darwinian evolution as a necessary step for the origin of life [64], we see no reason that independently-derived replicators would be prevented from forming collectives characterized by life cycles that potentiate higher-level adaptation, especially over planetary scales of size and time. While other factors may limit the origin of complex life [65], the potential for evolutionary innovation is probably not a major constraint.

Acknowledgements

This work was supported by NASA Exobiology grant NNX15AR33G (WCR, EL and MDH), NSF grant DEB-1456652 (WCR and MDH), NASA Cooperative Agreement Network 7 (MDH), NSF Graduate Research Fellowship under grant number DGE-1256082 (PLC), and the Packard Foundation (WCR). We would like to thank Elliot Sober and three excellent referees for helpful and constructive comments.

Author contributions

All authors contributed equally to the planning and writing of this paper.

BIBLIOGRAPHY

[1] Michod R E, Roze D. (1997) Transitions in individuality. *Proc. Biol. Sci.* **264**, 853–-857.

[2] Smith, J M, and E Szathmary. (1997) The major transitions in evolution. Oxford University Press.

[3] Wade, M. J. (1978). A critical review of the models of group selection. *The Quarterly Review of Biology*, **53**(2), 101–114.

[4] Williams, G. C. (1966). *Adaptation and natural selection: A critique of some current evolutionary thought.* Princeton University Press.

[5] Godfrey-Smith P. (2009) Darwinian Populations and Natural Selection. (Oxford University Press).

[6] Clarke, E. (2010). The problem of biological individuality. *Biological Theory*, **5**(4), 312–325

[7] Sober, E. (1991). Organisms, individuals, and units of selection. In *Organism and the origins of self* (pp. 275-296). Springer Netherlands.

[8] Lewontin R C (1970) The units of selection. *Annu. Rev. Ecol. Syst.* **1**: 1–-18.

[9] de Visser, J. A. G. M., Hermisson et al. (2003). Perspective: evolution and detection of genetic robustness. *Evolution*, **57**(9), 1959–1972.

[10] Wagner, A. (2008). Gene duplications, robustness and evolutionary innovations. *Bioessays*, **30**(4), 367–373.

[11] Pigliucci, M. (2008). Is evolvability evolvable? *Nature Reviews Genetics*, **9**(1), 75–82.

[12] Buss, Leo W. *The evolution of individuality.* Princeton University Press, 2014.

[13] Rainey, P. B., and De Monte, S. (2014). Resolving conflicts during the evolutionary transition to multicellular life. *Annual Review of Ecology, Evolution, and Systematics,* **45**, 599-620.

[14] Merlo, L. M., Pepper, J. W., Reid, B. J., and Maley, C. C. (2006). Cancer as an evolutionary and ecological process. *Nature Reviews Cancer*, **6**(12), 924-935.

[15] Taylor, D. R., Zeyl, C., and Cooke, E. (2002). Conflicting levels of selection in the accumulation of mitochondrial defects in Saccharomyces cerevisiae. *Proceedings of the National Academy of Sciences*, **99**(6), 3690–3694.

[16] Austin, B. U. R. T., Trivers, R., and Burt, A. (2009). *Genes in conflict: the biology of selfish genetic elements.* Harvard University Press.

[17] Grosberg R K, Strathmann R R (1998) One cell, two cell, red cell, blue cell: the persistence of a unicellular stage in multicellular life histories. *Trends Ecol. Evol.* **13**: 112–-116.

[18] Roze D, Michod R E (2001) Mutation, multilevel selection, and the evolution of propagule size during the origin of multicellularity. *Am. Nat.* **158**: 638–-654.

[19] Ratcliff, W. C., Fankhauser, J. D., Rogers, D. W., Greig, D., and Travisano, M. (2015). Origins of multicellular evolvability in snowflake yeast. *Nature communications*, **6**. 6102.

[20] Queller D C. (1997) Cooperators since life began. *The Quarterly Review of Biology* **72**2: 184–188.

[21] Fisher R A (1930) The Genetical Theory of Natural Selection, Clarendon Press, Oxford.

[22] O'Toole, G., Kaplan, H. B., and Kolter, R. (2000). Biofilm formation as microbial development. *Annual Reviews in Microbiology*, **54**(1), 49–79.

[23] Nadell, C. D., Drescher, K., and Foster, K. R. (2016). Spatial structure, cooperation and competition in biofilms. *Nature Reviews Microbiology.* **14**,589–-600.

[24] Clarke E (2016) Levels of selection in biofilms: multispecies biofilms are not evolutionary individuals. *Biol. Philos.* **31**: 191–-212.

[25] Bantinaki, E., Kassen, R., Knight, C. G., Robinson, Z., Spiers, A. J., and Rainey, P. B. (2007). Adaptive divergence in experimental populations of *Pseudomonas fluorescens*. III. Mutational origins of wrinkly spreader diversity. *Genetics*, **176**(1), 441–453.

[26] Hammerschmidt, K., Rose, C. J., Kerr, B., and Rainey, P. B. (2014). Life cycles, fitness decoupling and the evolution of multicellularity. *Nature*, **515**(7525), 75–79.

[27] Rainey, P. B. and Kerr, B. (2010). Cheats as first propagules: A new hypothesis for the evolution of individuality during the transition from single cells to multicellularity. *Bioessays*, **32**(10), 872–880.

[28] Beaumont, H.J., Gallie, J., Kost, C., Ferguson, G.C. and Rainey, P.B., (2009). Experimental evolution of bet hedging. *Nature*, **462**(7269), 90–93.

[29] Libby, E. and Rainey, P. B. (2011). Exclusion rules, bottlenecks and the evolution of stochastic phenotype switching. *Proceedings of the Royal Society B*, **278**(1724), 3574–83.

[30] Libby, E. and Rainey, P. B. (2013). Eco-evolutionary feedback and the tuning of protodevelopmental life cycles. *PLoS One*, **8**(12), e82274.

[31] Wolinsky, E. and Libby, E. (2015). Evolution of regulated phenotypic expression during a transition to multicellularity. *Evolutionary Ecology*, **30**(2), 235–250.

[32] Ratcliff, W. C., Denison, R. F., Borrello, M., and Travisano, M. (2012). Experimental evolution of multicellularity. *Proceedings of the National Academy of Sciences*, **109**(5), 1595–1600.

[33] Ratcliff, W. C., Pentz, J. T., and Travisano, M. (2013). Tempo and mode of multicellular adaptation in experimentally evolved *Saccharomyces cerevisiae*. *Evolution*, **67**(6), 1573–1581.

[34] Cross, F. R., and Umen, J. G. (2015). The Chlamydomonas cell cycle. *The Plant Journal*, **82**(3), 370–392.

[35] Lurling, M. and Beekman, W. (2006). Palmelloids formation in *Chlamydomonas reinhardtii*: defence against rotifer predators?. *Annales de Limnologie-International Journal of Limnology* **42**(2) 65–72.

[36] Hanschen, E. R., Marriage, et al. (2016). The Gonium pectorale genome demonstrates co-option of cell cycle regulation during the evolution of multicellularity. *Nature communications,* 7: 11370.

[37] Olson B J S C, Nedelcu A M (2016) Co-option during the evolution of multicellularity and developmental complexity in the volvocine green algae. *Curr. Opin. Genet. Dev.* **39**: 107–-115.

[38] Carr, M., Leadbeater, B. S., Hassan, R., Nelson, M., and Baldauf, S. L. (2008). Molecular phylogeny of choanoflagellates, the sister group to Metazoa. *Proceedings of the National Academy of Sciences*, **105**(43), 16641-16646.

[39] Dayel, M. J., Alegado, R. A., Fairclough, S. R., Levin, T. C., Nichols, S. A., McDonald, K., and King, N. (2011). Cell differentiation and morphogenesis in the colony-forming choanoflagellate *Salpingoeca rosetta*. *Developmental biology*, **357**(1), 73-82.

[40] Fairclough, S. R., Dayel, M. J., and King, N. (2010). Multicellular development in a choanoflagellate. *Current Biology*, **20**(20), R875-R876.

[41] Abedin M,King N (2010) Diverse evolutionary paths to cell adhesion. *Trends Cell Biol.* **20**: 742–-734.

[42] Tarnita C E, Taubes C H, Nowak M A (2013) Evolutionary construction by staying together and coming together. *J. Theor. Biol.* **320**: 10–-22.

[43] Herron M D, Michod R E (2008) Evolution of complexity in the volvocine algae: transitions in individuality through Darwin's eye. *Evolution* **62**: 436–-451.

[44] Kirk D L (2005) A twelve-step program for evolving multicellularity and a division of labor. *BioEssays* **27**: 299–-310.

[45] Nozaki H, Itoh M, Watanabe M M, Kuroiwa T. (1996) Ultrastructure of the vegetative colonies and systematic position of *Basichlamys* (Volvocales, Chlorophyta). *Eur. J. Phycol.* **31**: 67–-72.

[46] McShea D W (1996) Perspective: metazoan complexity and evolution: is there a trend? *Evolution* **50**: 477–-492.

[47] Viamontes G I, Kirk D L (1977) Cell shape changes and the mechanism of inversion in *Volvox*. *J. Cell Biol.* **75**: 719-–730.

[48] Höhn S, Honerkamp-Smith A R, Haas P A, Trong P K, Goldstein R E (2015) Dynamics of a *Volvox* embryo turning itself inside out. *Phys. Rev. Lett.* **114**: 1–-5.

[49] Lynch M, Walsh B (1998) *Genetics and Analysis of Quantitative Traits* (Sunderland, MA: Sinauer Associates, Inc.)

[50] Herron M D, Ratcliff W C (2016) Trait heritability in major transitions. bioRxiv 041830; doi: 10.1101/041830

[51] Queller D C (2000) Relatedness and the fraternal major transitions. *Philos. Trans. Biol. Sci.* **355**: 1647–-1655.

[52] Simpson C (2011) How many levels are there? How insights from evolutionary transitions in individuality help measure the hierarchical complexity of life. in *The Major Transitions in Evolution Revisited* (eds. Calcott B, Sterelny K) 199–-225 (The MIT Press).

[53] Shelton D, Michod R (2014) Group selection and group adaptation during a major evolutionary transition: insights from the evolution of multicellularity in the volvocine algae. *Biol. Theor.* **9**: 452–469.

[54] Libby E, Ratcliff W C (2014) Ratcheting the evolution of multicellularity. *Science* **346**: 426–427.

[55] Libby E, Conlin P L, Kerr B, Ratcliff W C (2016) Stabilizing multicellularity through ratcheting. *Phil. Trans. Roy. Soc. B.* **371**: 20150444.

[56] Grosberg, R. K. and Strathmann, R. R. (2007). The evolution of multicellularity: a minor major transition?. *Annu. Rev. Ecol. Evol. Syst.*, **38**, 621–654.

[57] Hughes, W. O., Oldroyd, B. P., Beekman, M., and Ratnieks, F. L. (2008). Ancestral monogamy shows kin selection is key to the evolution of eusociality. *Science*, **320**(5880), 1213–1216.

[58] Dunn, C. W., and Wagner, G. P. (2006). The evolution of colony-level development in the Siphonophora (Cnidaria: Hydrozoa). *Development genes and evolution*, **216**(12), 743–754.

[59] Delwiche, C. F., and Palmer, J. D. (1997). The origin of plastids and their spread via secondary symbiosis. In *Origins of algae and their plastids* (pp. 53-86). Springer Vienna.

[60] Greiner, S., Sobanski, J., and Bock, R. (2015). Why are most organelle genomes transmitted maternally? BioEssays, 37(1), 80-94.

[61] Chen, I. A., Roberts, R. W., and Szostak, J. W. (2004). The emergence of competition between model protocells. *Science*, **305**(5689), 1474-1476.

[62] Knoll, A. H. (2011). The multiple origins of complex multicellularity. *Annual Review of Earth and Planetary Sciences*, **39**, 217-239.

[63] Butterfield, N. J. (2000). *Bangiomorpha pubescens* n. gen., n. sp.: implications for the evolution of sex, multicellularity, and the Mesoproterozoic/Neoproterozoic radiation of eukaryotes. *Paleobiology* 26:386–404.

[64] Benner, S. A. (2010). Defining life. *Astrobiology*, **10**(10), 1021-1030.

[65] Lane, N. (2014). Bioenergetic constraints on the evolution of complex life. *Cold Spring Harbor perspectives in biology*, **6**(5), a015982.

Chapter 4

EXPERIMENTAL EVOLUTION OF ADAPTIVE PHENOTYPIC PLASTICITY IN A TEMPORALLY VARYING ENVIRONMENT

Peter L. Conlin[1,*] Samuel E. Reed[1] Joseph H. Marcus[1] William C. Ratcliff[2] Benjamin Kerr[1]

[1]Department of Biology and BEACON Center for the Study of Evolution in Action, University of Washington, Seattle, WA 98195, United States of America

[2]Department of Biology, Georgia Institute of Technology, Atlanta, GA 30332, United States of America

∗ **corresponding author, email: pconlin2@uw.edu**

Keywords: phenotypic plasticity | G x E interaction | cue reliability | evolution

Abstract

Phenotypic plasticity, the ability of a single genotype to produce different phenotypes in response to changes in the environment, is common in nature. Its commonness, however, should not be taken as an indication that plasticity is necessarily adaptive: Theory suggests that the adaptive value of plasticity depends on the degree of environmental heterogeneity and the existence of environmental cues that provide reliable information about selective conditions. We tested this prediction using experimental evolution. Populations of cluster-forming "snowflake" yeast were grown in alternating environments with selection for either small or large size following each 24-hour growth phase. We manipulated cue reliability (the degree to which environmental cues and selective conditions are correlated) by pairing selection for small or large cluster size to pairs of growth media environments in different combinations. We find that temporally varying selection can favor the evolution of phenotypic plasticity in experimental populations of snowflake yeast when selection is predictable. When selection is unpredictable, we find that phenotypic plasticity is frequently lost; populations evolve flat reaction norms. Furthermore, the adaptive benefits of evolved plasticity under different regimes of environmental change were shown to be specific to the exact pairs of growth environment and size selection experienced during the evolution experiment. Microscopic analysis of single-cell morphology revealed a plausible physical mechanism to explain how plastic changes in cluster size are achieved. These findings support a critical role for cue reliability in the evolution of phenotypic plasticity and suggest that adaptive phenotypic plasticity can evolve rapidly.

Introduction

Organisms living in variable environments must contend with changing, often opposing, selection pressures or risk extinction (Burger and Lynch 1995; Bell and Collins 2008). In order to buffer against the risk of environmental change, organisms may evolve strategies that ensure

successful reproduction across a range of environments (Simons 2011). One way to do this is to be a generalist, producing an intermediate phenotype that performs moderately well in most environments but excels in none, a strategy also referred to as conservative bet hedging (Seger and Brockmann 1987). In other cases, it may be advantageous to evolve high variance in the phenotype under selection so that some proportion of offspring will successfully reproduce regardless of environmental conditions, a strategy called diversification bet hedging (Cohen 1966; Seger and Brockmann 1987). Both of the above strategies maximize long-term fitness in unpredictably changing environments by reducing the variance in fitness across environments (Slatkin 1974; Seger and Brockmann 1987; Philippi and Seger 1989; Starrfelt and Kokko 2012). If changing selective conditions are instead predictable, organisms may evolve to alter their phenotype based on the state of the environment; phenotypic plasticity may evolve (Scheiner 1993).

Phenotypic plasticity is the ability of a single genotype to produce different phenotypes in response to changes in the environment (Bradshaw 1965; Via et al. 1995; DeWitt and Scheiner 2004). Plasticity can occur for almost any phenotype and is found across all levels of biological complexity. For instance, plants elongate in response to shading (Schmitt et al. 1999; Smith 2000), water fleas grow protective head shields in the presence of predators (Dodson 1988; Tollrian 1995), and soil bacteria sporulate in nutrient-poor environments (López and Kolter 2010). Plasticity may confer an adaptive benefit, as expected in the examples above, but it can also be maladaptive or neutral (Ghalambor et al. 2007). The adaptive value of phenotypic plasticity depends on many factors that can be broadly grouped as either costs or limits of plasticity (Dewitt et al. 1998; Murren et al. 2015). Costs include any energetic demands associated with the sensory or developmental machinery necessary for a plastic response whereas limits refer to anything that might lead to the expression of a maladapted phenotype such as the lag-time between the environmental change and phenotypic response due to development.

As suggested above, the availability of reliable cues is thought to be a central constraint on

the evolution of phenotypic plasticity. We define a cue as any environmental factor, biotic or abiotic, that could be used as a guide for future action (Hasson 1994; Maynard Smith and Harper 2003). In some cases, the cue can be the same as the environmental factor imposing the selective pressure (e.g., upregulating heat shock genes in response to heat stress). However, it is commonly the case that development of the phenotype must occur before the organism faces the selective conditions. This type of predictive plasticity is the focus of our present study. Theory predicts that predictive plasticity should be favored under conditions when environments fluctuate temporally, environmental cues provide reliable information about selection, and the costs of plasticity are low (Moran 1992; Tufto 2000; Sultan and Spencer 2002; Scheiner and Holt 2012). This prediction is supported by the observation that the degree of plasticity observed in natural populations is positively correlated with environmental heterogeneity (Lind and Johansson 2007; Van Buskirk 2017) and by experiments that demonstrate a selective advantage of plasticity in response to relevant environmental cues (Lively 1986; Van Buskirk and Relyea 1998). Similar constraints are thought to apply to the origin of an adaptive plastic response to a novel environmental cue. However, the extent to which plasticity can evolve, even under favorable conditions, depends on the availability of genetic variation (Via and Lande 1985; Scheiner 1993) and the existence of genetic constraints, which may depend on the type of environmental factors that covary with selection (Izem and Kingsolver 2005; Snell-Rood et al. 2010; Murren et al. 2015).

Here we investigate the role of cue reliability on the *de novo* evolution of phenotypic plasticity. We experimentally evolved multicellular "snowflake" yeast (Ratcliff et al. 2012) under alternating growth environments with paired selection for either small or large size following each 24-hour growth phase. Cue reliability was manipulated by changing the correlation between growth environment and post-growth size selection. Using this approach, we explored the evolution of plasticity for cluster size under three different cue reliability regimes. Here we report the rapid evolution of adaptive phenotypic plasticity in response to divergent selection in alternating growth environments. We present data on the fitness

effects of evolved plasticity under different regimes of environmental change and discuss constraints on the evolution of phenotypic plasticity in relation to the complexity of environmental variation. Finally, using microscopic analysis of individual yeast cells, we identified environment-dependent shifts in an aspect of cellular morphology, cell aspect ratio, that could serve as the mechanism for plastic changes in cluster size.

Study system

Multicellular 'snowflake yeast' clusters were previously evolved from a heterozygous diploid strain of *Saccharomyces cerevisiae* under daily selection for rapid sedimentation in liquid media (Ratcliff et al. 2012). The multicellular phenotype is a consequence of a cell separation defect caused by a loss-of-function mutation in the transcription factor *ACE2* that results in the formation of multicellular clusters (Nelson et al. 2003; Voth et al. 2005; Oud et al. 2013; Ratcliff et al. 2015). Snowflake yeast clusters grow via budding of existing cells and reproduce by fragmentation when internal stresses caused by physical crowding of cells become too great (Ratcliff et al. 2015; Jacobeen et al. 2017, 2018). As a consequence of fragmentation, snowflake yeast strains produce a distribution of cluster sizes at the end of a 24-hour growth cycle in liquid media (Fig. 1a). Interestingly, we found that the distribution of cluster sizes at the end of a 24-hour growth cycle was variable in different growth environments (evidence of preexisting plasticity; Fig. 1b) and for different snowflake yeast genotypes (evidence of GxE interaction; Fig. S1). We discuss all four of the growth environments depicted in Fig. 1b further in the following section.

Experimental evolution and predictions

Populations of snowflake yeast were grown in alternating environments (denoted E_1 and E_2) with selection for either small or large size (denoted S_S and S_L) following each 24-hour growth phase (Fig. 2a). Briefly, size selection was performed by pre-diluting overnight cultures 1:10 into 900ml of sterile growth media in a 1.5ml microcentrifuge tube and then passaging the

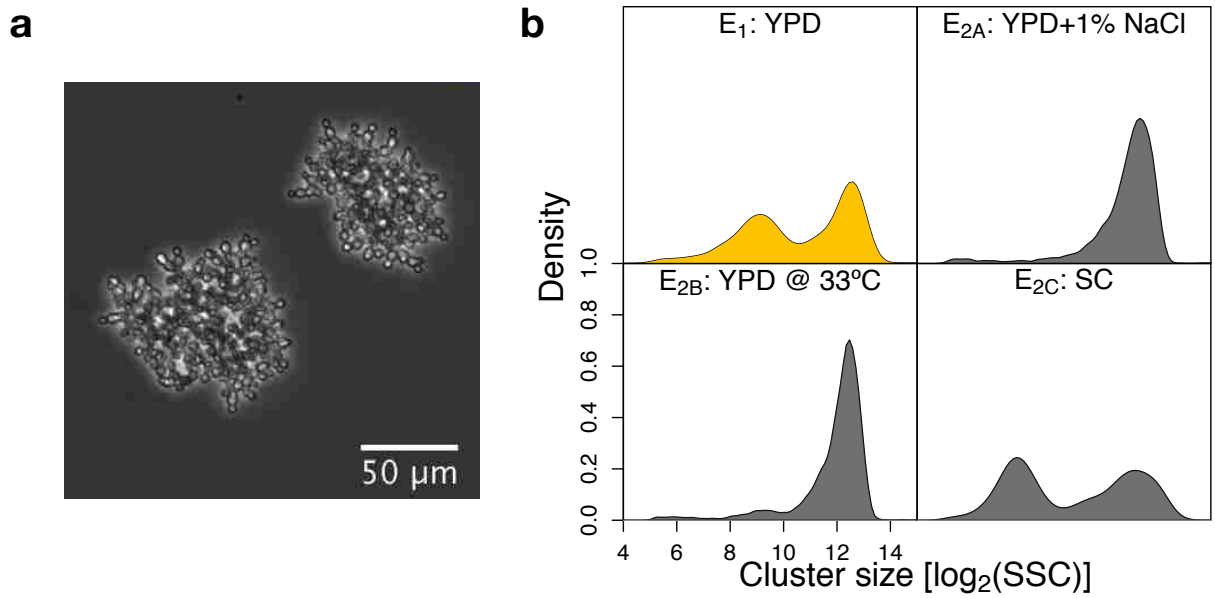

Figure 4.1: **(a) Bright-field image of snowflake yeast clusters. (b) Cluster size distributions of the ancestral C1W6 genotype after 24-hour growth in different media types.** The standard growth medium for our experiments, Yeast Peptone Dextrose (YPD), is shown in yellow (top right). Additional growth media types used in our evolution experiment appear in grey: YPD+1%NaCl, (bottom left) YPD incubated at 33ºC, (bottom right) Synthetic complete (SC) media. All cluster size measurements done by flow cytometry.

sample through a sterile nylon mesh filter. For small selection, a 30µm was used and the flow-through was propagated. For large selection, a 70µm nylon mesh filter was used and the filter was back-flushed to collect and propagate clusters that were larger than 70µm. A full description of our size selection protocols can be found in "Methods". The evolution experiment was run for a total of 56 transfers. Whole population samples were frozen each week.

We manipulated cue reliability by pairing selection for small or large size to environments E_1 and E_2 with different probabilities to form three "cue reliability regimes" (Fig. 2b). In our first regime, growth in E_1 was always followed by selection for large size and growth in E_2 always followed by selection for small size. Because there is perfect correlation between the growth environment and subsequent size selection, this regime is said to be "predictable". To visualize the plastic strategy predicted to evolve under these conditions we use the reaction norm, a curve that describes the range of phenotypes produced by a given genotype across a range of environments (Schlichting and Pigliucci 1998). In our case, the phenotype under investigation is mean cluster size (shown on the y-axis) and the range of environments are simply E_1 and E_2 (on the left and right sides of the x-axis, respectively). Clusters should evolve to be larger in E_1 and smaller in E_2. Thus, we predict that the evolved reaction norms will have a negative slope (Fig. 2c, left). Accordingly, we designate this regime P- (predictable, favoring negatively sloped reaction norms). Our second regime is exactly the inverse of the P- regime: growth in E_1 was always followed by selection for small size and growth in E_2 always followed by selection for large size; we call this the P+ regime (predictable, favoring positively sloped reaction norms; Fig. 2c, right). For the third cue reliability regime, the growth environment alternated in the same way as above, but size selection was random with respect to growth environment. Importantly, selection for small and large size occurred with equal frequency but in a random order so as to eliminate the correlation between growth environment and size selection without biasing selection in favor of one size or the other. We refer to this as the U regime (unpredictable). Here plasticity is

expected to be unfavorable so we predict a flat reaction norm (Fig. 2c, middle).

To maximize our chances of observing the evolution of phenotypic plasticity, three different pairs of growth environments were used to form three "cue identity treatments" which we refer to as ΔOsmolarity, ΔTemperature, and ΔNutrients. Yeast Peptone Dextrose (YPD: 10 g l^{-1} yeast extract, 20 g l^{-1} peptone and 20 g l^{-1} dextrose) was used as E_1 for all three cue identity pairs. E_2 varied according to treatment as follows: In the ΔOsmolarity treatment, E_{2A} was YPD with an additional 1% NaCl (YPD + 10 g l^{-1} NaCl). In the ΔTemperature treatment, E_{2B} was YPD incubated at 33ºC rather than the standard 30ºC. And in the ΔNutrients treatment, E_{2C} was Synthetic Complete medium (SC: 6.7 g l^{-1} yeast nitrogen base with amino acids + 20 g l^{-1} dextrose).

Results

Mean trait value evolution

Cluster size distributions were measured by flow cytometry twice weekly on consecutive days to track changes in cluster size over time in environments E_1 and E_2. We found that the average size of yeast clusters across both environments E_1 and E_2 decreased uniformly in nearly all replicate populations regardless of cue identity or cue reliability treatment (Fig. S2). This was somewhat expected since the large size filter cutoff of 70 μm is smaller than the average snowflake yeast cluster of our ancestral strain in most environments. Changes in mean trait value were least pronounced in the ΔNutrients treatment where mean trait value started off much lower.

Reaction norm evolution

At the end of the evolution experiment, four single colony isolates were collected from each of the 45 evolved populations to characterize evolved reaction norms. Each individual genotype was then grown for 24 hours in each of the two cue environments it experienced during the

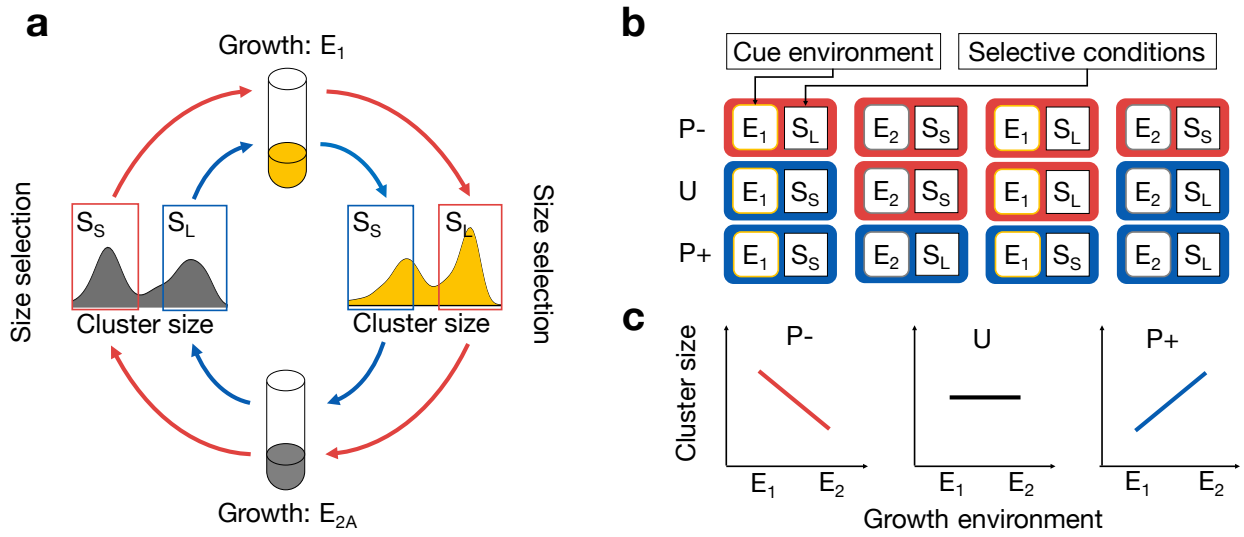

Figure 4.2: **(a) Structure of evolution experiments.** E_1 and E_2 represent cue environments, and S_S and S_L represent selective conditions. Environment E_2 takes on three different identities in our experiment that define our three "cue identity" regimes. Environment E_{2A} is shown here for the purpose of illustration. **(b) Cue reliability regimes.** Cue reliability regimes are defined by the associations between growth environment and size selection. Here we highlight the combinations that occur in each of our three cue reliability treatments: P- (predictable, favoring negative slopes), U (unpredictable), and P+ (predictable, favoring positive slopes). Each cue-selection pair is color-coded: E_1S_L, E_2S_S in red and E_1S_S, E_2S_L in blue. Only four days are shown in the diagram, but the evolution experiment was run for a total of 56 transfers. **(c) Predictions.** Qualitatively different reaction norms are expected to evolve in response to our three cue reliability regimes. High cue reliability is predicted to lead to phenotypic plasticity while unpredictable environmental change should select for non-plastic, flat reaction norms.

evolution experiment and cluster size distributions were measured in triplicate using flow cytometry (45 samples x 4 single strain isolates x 2 environments x 3 technical replicates for a total of 1080 measurements). Here we examine the patterns of reaction norm evolution across all treatments to assess general patterns at the aggregate level and within treatments to assess cue environment pair specific patterns.

We found significant variation in our evolved isolates for reaction norm slope indicating a significant effect of cue reliability (Fig. 3a; significant cue identity by cue reliability treatment interaction; mixed effects ANOVA, F=0.007184, p=0.001). Phenotypic plasticity was maintained under all environments where the slope of the preexisting reaction norm was expected to be coincidentally adaptive and more frequently lost in the unpredictably fluctuating environment than in either of the predictable ones (reaction norm slopes between -0.1 and 0.1 were considered to be non-plastic; Fisher's exact test, two-tailed P=0.0072). When preexisting plasticity was maladaptive, however, we found that the response to selection varied widely depending on the cue environment pair. We observed the evolution of adaptive plasticity from initially maladaptive plasticity in the ΔNutrients treatment (Fig. 3b). Because each pair of cue environments in our study is an independent experiment with the same structure, we perform separate analyses for each cue environment treatment below.

We used generalized linear models to compare differences in the slopes of reaction norms evolved in different populations and under different cue reliability treatments. We found statistically significant differences in evolved slopes for 7/9 pairwise comparisons conducted (indicated by an asterisk, Fig. 3b) and 6/7 significant differences are in the direction predicted. Most interestingly, reaction norm slopes shifted from negative to positive in 4/5 populations from the ΔNutrients P+ treatment.

Changes in relative fitness

One pair of cue environments produced results entirely consistent with theoretical predictions, ΔNutrients. To determine whether the changes in plasticity observed in this treatment

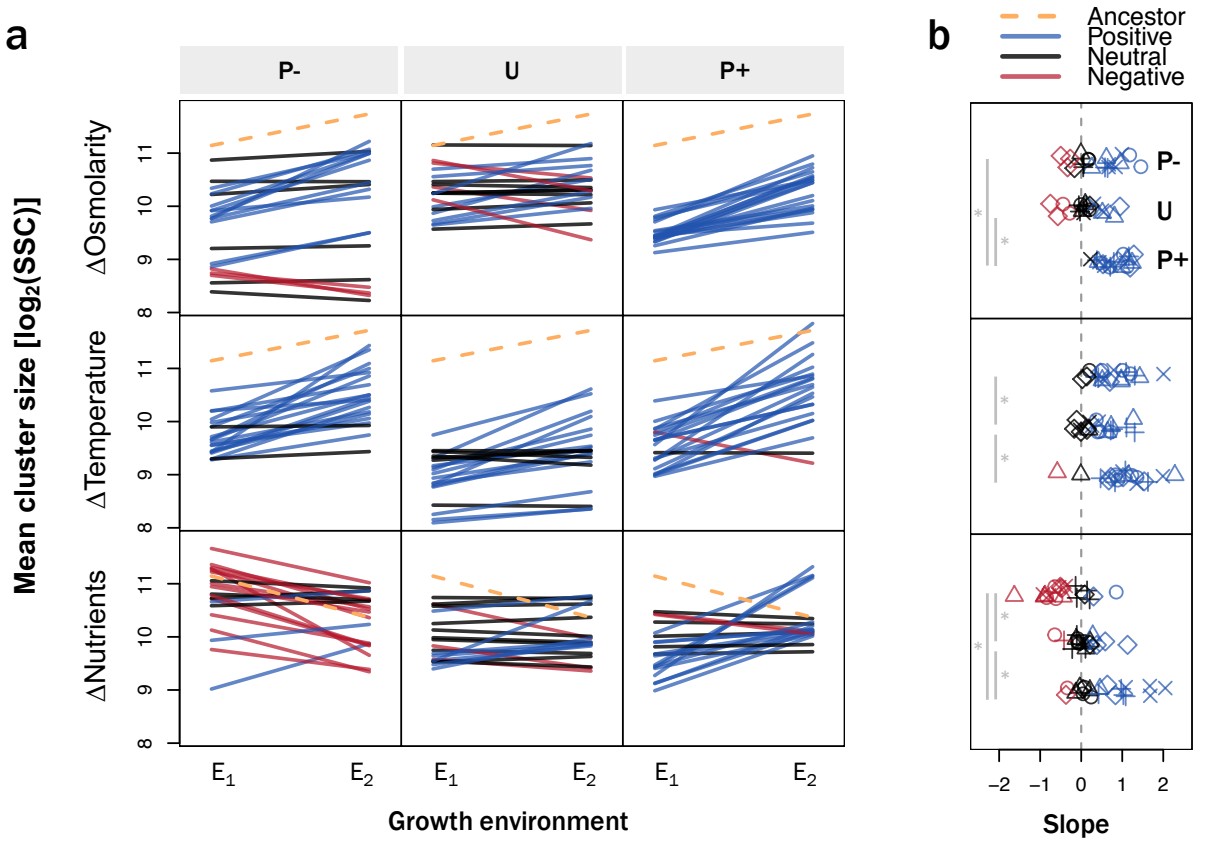

Figure 4.3: **(a) Comparison of evolved reaction norms.** Reaction norms illustrate differences in the way that mean cluster size in the two cue environments has changed after 56 days of evolution. The ancestral reaction norm for each cue environment pair is shown by the orange dotted line. Evolved isolates exhibiting a positive slope are colored in blue; neutral in black; negative in red. **(b) Comparison of evolved slopes.** These plots highlight two key aspects of the data shown in Figure 4a, slope and origin of the single colony isolates. Slope = $\log_2$(size in E_2 / size in E_1). Isolates from different replicate populations are marked with a different symbol. Comparison of evolved slopes was carried out using linear mixed-effects models with cue reliability treatment as a fixed factor and variance among isolates derived from replicate populations as random effects followed by post-hoc Tukey's pairwise comparisons. An asterisk indicates statistically significant differences in evolved slopes within a given set of cue environments.

were adaptive, we performed a set of pairwise competitions (Lenski et al. 1991). We selected evolved strains from the ΔNutrients P- and P+ treatments that exhibited either the minimum or maximum reaction norm slopes to get an idea of the range of phenotypes selected under different cue reliability regimes (Fig. 4a). Each selected strain was labeled with an inducible fluorescent GFP to enable competitions using the flow cytometer. Selective neutrality of the fluorescent markers was confirmed by competing GFP-labeled strains against an otherwise isogeneic unlabeled strain in the absence of size selection to confirm that there was no cost associated with the fluorescent marker (Fig. S3).

In order to closely replicate the conditions of growth and selection during the evolution experiment, we exposed the co-cultures to both combinations of growth environment and size selection experienced by either the P- or the P+ selection treatment according to the cue reliability conditions experienced by the focal strain. Competitions involving the evolved strains from the U treatment were not performed because of the difficulties associated with reproducing the selective pressures experienced by populations evolved under this regime of environmental change (4 different pairs of growth environment and post-growth size selection are possible).

We first competed each evolved strain in its native conditions against the ancestor. We found that the fitness of the evolved isolates is greater than or equal to that of the ancestral strain (Fig. 4b-c; grey bars); indicating that some adaptation has occurred. Next, we performed "reciprocal transplant" competitions by measuring the fitness of evolved strains in their native conditions against strains that had evolved in the opposite cue reliability conditions. We found that all focal strains had higher fitness when competing under their native cue reliability conditions than when serving as competitor strain in the transplant environment (e.g., fitness of P- strains in the P- environment > fitness of P- strains in the P+ environment). This suggests that adaptation is specific to the exact pairs of growth environment and size selection experienced during the evolution experiment.

We predicted that more negatively sloped reaction norms would be favored in the P-

environment while more positively sloped reaction norms would be favored in the P+ environment. In keeping with these predictions, we found that P-min had a consistently higher fitness than P-max across each of the three pairs of competitions in the P- environment. In the P+ environment, P+max had a higher fitness than P+min across all three competitions. A simple linear regression was performed to determine if competitive fitness could be explained by the difference in the reaction norm slopes of the focal strain and its competitor. In the P- environment, we found a negative relationship between the difference in reaction norm slopes and competitive fitness (Fig. 4d; β = -0.03612) but the difference was non-significant (adjusted $r^2 = 0.529$, $F_{1,4} = 6.618$, $p = 0.06181$). In the P+ environment, relative fitness of the focal strain increased as the difference in reaction norm slopes increased (Fig. 4e; $\beta = 0.10870$, adjusted $r^2 = 0.6585$, $F_{1,4} = 10.64$, $p = 0.03103$).

Phenotypic changes associated with adaptive plasticity

To investigate the mechanistic basis for the evolved changes in phenotypic plasticity we visualized populations of snowflake yeast with different reaction norms slopes after growth in either YPD or SC media. We hypothesized that changes in yeast cell morphology could have led to the observed changes in cluster size distribution. For example, cell shape has a pronounced effect on the size at which snowflake yeast clusters fracture: more elongate cells produce larger clusters (Jacobeen et al. 2017, 2018). Environment-dependent changes in cell aspect ratio could be a possible route to adaptive changes in mean cluster size. Similarly, environment-dependent changes in cell size (with shape held constant) could lead to an adaptive shift in the stationary phase cluster size distribution, assuming that cluster size scales linearly with cell size. We manually measured aspect ratio and area for 50 budded yeast cells after 24 hours of growth in either YPD or SC for three representative evolved strains from the P-, U, and P+ treatments and the ancestor using the ellipse drawing tool in ImageJ (Rueden et al. 2017).

We tested for significant differences in cell aspect ratio and cell size using a Mann-Whitney

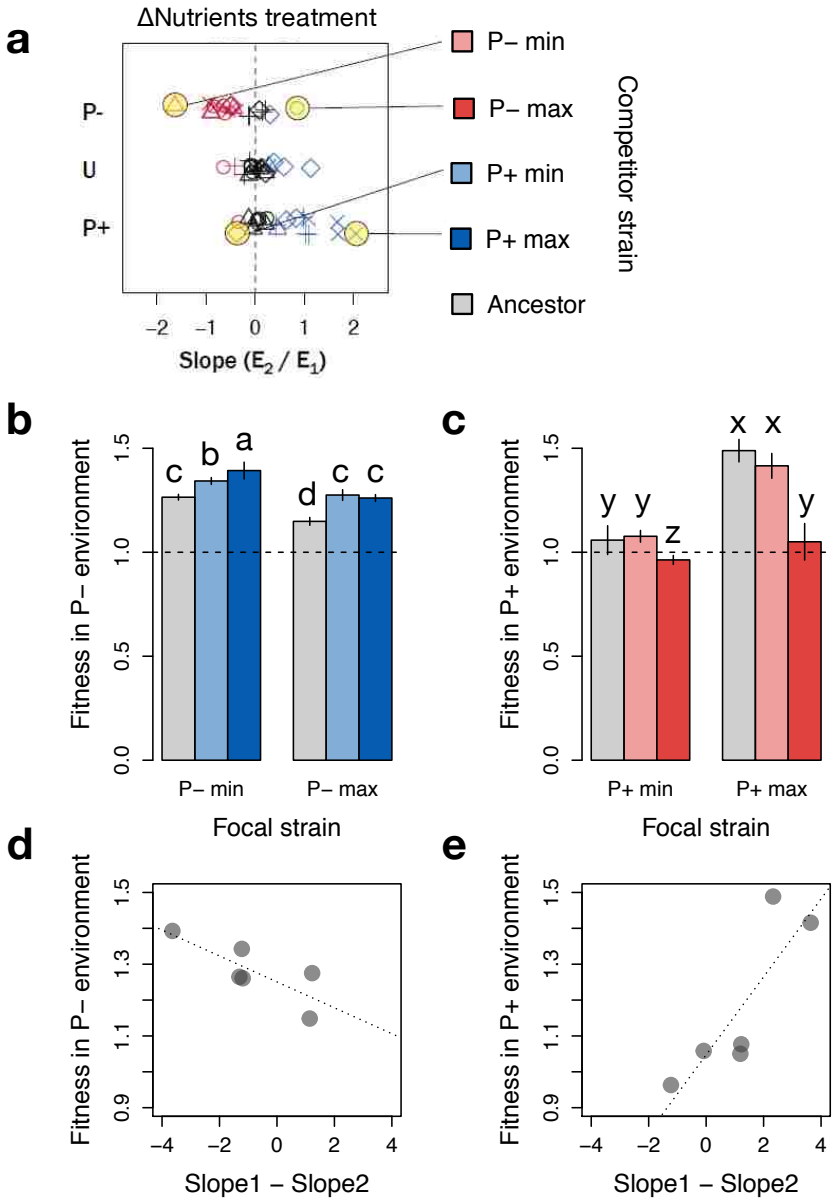

Figure 4.4: **(a) Selecting strains for pairwise competitions.** To compare strains evolved under different regimes of environmental change, we chose isolates with the minimum and maximum slope from each treatment. Each highlighted strain was transformed with an inducible GFP and competed against an unlabeled version of itself to test for a fitness cost of the marker. **(b-c) Competitive fitness of evolved strains.** Relative fitness of the focal strain is reported as the ratio of Malthusian parameters. Bars are grouped by focal strain and colored according to the competitor strain. Letters indicate statistically significant differences between fitness values (determined with a one-way ANOVA and a post-hoc Tukey's HSD test). **(d-e) Relationship between reaction norm slopes and relative fitness.** Fitness values from the corresponding panel above are plotted against the difference between reaction norm slope of the focal strain minus that of the competitor strain.

U test with a Bonferroni correction for multiple comparisons. We found that cell aspect ratio was significantly smaller in the SC environment for both the Ancestral strain and the evolved strain from the P- treatment ($p = 4.208 \times 10^{-10}$ and $p = 8.623 \times 10^{-3}$, respectively) but significantly larger in SC for the evolved strain from the P+ treatment ($p = 9.677 \times 10^{-5}$; Fig. 5a). The evolved strain from the U treatment showed no significant difference in cell aspect ratio between YPD and SC ($p = 0.428$). This pattern is entirely consistent with the hypothesis that more elongate cells will produce larger clusters. Significant differences in cell size were also detected for both the P+ treatment and the U treatment ($p = 4.851 \times 10^{-3}$ and $p = 7.295 \times 10^{-4}$, respectively). However, the differences in cell size were opposite of that which would be expected if environment-dependent changes in cell size were responsible for the observed changes in cluster size.

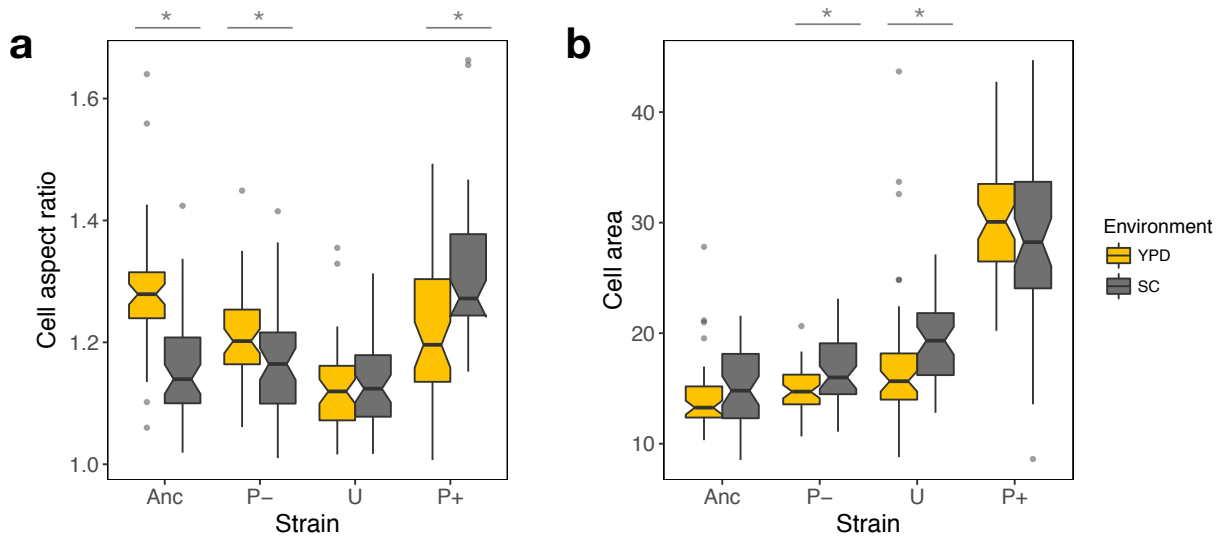

Figure 4.5: **(a) Cell aspect ratio measurements and (b) cell area measurements.** Yellow box plots indicate measurements taken after 24-hour growth in Yeast Peptone Dextrose (YPD) media. Grey box plots indicate measurements take after 24-hour growth in Synthetic Complete (SC) media. Significant differences between mean trait value in YPD versus SC, indicated by a grey bar and asterisk, were determined using a Mann-Whitney U test with a Bonferroni correction for multiple comparisons ($p < 0.0125$).

Discussion

Predictable environmental fluctuations have been suggested to select for phenotypic plasticity when different environments favor different phenotypes and fluctuations occur between organismal generations. Here we provide direct evidence in support of this prediction using experimental evolution. In the ΔNutrients treatment, we found that plasticity was maintained under conditions where it was coincidentally adaptive, commonly lost in the unpredictably fluctuating environments, and we observed major changes in the slope of the reaction norm in the form of multiple independent shifts from negative to a positive. Pairwise reciprocal transplant competitions with evolved isolates in the P- and P+ environments suggest that evolved reaction norms are adaptive and specific to the exact pairs of growth environment and size selection experienced during the evolution experiment.

Unexpected changes in reaction norms

In the other two cue identity treatments (ΔOsmolarity and ΔTemperature), evolutionary outcomes differed significantly from our predictions. Specifically, populations in these treatments failed to evolve adaptive plasticity when preexisting plasticity was initially maladaptive. It is possible that trade-offs with other traits, or across life history stages, may have constrained the evolution of plastic responses to certain types of environmental change more than others (Dewitt et al. 1998; Scheiner and Berrigan 1998). Plastic responses to temperature, in particular, have been previously suggested to be highly constrained due to the strong influence of temperature on the rate of biochemical reactions (Huey and Kingsolver 1989). Perhaps this could help to explain why evolved changes in phenotypic plasticity for cluster size were so limited in the ΔTemperature treatment in our study. Interestingly, plastic responses to temporally varying selection were also found to be very weak or absent in two other experimental evolution studies that examined the effect of cue reliability in alternating thermal environments (Scheiner and Yampolsky 1998; Manenti et al. 2015).

Another possible explanation for the observed differences between cue identity treatments is that the complexity of environmental variations can influence an organism's ability to evolve predictive plasticity. Although we did not design this experiment with the intention to explore the effects of environmental complexity, we find it interesting that adaptive plastcity repeatedly evolved in the ΔNutrients treatment (where multiple correlated environmental factors varied simultaneously) while reaction norm evolution was more constrained in the ΔOsmolarity and ΔTemperature treatments (where only a single environmental factor varied). We speculate that it may be easier to evolve new associations between cue and phenotype in the ΔNutrients treatment because several correlated environmental factors were varied simultaneously. Our rationale is two-fold. First, the use of multiple covarying environmental factors as a cue for plastic changes in morphology could be favored because the combination of environmental variables acts as a stronger predictor of future selective pressures. A second possible explanation is that the availability of multiple environmental factors that could serve as cues simply provided a larger set of possible evolutionary responses due to an increase in genetic variation for plastic responses to the individual environmental components. Chevin and Lande (2015) modeled the evolution of linear reaction norms in response to several correlated environmental variables in a population undergoing stationary environmental fluctuations and found that populations evolved to use a combination of environmental variables as cues for the plastic trait under selection. Consequently, plastic responses to any single environmental variable were sometimes found to be maladaptive (Chevin and Lande 2015). Understanding the role of multiple environmental cues for plasticity remains a critically important area for future study.

Mechanistic basis of phenotypic plasticity

One unique aspect of this work is that we were able to identify a plausible physical mechanism for the plastic changes in cluster size we observe in the evolved strains isolated from the ΔNutrients treatment. We identified environment-dependent changes in an aspect of cellular

morphology, cell aspect ratio, that are positively correlated with changes in mean cluster size. The discovery of this correlation was facilitated by the relative simplicity of the snowflake yeast growth form and the existence of earlier studies into the biophysics of cluster growth and fragmentation (Jacobeen et al. 2017, 2018). Prior work showed that cells evolved an 8% increase in cellular aspect ratio in response to 7 weeks of selection for increased cluster size; this change accounted for a 1.7-fold increase in the radius of snowflake yeast clusters (Jacobeen et al. 2017). Here we observe comparable differences in cellular aspect ratio when snowflake yeast are grown in different media types and an associated change in cluster size. The link between cell aspect ratio and cluster size is of interest because it illustrates how subtle changes in cellular morphology can filter up to affect morphology on a macroscopic level. The finding that simple multicellular clusters of yeast can evolve to conditionally express cell-level phenotypes in response to external environmental cues may also have important implications for the evolution of multicellular development.

Limitations and future directions

An important limitation of our study is that we able to explore only the extremes of cue reliability: perfect information (P+ and P- treatments) and total lack of information (U treatment). Our predictions were accordingly simple: perfect phenotypic plasticity should evolve in the P+ and P- treatments while the U treatment should favor a non-plastic bet-hedging strategy of some sort. Phenotypic plasticity and bet-hedging, however, should not be thought of as mutually exclusive possibilities. When incomplete information about the state of the environment is available, the optimal strategy may involve some combination of the two (Donaldson-Matasci et al. 2013; Simons 2014; Maxwell and Magwene 2017). For example, Emex spinosa, an amphicarpic annual plant that produces two types of propagules with different dispersal abilities, changes the proportion of short vs. long-range propagules in response to nutrient availability and the density of neighboring plants (Sadeh et al. 2009). In the same way that mean cluster size changes over evolutionary time, snowflake yeast

can evolve to increase or decrease the variance in cluster size around the phenotypic mean. If we allow for some looseness in the application of the term "bet-hedging", equating bet-hedging with the simple generation of phenotypic variance within a single environment, we can measure how both phenotypic plasticity and bet-hedging change in response to different degrees of cue reliability as well as exploring their joint expression (DeWitt and Langerhans 2004).

Conclusion

Selection experiments have been used for decades to investigate the evolution of phenotypic plasticity (Scheiner 2002) and have played a central role in advancing our understanding of nearly all aspects of phenotypic plasticity. Early studies demonstrated that plasticity was a heritable trait that could be directly selected (Waddington 1960; Kindred 1965; Druger 1967; Brumpton et al. 1977; Jinks et al. 1977). Later, selection experiments helped to establish the adaptive significance of phenotypic plasticity and began to probe the genetic bases of plastic traits (Van Buskirk and Relyea 1998; Schmitt et al. 1999; Dorn et al. 2000). Our study adds to this growing body of work in a few ways. First, our results provide further evidence that adaptive changes in plasticity can evolve rapidly (Sikkink et al. 2014; Yi and Dean 2016; López García de Lomana et al. 2017). Second, we demonstrate that adaptive plasticity can evolve in response to temporally heterogeneous selection for opposing phenotypes in different environments. This has been shown previously by laboratory evolution experiments (Bell and Reboud 1997; Reboud and Bell 1997; Kassen and Bell 1998), but direct experimental tests of the conditions favoring the evolution of adaptive phenotypic plasticity remain relatively rare. Lastly, we confirm the critical role that cue reliability plays in shaping the evolution of reaction norms. Because natural environments are more complex than the environments studied here and because unpredictable environmental changes are increasingly common, we encourage future studies of plasticity evolution that consider multiple environmental cues and/or intermediate degrees of cue reliability.

Methods

Strain construction

A detailed list of all strains used in this study can be found in Table S1.

All populations for the evolution experiment were initiated with a homozygous diploid strain of *Saccharomyces cerevisiae* Y55 derived from a previously described strain (C1W6) (Ratcliff et al. 2012). Briefly, the ancestral strain for our study was obtained by autodiploidization of a single spore collected via tetrad dissection onto Yeast Peptone Dextrose agar plates (YPD agar: 10 g l^{-1} yeast extract, 20 g l^{-1} peptone, 20 g l^{-1} dextrose, 15 g l^{-1} agarose). Fluorescently-labeled strains prepared for competition experiments were derived from single colony isolates and transformed with an inducible *ura3::met25*-GFP using the LiAc/SS-DNA/PEG method of transformation (Gietz and Schiestl 2007).

Culture conditions and storage

Unless otherwise stated, strains were grown in 10 ml of media in 25mm tubes shaken at 250 rpm at 30ºC for approximately 20 hours. Freezer stocks of single strain isolates and whole populations were prepared by mixing 0.7ml of an overnight culture with 0.3ml of 70% glycerol and stored at -80ºC.

Microscopy

Microscopic measurements of yeast clusters were conducted using an inverted fluorescence microscope (Nikon, Eclipse Ti). Large-field mosaic images were collected for each isolate by combining 24 separate images (each collected at 100 magnification) using a Nikon Eclipse Ti inverted microscope with a computer-controlled Prior stage, resulting in a 17424x17134 pixel composite image. This technique results in large sample sizes and minimizes sample bias arising from single images in which yeast touching the edge of the field of view are discarded.

Images were analyzed using ImageJ and Fiji image analysis software tools (Schindelin et al. 2012; Rueden et al. 2017).

Flow cytometry

All flow cytometry was carried out on a CyFlow Cube8 with autoloading station and cell-sorting cuvette (Sysmex). Samples can be loaded manually or automatically using an integrated autoloading station capable of handling up to 192 samples at a time (two 96-well plates). Prior to measurement, samples were diluted 1:10 into DI water, mixed by inverted (or using a custom mixing script in the case of the autoloader) and then run through the flow cytometer for 15 seconds to prime the instrument. After the flow rate reached equilibrium, data was cleared and collection began. After each sample, we performed the same procedure with DI water followed by a wash cycle to flush the instrument of any remaining yeast clusters.

FCS files were exported as CSV files using FSC Express software and analyzed in R (R Core Team 2018).

Measuring cluster size distributions

Cultures were acclimated in YPD prior to growth in the cue environment but experienced no size selection prior to measurement. Size measurements were collected via flow cytometry using side scatter (SSC) as a proxy for cluster size to enable high-throughput measurement. SSC was chosen as a proxy for cluster size because in a comparison of flow cytometric data collection channels (FSC, SSC, FL1) against cluster area measurements collected via microscopy, SSC was found to have the lowest Kullback-Leibler divergence (KLD = 0.0412 compared to 0.1137 and 0.0842 for FSC and FL1, respectively; see supplement for details, Fig. S3).

Size selection

Nylon mesh filters were used to selection for small or large yeast cluster sizes. Given the variance in mean cluster size across the 3 cue identity treatments, we tried to choose size thresholds that would select for small and large size, respectively, regardless of treatment. Selection for small cluster size was performed by passaging yeast cultures through a sterile 30μm nylon mesh filter (Sysmex, CellTrics®) and propagating only clusters that were small enough to pass through. Selection for large cluster size was performed by passaging yeast cultures through a sterile 70μm nylon mesh filter (Fisher Scientific, Corning®) then back-flushing to collect clusters that were too large to pass through. Filters were re-sterilized each day after use as follows: nylon filters were first soaked in a 1% bleach solution for >10 minutes, rinsed repeatedly in DI water (washed >5X), transferred to a 70% ethanol bath for 15 minutes, and then left to dry in an open sterile glass container inside of a laminar flow hood. Mesh filters were reused until they showed signs of wear.

Competition assay

Relative fitness of evolved isolates was assessed using pairwise competitions against a fluorescently marked competitor (Lenski et al. 1991; Desai et al. 2007). GFP-labeled strains were mixed with unlabeled strains at a 1:1 ratio by cluster number and grown in alternating environments (E_1, E_2, E_1) with selection for small and large size according to the cue reliability conditions experienced by the focal strain. Samples were taken at the beginning and end of the competition ($t = 0$ and $t = 72$), diluted 1:5 into 4ml of Methionine dropout media (6.7 g l^{-1} yeast nitrogen base without amino acids + 845 mg l^{-1} amino acid mix + 10 g l^{-1} dextrose) and grown for 2 hours to induce expression of GFP. Flow cytometry was used to determine the ratio of GFP-labeled and unlabeled strains. Six replicate competitions were run in parallel for each pair of strains. Relative fitness of fluorescently labeled strains was assessed as described above but in the absence of size selection in order to account for any potential negative effects on growth rate.

Statistical analyses

All statistical analyses were performed using the R software environment (R Core Team 2018).

Author contributions

All authors participated in the design of the evolution experiment; PLC, SER, and JHM conducted the pilot study; PLC performed the evolution experiment, data analyses and wrote the first draft of the manuscript.

Acknowledgements

We wish to thank Troy von Beck and Jennifer Pentz for help with the transformation of evolved yeast strains with an inducible GFP marker. Furthermore, we would like to thank members of the Kerr and Ratcliff labs for thoughtful comments on this project. This work was supported by NASA Exobiology grant #NNX15AR33G to WCR and the BEACON Center for the Study of Evolution in Action through NSF cooperative agreement number DBI-0939454 to BK. PLC was supported by the National Science Foundation Graduate Research Fellowship under Grant No. DGE-1256082 and funds made available by the UW Biology department.

References

Bell, G., and X. Reboud. 1997. Experimental evolution in *Chlamydomonas*. II. Genetic variation in strongly contrasted environments. Heredity 78:1–11.

Bradshaw, A. D. 1965. Evolutionary significance of phenotypic plasticity in plants. Advances in Genetics 13:115–155.

Chevin, L.-M., and R. Lande. 2015. Evolution of environmental cues for phenotypic plasticity. Evolution 69:2767–2775.

Cohen, D. 1966. Optimizing reproduction in a randomly varying environment. Journal of Theoretical Biology 12:119–129.

Desai, M. M., D. S. Fisher, and A. W. Murray. 2007. The speed of evolution and maintenance of variation in asexual populations. Current Biology 17:385–394.

DeWitt, T. J., and R. B. Langerhans. 2004. Integrated solutions to environmental heterogeneity: theory of multimoment reaction norms. Pages 98–111 in Phenotypic Plasticity: Functional and Conceptual Approaches. Oxford University Press.

DeWitt, T. J., and S. M. Scheiner. 2004. Phenotypic Plasticity: Functional and Conceptual Approaches. Oxford University Press.

Dewitt, T. J., A. Sih, and D. S. Wilson. 1998. Costs and limits of phenotypic plasticity. Trends in Ecology and Evolution 13:77–81.

Donaldson-Matasci, M. C., C. T. Bergstrom, and M. Lachmann. 2013. When unreliable cues are good enough. The American Naturalist 182:313–327.

Dorn, L. A., E. H. Pyle, and J. Schmitt. 2000. Plasticity to light cues and resources in *Arabidopsis thaliana*: Testing for adaptive value and costs. Evolution 54:1982–1994.

Ghalambor, C. K., J. K. McKay, S. P. Carroll, and D. N. Reznick. 2007. Adaptive versus non-adaptive phenotypic plasticity and the potential for contemporary adaptation in new environments. Functional Ecology 21:394–407.

Gietz, R. D., and R. H. Schiestl. 2007. Quick and easy yeast transformation using the LiAc/SS carrier DNA/PEG method. Nature Protocols 2:35–37.

Hasson, O. 1994. Cheating signals. Journal of Theoretical Biology.

Huey, R. B., and J. G. Kingsolver. 1989. Evolution of thermal sensitivity of ectotherm performance. Trends in Ecology and Evolution 4:131–135.

Izem, R., and J. G. Kingsolver. 2005. Variation in continuous reaction norms: quantifying directions of biological interest. The American Naturalist 166:277–289.

Jacobeen, S., E. C. Graba, C. G. Brandys, T. C. Day, W. C. Ratcliff, and P. J. Yunker. 2018. Geometry, packing, and evolutionary paths to increased multicellular size. bioRxiv 1–8.

Jacobeen, S., J. T. Pentz, E. C. Graba, C. G. Brandys, W. C. Ratcliff, and P. J. Yunker. 2017. Cellular packing, mechanical stress and the evolution of multicellularity. Nature Physics 1:1–6.

Kassen, R., and G. Bell. 1998. Experimental evolution in *Chlamydomonas*. IV. Selection in environments that vary through time at different scales. Heredity 80:732–741.

Lenski, R. E., M. R. Rose, S. C. Simpson, and S. C. Tadler. 1991. Long-term experimental evolution in *Escherichia coli*. I. Adaptation and divergence during 2,000 generations. The American Naturalist 138:1315–1341.

Lind, M. I., and F. Johansson. 2007. The degree of adaptive phenotypic plasticity is correlated with the spatial environmental heterogeneity experienced by island populations of *Rana temporaria*. Journal of Evolutionary Biology 20:1288–1297.

Lively, C. M. 1986. Predator-induced shell dimorphism in the acorn barnacle *Chthamalus anisopoma*. Evolution 40:232.

López, D., and R. Kolter. 2010. Extracellular signals that define distinct and coexisting cell fates in *Bacillus subtilis*. FEMS microbiology reviews 34:134–49.

López García de Lomana, A., A. Kaur, S. Turkarslan, K. D. Beer, F. D. Mast, J. J. Smith, J. D. Aitchison, et al. 2017. Adaptive prediction emerges over short evolutionary time scales. Genome Biology and Evolution 9:1616–1623.

Manenti, T., V. Loeschcke, N. N. Moghadam, and J. G. Sørensen. 2015. Phenotypic plasticity is not affected by experimental evolution in constant, predictable or unpredictable fluctuating thermal environments. Journal of Evolutionary Biology 28:2078–2087.

Maxwell, C. S., and P. M. Magwene. 2017. When sensing is gambling: an experimental system reveals how plasticity can generate tunable bet-hedging strategies. Evolution 71:859–871.

Maynard Smith, J., and D. Harper. 2003. Animal Signals. Oxford University Press.

Moran, N. A. 1992. The evolutionary maintenance of alternative phenotypes. The American Naturalist 139:971–989.

Murren, C. J., J. R. Auld, H. S. Callahan, C. K. Ghalambor, C. A. Handelsman, M. A. Heskel, J. G. Kingsolver, et al. 2015. Constraints on the evolution of phenotypic plasticity: limits and costs of phenotype and plasticity. Heredity 115:293–301.

Nelson, B., C. Kurischoko, J. Horecka, M. Mody, P. Nair, L. Pratt, A. Zougman, et al. 2003. RAM: a conserved signaling network that regulates Ace2p transcriptional activity and polarized morphogenesis. Molecular Biology of the Cell 14:3782–3803.

Oud, B., V. Guadalupe-Medina, J. F. Nijkamp, D. de Ridder, J. T. Pronk, A. J. a van Maris, and J.-M. Daran. 2013. Genome duplication and mutations in *ACE2* cause multicellular, fast-sedimenting phenotypes in evolved *Saccharomyces cerevisiae*. Proceedings of the National Academy of Sciences of the United States of America 110:E4223-31.

Philippi, T., and J. Seger. 1989. Hedging one's evolutionary bets, revisited. Trends in Ecology and Evolution 4:41–44.

R Core Team. 2018. R: A language and environment for statistical computing. R Foundation for Statistical Computing, Vienna, Austria.

Ratcliff, W. C., R. F. Denison, M. Borrello, and M. Travisano. 2012. Experimental evolution of multicellularity. Proceedings of the National Academy of Sciences 109:1595–600.

Ratcliff, W. C., J. D. Fankhauser, D. W. Rogers, D. Greig, and M. Travisano. 2015. Origins of multicellular evolvability in snowflake yeast. Nature Communications 6:6102.

Reboud, X., and G. Bell. 1997. Experimental evolution in *Chlamydomonas*. III. Evolution of specialist and generalist types in environments that vary in space and time. Heredity 78:507–514.

Rueden, C. T., J. Schindelin, M. C. Hiner, B. E. DeZonia, A. E. Walter, E. T. Arena, and K. W. Eliceiri. 2017. ImageJ2: ImageJ for the next generation of scientific image data. BMC Bioinformatics 18:1–26.

Sadeh, A., H. Guterman, M. Gersani, and O. Ovadia. 2009. Plastic bet-hedging in an amphicarpic annual: an integrated strategy under variable conditions. Evolutionary Ecology 23:373–388.

Scheiner, S. M. 1993. Genetics and evolution of phenotypic plasticity. Annual Review of Ecology and Systematics 24:35–68.

Scheiner, S. M. 2002. Selection experiments and the study of phenotypic plasticity. Journal of Evolutionary Biology 15:889–898.

Scheiner, S. M., and D. Berrigan. 1998. The genetics of phenotypic plasticity. VIII. The cost of plasticity in *Daphnia pulex*. Evolution 52:368.

Scheiner, S. M., and R. D. Holt. 2012. The genetics of phenotypic plasticity. X. Variation versus uncertainty. Ecology and evolution 2:751–67.

Scheiner, S. M., and L. Y. Yampolsky. 1998. The evolution of *Daphnia pulex* in a temporally varying environment. Genetic Research Cambridge 72:25–37.

Schindelin, J., I. Arganda-Carreras, E. Frise, V. Kaynig, M. Longair, T. Pietzsch, S. Preibisch, et al. 2012. Fiji: An open-source platform for biological-image analysis. Nature Methods 9:676–682.

Schlichting, C. D., and M. Pigliucci. 1998. Phenotypic Evolution: A Reaction Norm Perspective. Sinauer Associates Incorporated.

Schmitt, J., S. A. Dudley, and M. Pigliucci. 1999. Manipulative approaches to testing

adaptive plasticity: phytochrome-mediated shade-avoidance responses in plants. The American Naturalist 154:S43–S54.

Seger, J., and H. J. Brockmann. 1987. What is bet-hedging? Pages 182–211 in P. H. Harvey and L. Partridge, eds. Oxford Surveys in Evolutionary Biology (Vol. 4). Oxford University Press.

Sikkink, K. L., R. M. Reynolds, C. M. Ituarte, W. A. Cresko, and P. C. Phillips. 2014. Rapid evolution of phenotypic plasticity and shifting thresholds of genetic assimilation in the nematode *Caenorhabditis remanei*. G3 4:1103–1112.

Simons, A. M. 2014. Playing smart vs. playing safe: The joint expression of phenotypic plasticity and potential bet hedging across and within thermal environments. Journal of Evolutionary Biology 27:1047–1056.

Slatkin, M. 1974. Hedging one's evolutionary bets. Nature 250:704–705.

Smith, H. 2000. Phytochromes and light signal perception by plants–an emerging synthesis. Nature 407:585–91.

Snell-Rood, E. C., J. D. Van Dyken, T. Cruickshank, M. J. Wade, and A. P. Moczek. 2010. Toward a population genetic framework of developmental evolution: The costs, limits, and consequences of phenotypic plasticity. BioEssays 32:71–81.

Starrfelt, J., and H. Kokko. 2012. Bet-hedging – a triple trade-off between means, variances and correlations. Biological Reviews 87:742–755.

Sultan, S. E., and H. G. Spencer. 2002. Metapopulation structure favors plasticity over local adaptation. The American Naturalist 160:271–283.

Tufto, J. 2000. The evolution of plasticity and nonplastic spatial and temporal adaptations in the presence of imperfect environmental cues. The American Naturalist 156:121–130.

Van Buskirk, J. 2017. Spatially heterogeneous selection in nature favors phenotypic plasticity in anuran larvae. Evolution 71:1670–1685.

Van Buskirk, J., and R. A. Relyea. 1998. Selection for phenotypic plasticity in *Rana sylvatica* tadpoles. Biological Journal of the Linnean Society 65:301–328.

Via, S., R. Gomulkiewicz, G. De Jong, S. M. Scheiner, C. D. Schlichting, and P. H. Van Tienderen. 1995. Adaptive phenotypic plasticity: consensus and controversy. Trends in Ecology & Evolution 10:212–217.

Via, S., and R. Lande. 1985. Genotype-environment interaction and the evolution of phenotypic plasticity. Evolution 39:505–522.

Voth, W. P., A. E. Olsen, M. Sbia, K. H. Freedman, and D. J. Stillman. 2005. *ACE2*, *CBK1*, and *BUD4* in budding and cell separation. Eukaryot. Cell 4:1018–1028.

Yi, X., and A. M. Dean. 2016. Phenotypic plasticity as an adaptation to a functional trade-off. eLife 5:1–12.

Chapter 5

TRADE-OFFS DRIVE THE EVOLUTION OF INCREASED COMPLEXITY IN NASCENT MULTICELLULAR DIGITAL ORGANISMS

Peter L. Conlin[1] William C. Ratcliff[2,*]

[1]Department of Biology and BEACON Center for the Study of Evolution in Action, University of Washington, Seattle, WA 98195, United States of America

[2]Department of Biology, Georgia Institute of Technology, Atlanta, GA 30332, United States of America

∗ **corresponding author, email: will.ratcliff@biology.gatech.edu**

Keywords: multicellularity | trade-offs | complexity | digital evolution

Introduction

The transition to multicellularity was a major step in the evolution of large, complex life on Earth (Maynard Smith and Szathmáry 1995). Unlike other major evolutionary transitions, which have occurred only once (e.g., prokaryotes to eukaryotes), multicellularity has evolved multiple times in diverse lineages including archaea (Jahn et al. 2008), bacteria (Velicer and Vos 2009; Overmann 2010; Schirrmeister et al. 2011), and eukaryotes (Bonner 1998; King 2004; Grosberg and Strathmann 2007; Herron et al. 2013). Prior work suggests that the formation of simple clusters of cells, the first step in the transition to multicellularity, may be adaptive under a number of distinct ecological scenarios. For example, clusters may provide protection from predation (Kessin et al. 1996; Boraas et al. 1998), protection from environmental stress (Smukalla et al. 2008), or improved utilization of diffusible nutrients (Pfeiffer and Bonhoeffer 2003, Koschwanez et al. 2011; Koschwanez et al. 2013). Nevertheless, how and why nascent multicellular lineages evolve increased complexity remains a fundamental question in evolutionary biology. Progress has been impeded by a lack of experimental systems due to the fact that most nascent multicellular lineages have been lost to extinction.

To sidestep this historical limitation, we (and colleagues) have been using experimental evolution to re-create this major transition under controlled laboratory conditions (reviewed in Ratcliff and Travisano, 2014). Starting with outbred diploid unicellular yeast, we selected for cluster formation by favoring yeast that settle rapidly through liquid medium. In all ten replicate populations, cluster-forming 'snowflake' yeast readily evolved and displaced their unicellular ancestors. Snowflake yeast consist of daughter cells that remain attached after mitotic division, forming spherical branched structures of genetically-identical cells. Over the next several hundred generations, several traits of interest evolved as snowflake yeast further adapted to this selection regime.

In response to selection for rapid settling, snowflake yeast first evolved to form clusters

that contain more cells. Later, snowflake yeast evolved a 2.1-fold increase in the volume of individual cells, further increasing cluster biomass and thus settling speeds (Ratcliff et al. 2013). Large-bodied yeast also evolved higher rates of programmed cell death, hereafter referred to as apoptosis. Prior experiments suggest that these dead cells act as 'weak links' in the chains of cells that make up the cluster, resulting in greater reproductive asymmetry (i.e., smaller propagules relative to cluster size). This conclusion is based on comparisons between high and low-apoptosis strains, direct experiments modifying the frequency of apoptosis chemically, and the observation that dead cells are found at the site of propagule scission ~12 times more frequently than is expected by chance (Ratcliff et al. 2012).

Fitness trade-offs, while central to all of life history theory (Roff 2001), are thought to take on a particularly important role during major evolutionary transitions such as the evolution of multicellularity (Michod et al. 2006). Specifically, trade-offs between survival and reproduction may drive increases in complexity and cellular differentiation (Michod et al. 2006). Perhaps the best-known example comes from the evolution of multicellularity in the volvocine algae: individual cells cannot reproduce and phototax simultaneously (Koufopanou 1994), favoring the evolution of divided labor through germ-soma differentiation (Koufopanou 1994; Solari et al. 2006). More generally, simple clusters of cells may benefit from increased size (e.g., reduced consumption by predators [Boraas et al. 1998; Becks et al. 2012]), but cellular clusters face greater diffusional limitation than single-cells, impeding resource uptake from their environment (Lavrentovich et al. 2013). Our experimental results suggest that trade-offs also play a role in the evolution of multicellularity in snowflake yeast. Evolving larger clusters increases settling speed, but decreases growth rates, likely because cells in the interior of large clusters become resource limited as a result of greater diffusional impedance (Ratcliff et al. 2012; Lavrentovich et al. 2013). Similarly, increasing cell size may decrease the rate at which individual cells are produced, again because larger cells have a proportionally greater surface area to volume ratio (but see Jorgensen et al. 2002). The effects of apoptosis are a bit more complicated. A small fraction of the cells in the cluster (~1.5-2.5%) die, a

direct viability cost. However, by producing proportionally smaller propagules, large clusters produce offspring that are less diffusionally-limited. Thus, apoptosis increases growth rates but decreases survival during settling selection, and will only be adaptive when the sum of these effects is positive.

Here we investigate the role of simple trade-offs during the evolution of increased multicellular complexity in snowflake yeast by modeling the evolution of simple multicellular digital organisms. We find that apoptosis, which results in the production of smaller propagules at the expense of the acting cell's life, is adaptive under a broad suite of conditions. This is because it can increase growth rates enough to compensate for the loss of apoptotic cells and reduced survival during settling selection. In our models, competition for faster settling results in an evolutionary arms race that drives a modest (maximum of 150 cells) increase in cluster size and apoptosis. Much larger clusters only evolved if the size required for surviving settling selection was increased through time. Using a two-player tournament-style evolutionary algorithm, we find that snowflake yeast that are initially mismatched in size will niche partition, with the smaller strain evolving into a growth specialist and the larger strain a settling specialist. Finally, we find that increasing the dimensionality of the multicellular trait space from two (cells per cluster and apoptosis) to three (adding cell size) increases the degree to which competing strains in a single population will diverge. This work demonstrates that multicellular complexity readily arises when trade-offs between group size and growth rates are ameliorated by the evolution of novel multicellular traits.

Model description

Cluster growth and reproduction

The model we develop here considers competition occurring between two genetically distinct snowflake yeast strains within a single population. As in our laboratory experiments, the transfer cycle involves two discrete phases: growth and settling selection (summarized in Figure 1). For each time step, clusters grow by adding cells in proportion to their initial number following the equation:

$$n' = n(2 - nd) - na, \tag{5.1}$$

where n is cell number per cluster, d is the diffusional limitation cost (ranging from 0.001 to 0.002) and a is the rate of apoptosis (see Table 1 for a summary of model parameter). In comparison to single-cells, clusters are diffusionally-limited, and thus grow less rapidly (Ratcliff et al. 2012). For simplicity, we model the cost of diffusional limitation as a linear trade-off between cluster size (# of cells) and growth rate, such that a single cell doubles during each time step, and larger clusters grow to size $n(2 - nd)$ cells. Cluster growth is offset by apoptosis where the number of cells that undergo cell death at each time step is calculated as:

$$n(a) = \frac{n(\alpha - 0.5)}{50}, \tag{5.2}$$

Table 1: **Summary of model parameters**.

Parameter	Description	Base value
a	Rate of apoptosis	0.001
α	Reproductive asymmetry	0.55
d	Cost of diffusional limitation	0.001

Parameter	Description	Base value
n_{min}	Minimum number of cells within a cluster	1
n_{max}	Maximum number of cells within a cluster	2000
N	Population size	8×10^6
r	Size at reproduction	150
s	Size threshold for settling selection	140

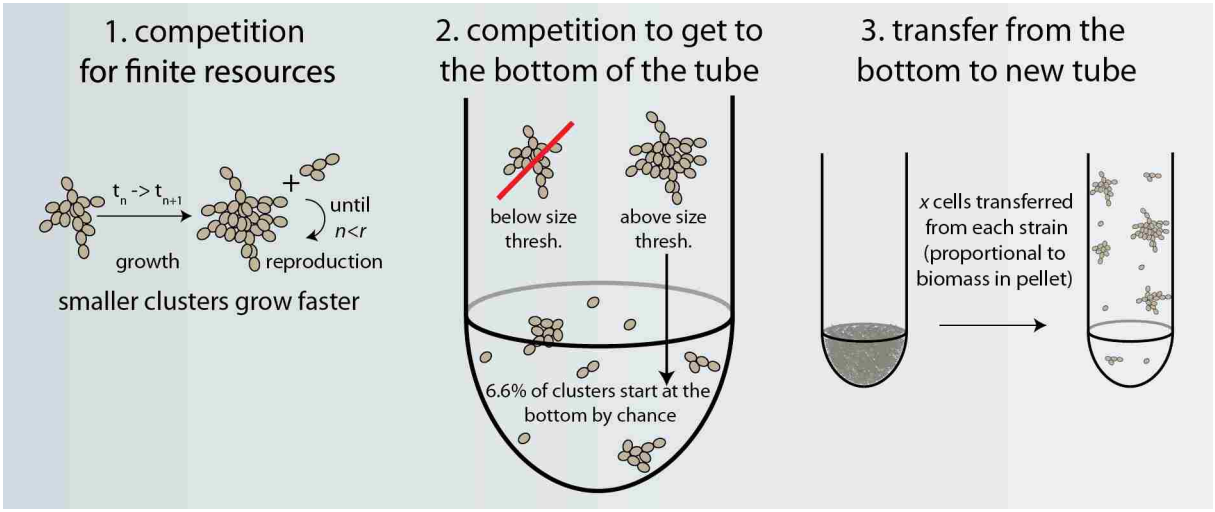

Figure 5.1: **Model schematic**. The model is separated into two distinct phases. First, clusters grow, competing for finite resources. Larger clusters face greater diffusional limitation and thus gain proportionally fewer cells during each time step. If a cluster's growth causes it to exceed its reproductive size r, then propagules are produced sequentially until cell number $n < r$. Settling selection is applied once resources are exhausted. All clusters above size threshold (thresh.) s settle to the bottom of the tube. Not all cells at the bottom are large, however: 6.6% of the clusters in the population simply start out there by chance. Finally, clusters are transferred to fresh medium. To allow for sufficient growth between rounds of settling selection, we transfer 1/20 of the stationary phase biomass to fresh medium. Clusters are transferred in proportion to the biomass of each strain in the pellet.

where α is reproductive asymmetry, a parameter that specifies the propagule size when a cluster undergoes reproduction (discussed below). For most of our simulations, the rate of apoptosis is equal to ~0.001 unless otherwise noted. For a 148-cell cluster growing up from

a 10-cell propagule during a single culture cycle, this corresponds to a cumulative death rate of 1.93%, which is similar to what we observe in our experiments (Ratcliff et al. 2012). Importantly, this step occurs before new cells are added so only cells $\geq$ one generation old are capable of dying from apoptosis.

When a cluster grows larger than r cells, they split, producing daughter propagules sequentially until they are smaller than the reproductive threshold. Offspring size depends on the cluster's reproductive asymmetry, α. Specifically, mean propagule size is $n(1-\alpha)$. Because snowflake yeast produce offspring that vary in size, we implemented a stochastic smoothing function into our model, such that asymmetry at each reproductive event is drawn from a uniform probability distribution bounded by $(\alpha - 0.05,\ \alpha + 0.05)$. Similarly, a cluster's size at reproduction is drawn from a uniform probability distribution bounded by $(r-5,\ r+5)$. This has the effect of preventing the accumulation of many clusters of exactly the same size, which can result in simulation artifacts (e.g., abrupt changes in fitness with small changes in traits). For all simulations, asymmetry was bounded between 0.5 and 0.9.

Population growth and settling selection

We model our experimental regime as two distinct phases, a growth phase and a settling phase. During the growth phase, resources are consumed by both strains of yeast until they are exhausted (in most simulation runs, we allow for 8×10^6 cellular reproductions) with each yeast strain growing and producing propagules according to the equations given above. After resource exhaustion, settling selection is applied. In our laboratory experiments, we transfer the cells found in the lower 100 µl of a microcentrifuge tube after settling selection to 10 ml of fresh medium. There are two ways that clusters can get to the bottom of the test tube: first, a small fraction of clusters (~6.6%) simply start out there after the tube is mixed. These clusters need not be large – they are simply lucky. Second, clusters can settle rapidly enough to sink to the bottom of the tube. Here, we impose a simple threshold, such that clusters containing more than s cells make it to the bottom of the test tube, and those smaller

do not. In our laboratory experiments, settling selection results in a 20 to 25-fold dilution per day for relatively fast-settling snowflake yeast. We model this by selecting clusters from each strain (in proportion to their biomass in the pellet) until 1/20 of the carrying capacity of the population is met. These clusters are then transferred to fresh medium and the cycle repeated.

In reality, settling selection is less precise: small clusters starting out just above the lower 100 µl may still join the pellet, while larger cluster starting at the very top of the tube may fail to make it to the bottom. Still, this simplifying assumption does not change the basic dynamics of size selection favoring larger sized clusters. Selection can be made more or less stringent by increasing or decreasing the threshold cluster size, s.

Results

Local fitness landscapes reveal the conditions favoring elevated apoptosis

We first examined the snowflake yeast fitness landscape under different nutrient diffusion regimes, d, as a function of both the rate of apoptosis and cluster size at reproduction. In each case, we competed a single strain (demarcated by the black circle in Figure 2a-d) against 1554 different competitor strains that varied in these traits. We measure relative fitness as the change in frequency of strain 1 cells relative to strain 2 cells between stationary phase in transfer two and stationary phase in transfer three. The threshold for surviving settling selection s was 140 cells, which is similar to what we have observed in early snowflake yeast (1-3 weeks of evolution). Competition between smaller clusters with little diffusional limitation (d=0.001) favors larger clusters with negligible apoptosis (Figure 2a). Increasing the severity of diffusional limitation ($d = 0.002$) favors elevated apoptosis (Figure 2c). We note, however, that the genotype with the highest fitness under these conditions still has the lowest rate of apoptosis. Among clusters that are much larger than the size necessary to survive settling selection (Figure 2b and 2d; which start out at size 225, but need only be

140 cells in size to survive selection), smaller size is beneficial. Importantly, higher rates of apoptosis can be selectively advantageous among these larger clusters, even when diffusional limitation is mild ($d = 0.001$).

Snowflake yeast compete in two key arenas: for resources during the 24 h of batch culture, and for a spot at the bottom of the tube during settling selection. It is in these two arenas where fitness trade-offs are realized. For example, large clusters settle quickly but grow slowly. By increasing reproductive asymmetry (reducing propagule size), increased rates of apoptosis should increase growth rates at the expense of survival during settling selection. Whether or not these traits are adaptive for a given environmental context depends on the benefit of faster growth relative to the cost of reduced survival during settling. To directly compare the magnitude of this fitness trade-off, we calculated the selection rate constants (following Travisano and Lenski 1996) for growth and settling for the landscape in Figure 2c. This approach allows us to compare each phase of competition using fitness as a common currency. As expected, elevated apoptosis increased growth rates, but reduced survival for settling selection, and larger cluster size was uniformly favored during settling (Figure 3). The benefits of faster growth out-weighed the cost of slower settling for part of the trait space (asymmetry between 0.62 and 0.75 and cluster size between 200-220 cells; Figure 2c). This result also highlights the fine-line being walked during the evolution of elevated apoptosis: mutations of large effect may produce strains with too much apoptosis, such that the costs of slower settling exceed the costs of faster growth.

Competition drives an evolutionary arms race for increased cluster size

Static fitness landscapes (e.g., Figures 2 and 3) are useful for examining the interaction between traits and fitness over only a limited range of conditions, because relative fitness is contextual and changes over evolutionary time along with the traits of the two competitors. To examine how cluster size and apoptosis rates might coevolve as the competitor also changes, we implemented a two-player evolutionary algorithm. For each time step, 10 deriva-

Figure 5.2: **Fitness landscapes vary depending on the extent of resource diffusion and on cluster size**. In each fitness landscape plotted above, a single strain (filled circle) competes against 1,554 competitor strains varying in cluster size at reproduction and apoptosis. Large size and low apoptosis are favored in small clusters with little diffusion limitation (A), while increasing the growth cost of diffusion favors smaller clusters with higher rates of apoptosis (C). Increasing cluster size at reproduction by 100 favors smaller cluster size (B, D). Apoptosis provides more of a benefit to larger clusters (lower region of B, D). Here $s = 140$, $d = 0.001$, and the growth phase contains sufficient resources for the production of 8×10^6 cells. The dashed line demarcates a relative fitness of 0.

Figure 5.3: **Disentangling fitness contributions from growth (a) and settling (b)**. We calculated the relative fitness consequences (as selection rate constants) during growth and settling for the landscape shown in figure 2c. Smaller cluster size at maturity and apoptosis increases fitness during growth at a cost to settling. Here $s = 140$, $d = 0.002$, and the growth phase contains sufficient resources for the production of 8×10^6 cells. The dashed line demarcates a selection rate constant of 0.

tives of each snowflake yeast genotype were generated, each with a 90% chance of mutation in cluster size at maturity or reproductive asymmetry. Each mutation was drawn from a normal distribution, with the mean being the former trait value with standard deviation of 1 (for cluster size at reproduction) or 0.003 (for reproductive asymmetry). All 10 variants of strain 1 were competed against last-round's strain 2 winner, then all 10 variants of strain 2 are competed against the best strain 1 variant. The strain with the highest relative fitness after three transfers was selected as the parent strain for the next round. For all simulations, the size threshold for surviving settling selection (s) was 140.

Figure 5.4: **Arms races and niche partitioning**. Larger clusters with higher rates of apoptosis evolve when both starting strains are similarly sized (a, b). If the initial size difference is substantial, arms-race dynamics are prevented, and instead the smaller strain evolves smaller size, becoming a growth specialist (c). The frequency of niche partitioning declines linearly as strain (Str.) 1's starting size increases from 150 to 160 (c, insert). Plotted are 100 simulations for each strain (strains 1 and 2 are demarcated by dark X's and light circles, respectively) over 150 transfers. Here $s = 140$, $d = 0.0015$, and the growth phase contains sufficient resources for the production of 2×10^6 cells.

When competition occurs between two similarly-sized strains, both readily evolve larger

cluster size and higher rates of apoptosis (Figure 4a and b). In contrast, when we compete two strains that vary substantially in size (150 vs. 200 cells at reproduction), snowflake yeast rapidly partition their niches (Figure 4c). Specifically, the 150-celled strain evolved to form clusters that were ~15 cells smaller than its ancestor over 150 rounds of competition against a 200-celled strain, while the same starting genotype evolved to form clusters that were an average of 67 cells larger when competed against another 150-celled strain (Figure 4a vs. 4c; $t_{157} = 114$, $p < 0.0001$, Bonferroni-corrected two-way t-test). This effect appears to be due to competitive exclusion during settling selection, driving the smaller strain to evolve smaller size and increased competitiveness during the growth phase of competition. We examined the size difference required for niche partitioning to occur, varying strain 1's starting size from 150 to 160 cells while leaving strain 2's starting size at 200 cells. For each competition, we ran 100 simulations for 150 transfers. The percent of runs in which strain 1 evolved to be a growth specialist declined linearly as their size increased ($y = 1503.9 - 9.3x$, $r^2 = 0.97$, $F_{1,10} = 254.9$, $p < 0.001$; Figure 4c, insert). Interestingly, we also found that the 200-celled strain evolved to form clusters that were ~30 cells larger when competing against another 200-celled strain, but not against a 150-celled strain (Figure 4b vs. 4c; $t_{196} = 30$, $p < 0.0001$, Bonferroni-corrected two-way t-test), further illustrating the importance of coevolution in our model. One caveat of this simulation is that it ensures coexistence of the two competing strains. It is possible that extinction in real populations would limit the ability for the evolution of niche partitioning.

The results of the two-player games (Figure 4) illustrate the importance of arms-race dynamics among similarly-sized competitors in the evolution of increased cluster size. The extent of directional change is limited, however, as the trade-off between settling and growth components of fitness result in stable coexistence at modest (250-340 cell) cluster size and low apoptosis (reproductive asymmetry ≈ 0.57, Figure 5a). To examine how size and apoptosis coevolve in response to different size-selection thresholds, we simulated competition in environments where the size threshold for surviving settling selection, s, varied from 50 to

750. We initialized each competition with two identical strains whose maximum size was just 10 cells larger than that required for settling, and then allowed them to come to equilibrium (1000 transfers per competition). While larger clusters readily evolved, they rarely got more than 150 cells larger than the threshold for surviving settling selection (Figure 5a, insert). Larger size clearly evolves in response to selection for faster settling, but imposing severe selection for rapid settling on small clusters can be counterproductive: selection cannot favor faster settling clusters if none survive. How then do large clusters evolve? In our experiments, we periodically increased the strength of settling selection (Ratcliff et al. 2013), favoring the progressive evolution of faster settling. We thus reran the above simulation, starting with a small snowflake yeast ($r = 140$), and increased the size of settling selection by 1 cell every 10 time steps. Here, much larger (>900 celled) clusters evolved, along with maximal rates of apoptosis (reproductive asymmetry ≈ 0.9 in strain 1, Figure 5B).

In our experiments, in addition to evolving an increased number of cells per cluster, snowflake yeast also evolved a 2.1-fold increase in cell size within two months (~400 generations, Ratcliff et al. 2013), increasing the settling speed of clusters. We thus modified the model to allow for the evolution of increased cell size, changing the settling selection step to count cluster biomass equivalents in addition to cell number. Further, we imposed a linear growth penalty for larger cells, assuming that cells with twice the volume grow at 98% the speed of a wild type cell. We repeated the two-player tournament simulations, allowing for mutations that increase cell size to occur with 90% probability (the distribution of mutational effect sizes was identical to that of reproductive asymmetry). Increasing the strength of settling selection was again essential for the evolution of both large and many-celled snowflake yeast (Figure 6).

Increasing the dimensionality of the multicellular trait space makes it possible for genetically and phenotypically distinct strains to arrive at the same multicellular solution (i.e., strains differing in cell size and cell number can nonetheless evolve the same overall cluster biomass). To examine how allowing a third multicellular trait to evolve affected

Figure 5.5: **Pushing the envelope—the evolution of large clusters**. (a) When the environment is constant ($s = 140$ for all 7,600 transfers), equilibrium dynamics rapidly establish themselves with the evolution of modest cluster size and low apoptosis. For a range of s from 50–750, cluster size at equilibrium (1,000 transfers, purple circles in 5a inset) is only modestly larger than required for surviving settling selection (black line, inset). (b) Slowly ratcheting up the threshold for settling to the bottom of the tube (s starts at 140 and increases by 1 every 10 transfers) results in the evolution of very large clusters with high rates of apoptosis. Filled circles and triangles refer to the two strains in competition. In these simulations the growth phase contains sufficient resources for the production of 2×10^6 cells and $d = 0.001$.

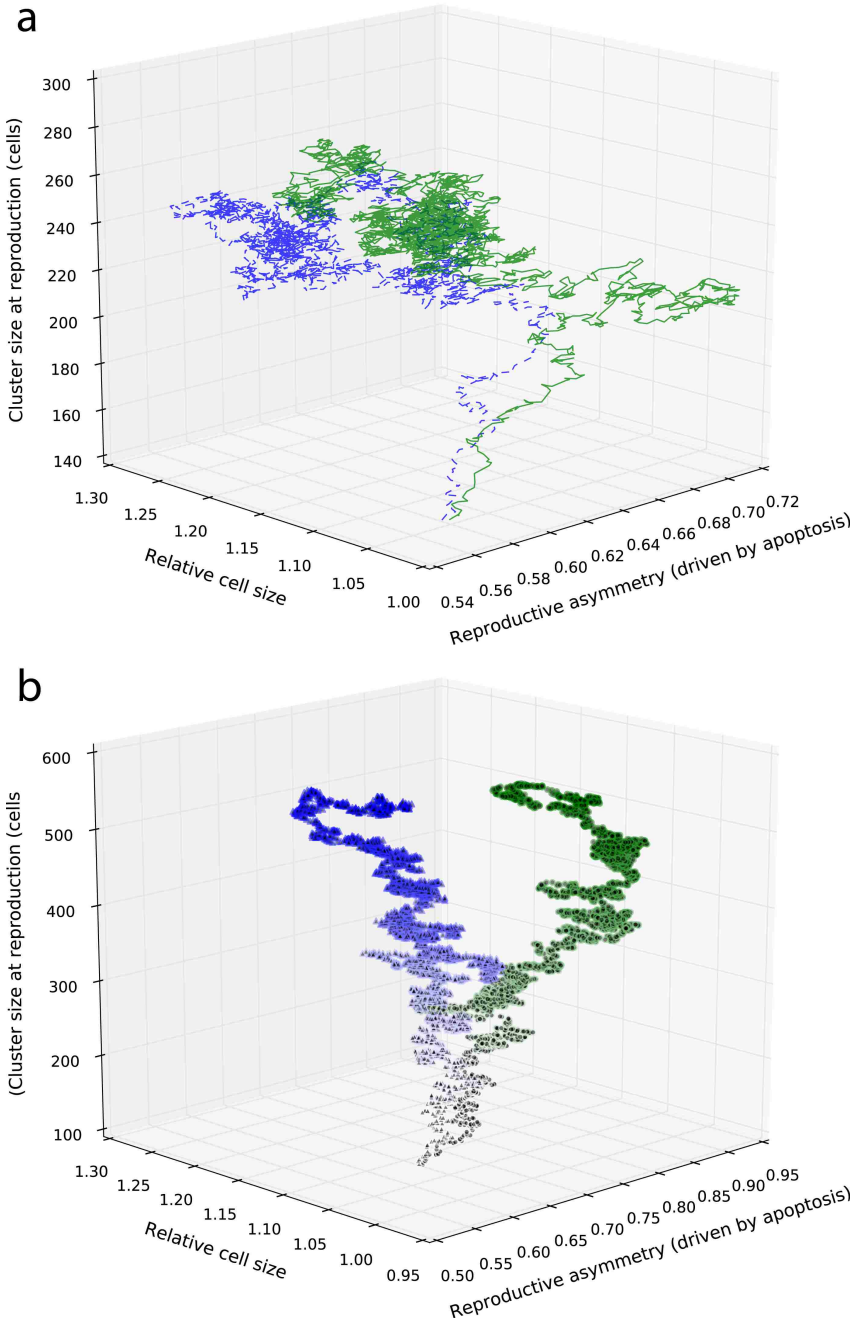

Figure 5.6: **Evolution of larger cell size**. Coevolution in a static ($s = 140$; a) or gradually more stringent size-selective environment (s starts at 140 and increases by 1 every 10 transfers; b). Increasing the strength of settling selection favors the evolution of all three key multicellular traits: large cluster size at reproductive maturity, high rates of apoptosis, and large individual cells. Here the growth phase contains sufficient resources for the production of 2×10^6 cells, $d = 0.001$, and marker shade reflects the yeast strain.

within-population divergence, we calculated the Euclidian distance of normalized trait values between competitors in each microcosm, either with or without cell size mutations, after equilibrium was reached (1000 time steps, $s = 140$). Increasing the dimensionality of the multicellular trait-space increased the opportunity for within-population diversification: competitors were an average of 32% more phenotypically divergent ($t_{196.7} = 3.07$, $p = 0.0024$, two-sided t-test) when cell size was allowed to evolve (Figure 7). Because there was only a 1% difference in cluster biomass (mean of 272 and 279 wild type cell equivalents for 2D and 3D simulations, respectively) and no difference in apoptosis (mean of 55.9% for both 2D and 3D simulations), it appears that yeast capable of evolving both greater cell number per cluster and larger cell size took different, though ecologically equivalent, paths to increased cluster size. This demonstrates that the evolution of additional multicellular traits may, as a side effect, increase the population's capacity to support the coexistence of ecologically equivalent (though genetically and phenotypically distinct) isolates.

Discussion

One of the most surprising results from our yeast experiments is the rapidity of adaptation after simple multicellularity evolves. After just ~400 generations, snowflake yeast evolve to form clusters containing twice as many cells, higher rates of apoptosis, and cells that are more than twice as large as the ancestor. These clusters settled 28% faster, on average (Ratcliff et al. 2013). Further, we have found that after a similar length of time (but in a different experiment), 9/10 replicate populations contained at least two strains that varied in size (Rebolleda-Gomez et al. 2012). The modeling results presented above help to explain both of these observations.

In both this model and in evolving populations of yeast (Ratcliff et al. 2012; Ratcliff et al. 2013), initially-small clusters of cells are under strong selection for increased size. The model described here shows why: even small increases in settling speed dramatically improve relative fitness, and at this small size, diffusional limitation is not yet very restrictive. As a

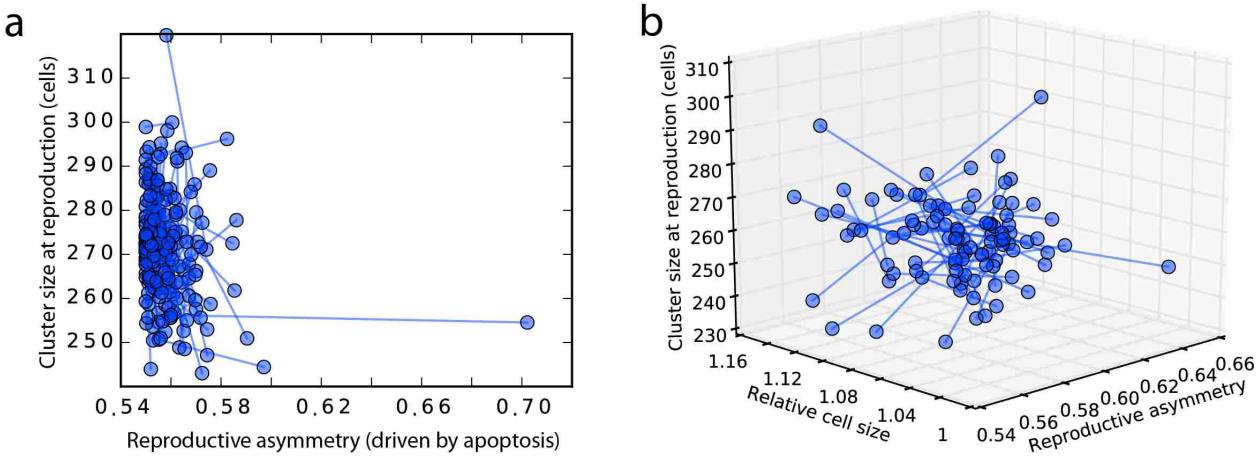

Figure 5.7: **Divergence in 2-D versus 3-D games**. Competing pairs of snowflake yeast evolved more divergent multicellular traits, measured as the Euclidian distance of each competitor after 1,000 generations. Plotted are the results of 2-D simulations where cell size was held constant (A) and 3-D simulations where cell size was allowed to evolve (B).

result, competition among co-evolving yeast results in a short-term arms race for increased size. As larger cluster size evolves, apoptosis becomes increasingly beneficial, allowing large-bodied yeast to produce proportionally smaller offspring that are temporarily freed from strong diffusional limitation. Competition in a static environment (no change in s) thus results in a modest increase in both size and apoptosis. However, we find that for very large, high apoptosis clusters to evolve, the strength of settling selection must increase through time. Long-term experiments running in our lab suggest that this increase in the strength of settling selection is also required for the in vitro evolution of large snowflake yeast clusters (unpublished).

Apoptosis readily evolves in this simple simulation model, ameliorating the growth rate cost incurred by large body size. This effect appears to be due to the fact that apoptosis produces proportionally smaller offspring that have a growth rate advantage when resource diffusion is more limiting. Specifically, increased rates of apoptosis are favored under conditions of low resource penetration into the cluster (high d), or for low values of d, as a

consequence of selection favoring the evolution of progressively larger slower growing clusters (but see Duran-Nebreda and Solé 2015 for a non-adaptive explanation for elevated rates of apoptosis). Apoptosis may therefore be a general solution to the biophysical constraint of diffusionally-limited growth so long as: i) selection favors larger clusters of cells, ii) larger clusters grow less rapidly than smaller clusters, iii) cell death results in propagule production, and iv) propagules that are produced by apoptosis are related (high Hamliton's r) (Hamilton 1964) to apoptotic cells. Both iii and iv likely require that clusters are formed through incomplete mother-daughter cell separation. Finally, it is also important that propagules have sufficient time to grow large enough to survive the next round of size-based selection.

Programmed cell death (PCD, a category of cell death mechanisms that includes apoptosis) plays a critical role in the evolution of multicellular complexity. In independently-evolved multicellular lineages, PCD is used to modify multicellular form during development (Jacobson et al. 1997; Pennell and Lamb 1997; Umar and Van Griensven 1997), plays a central role maintaining the multicellular body (e.g., removal of damaged [Jacobson et al. 1997], infected [Lam 2004] or cancerous cells [Lee and Bernstein 1995]), and can be useful in coordinated multicellular behaviors (e.g., leaf abscission [Bleecker and Patterson 1997]). Indeed, PCD plays such an important role in multicellular organization that it is difficult to imagine complex multicellular life in its absence. PCD, however, is not a multicellular invention: many diverse unicellular organisms possess active, genetically regulated cell death mechanisms (Nedelcu et al. 2011). Comparative work demonstrates that some PCD pathways in multicellular organisms arose in their unicellular ancestors (Nedelcu 2009), suggesting they were co-opted for novel use after the transition to multicellularity. The work presented here provides a simple, general explanation for how unicellular PCD can be co-opted for a novel multicellular purpose. See Duran-Nebreda et al. (this volume) for a discussion of how multicellular complexity can emerge as a consequence of interactions among the component cells.

Within-population diversity is present in both our lab experiments (Rebolleda-Gomez

et al. 2012), and this simulation model. The model predicts that some of this diversity may simply be the result of different lineages taking divergent trajectories during adaptation (Figures 5 and 6). This may be especially important when the multicellular trait-space is high dimensional, because, all else equal, these contain a greater number of ecologically equivalent trajectories. There are a number of potential multicellular traits that we did not include in the model, but which may be relevant and would further increase the dimensionality of the multicellular trait-space. For example, the architecture of snowflake yeast clusters (Libby et al. 2014) might change, affecting both d and how size relates to surviving during settling selection. This can be due to simple alterations, like the shape of individual cells, or more complex modifications. Indeed, after 227 days of selection, we see the evolution of more spherical, hydrodynamic clusters that settle 35% faster per increase in unit mass (Ratcliff et al. 2013). We do not yet know the mechanistic basis of this trait, but it is potentially due to a modified branching pattern, or changes in the location and timing of cellular apoptosis.

How multicellular complexity arises in evolution is a fundamental question in biology. In combination with our experimental work (Ratcliff et al. 2012; Rebolleda-Gomez et al. 2012; Ratcliff et al. 2013; Ratcliff et al. 2015), the results described here demonstrate that multicellular complexity readily arises as a solution to a trade-off between selection for fast growth and large size. While selection for rapid sedimentation is likely not a good proxy for natural systems, selection for large size is certainly common in microbial populations (e.g., cluster formation increases survival in the face of predators [Kessin et al. 1996; Boraas et al. 1998; Becks et al. 2012], but cluster formation slows growth [Yokota and Sterner 2011; Becks et al. 2012]). This work, along with other pioneering work experimentally evolving novel multicellularity (Boraas et al. 1998; Rainey and Rainey, 2003; Koschwanez et al. 2011; Koschwanez et al. 2013; Ratcliff et al. 2013), has shown that the first steps in this transition readily occur. The challenge before us is to determine how more complex, functionally integrated multicellular individuals (e.g., an organism that consists of multiple cell types whose multicellular life cycle is developmentally regulated) evolve from simple multicellular

ancestors.

Acknowledgements

We would like to thank Ben Kerr, Vidyanand Nanjundiah, Kayla Peck, and Jennifer Pentz for thoughtful comments on this manuscript and the Konrad Lorenz Institute for funding/hosting the meeting where this work was first presented. This work was supported by NASA Exobiology grant #NNX15AR33G.

References

Becks L., S. P. Ellner, L. E. Jones, and N. G. Hairston. 2012. The functional genomics of an eco-evolutionary feedback loop: linking gene expression, trait evolution, and community dynamics. *Ecology Letters*, 15: 492-501.

Bleecker A. B., and S. E. Patterson. 1997. Last exit: senescence, abscission, and meristem arrest in *Arabidopsis*. *Plant Cell*, 9: 1169-1179.

Bonner J. T. 1998. The origins of multicellularity. *Integrative Biology: Issues, News, and Reviews*, 1: 27-36.

Boraas M. E., D. B. Seale, and J. E. Boxhorn. 1998. Phagotrophy by a flagellate selects for colonial prey: a possible origin of multicellularity. *Evolutionary Ecology*, 12: 153-164.

Duran-Nebreda, S., and R. Solé. 2015. Emergence of multicellularity in a model of cell growth, death and aggregation under size-dependent selection. *Journal of The Royal Society Interface*, 12: 20140982.

Grosberg R. K., and R. R. Strathmann. 2007. The evolution of multicellularity: A minor major transition? *Annual Review of Ecology, Evolution, and Systematics*, 38: 621-654.

Hamilton W. D. 1964. The genetical evolution of social behavior. I. *Journal of Theoretical Biolology*, 7: 1-16.

Herron M. D., A. Rashidi, D. E. Shelton, and W. W. Driscoll. 2013. Cellular differentiation and individuality in the 'minor' multicellular taxa. *Biological Reviews*, 88: 844-861.

Herron M. D., J. D. Hackett, F. O. Aylward, and R. E. Michod. 2009. Triassic origin and early radiation of multicellular volvocine algae. *Proceedings of the National Academy of Sciences*, 106: 3254-3258.

Jacobson M. D., M. Weil, and M. C. Raff. 1997. Programmed cell death in animal development. *Cell*, 88: 347-354.

Jahn U., M. Gallenberger, W. Paper, B. Junglas, W. Eisenreich, K. O. Stetter, R. Rachel, and H. Huber. 2008. *Nanoarchaeum equitans* and *Ignicoccus hospitalis*: new insights into a unique, intimate association of two archaea. *Journal of Bacteriology*, 190: 1743-1750.

Jorgensen, P., Nishikawa, J. L., Breitkreutz, B. J., and M. Tyers. 2002. Systematic identification of pathways that couple cell growth and division in yeast. *Science*, 297: 395-400.

Kessin, R. H., Gundersen, G. G., Zaydfudim, V., and M. Grimson. 1996. How cellular slime molds evade nematodes. *Proceedings of the National Academy of Sciences*, 93: 4857-4861.

King N. 2004. The unicellular ancestry of animal development. *Developmental Cell*, 7: 313–325

Koufopanou, V. 1994. The evolution of soma in the Volvocales. *American Naturalist*, 143: 907-931.

Koschwanez J. H., Foster K. R., and A. W. Murray. 2013. Improved use of a public good selects for the evolution of undifferentiated multicellularity. *eLife*, 2: e00367.

Koschwanez J. H., Foster K. R., and A. W. Murray. 2011. Sucrose utilization in budding yeast as a model for the origin of undifferentiated multicellularity. *PLOS Biology*, 9: e1001122.

Lam E. 2004. Controlled cell death, plant survival and development. *Nature Reviews*

Molecular Cell Biology, 5: 305-315.

Lee J. M., and A. Bernstein. 1995. Apoptosis, cancer and the p53 tumour suppressor gene. *Cancer Metastasis Review*, 14: 149-161.

Libby E., W. Ratcliff, M. Travisano, and B. Kerr. 2014. Geometry shapes evolution of early multicellularity. *PLOS Computational Biology*, 10: e1003803 .

Maynard Smith J., and E. Szathmáry. 1995. *The major transitions in evolution*. Oxford University Press.

Michod, R. E., Viossat, Y., Solari, C. A., Hurand, M., and A. M. Nedelcu. 2006. Life-history evolution and the origin of multicellularity. *Journal of Theoretical Biology*, 239: 257-272.

Nedelcu A. 2009. Comparative genomics of phylogenetically diverse unicellular eukaryotes provide new insights into the genetic basis for the evolution of the programmed cell death machinery. *Journal of Molecular Evolution*, 68: 256-268.

Nedelcu A. M., W. W. Driscoll, P. M. Durand, M. D. Herron, and A. Rashidi. 2011. On the paradigm of altruistic suicide in the unicellular world. *Evolution*, 65: 3-20.

Overmann J. 2010. The phototrophic consortium "*Chlorochromatium aggregatum*"–a model for bacterial heterologous multicellularity. In P. C. Hallenbeck (Ed.), *Recent Advances in Phototrophic Prokaryotes* (pp. 15-29). Springer, NY.

Pennell R. I., and C. Lamb. 1997. Programmed cell death in plants. *Plant Cell*, 9: 1157-1168.

Pfeiffer, T., and S. Bonhoeffer. 2003. An evolutionary scenario for the transition to undifferentiated multicellularity. *Proceedings of the National Academy of Sciences*, 100: 1095-1098.

Rainey, P. B., and K. Rainey. 2003. Evolution of cooperation and conflict in experimental bacterial populations. *Nature*, 425: 72-74.

Ratcliff W. C., and M. Travisano. 2014. Experimental evolution of multicellular complexity in *Saccharomyces cerevisiae*. *BioScience*, 64: 383-393.

Ratcliff W. C., M. D. Herron, K. Howell, J. T. Pentz, F. Rosenzweig, and M. Travisano. 2013. Experimental evolution of an alternating uni-and multicellular life cycle in *Chlamydomonas reinhardtii*. *Nature Communications*, 4: 2742.

Ratcliff W. C., R. F. Denison, M. Borrello, and M. Travisano. 2012. Experimental evolution of multicellularity. *Proceedings of the National Academy of Sciences*, 109: 1595-1600.

Ratcliff W. C., J. T. Pentz, and M. Travisano. 2013. Tempo and mode of multicellular adaptation in experimentally-evolved *Saccharomyces cerevisiae*. *Evolution*, 67: 1573-1581.

Ratcliff, W. C., Fankhauser, J. D., Rogers, D. W., Greig, D., and M. Travisano. 2015. Origins of multicellular evolvability in snowflake yeast. *Nature Communications*, 6: 6102.

Rebolleda-Gomez M., W. Ratcliff, and M. Travisano. 2012. Adaptation and Divergence during Experimental Evolution of Multicellular *Saccharomyces cerevisiae*. In *Artificial Life* (Vol. 13, pp. 99-104).

Roff, D. A. 2002. *Life history evolution*. Sinauer Associates.

Schirrmeister B. E., A. Antonelli, and H. C. Bagheri. 2011. The origin of multicellularity in cyanobacteria. *BMC Evolutionary Biology*, 11: 45.

Smukalla, S., Caldara, M., Pochet, N., Beauvais, A., Guadagnini, S., Yan, C., … and K. J. Verstrepen. 2008. *FLO1* is a variable green beard gene that drives biofilm-like cooperation in budding yeast. *Cell*, 135: 726-737.

Solari, C. A., Kessler, J. O., and R. E. Michod. 2006. A hydrodynamics approach to the evolution of multicellularity: flagellar motility and germ-soma differentiation in Volvocalean green algae. *The American Naturalist*, 167: 537-554.

Travisano M., and R. E. Lenski. 1996. Long-term experimental evolution in *Escherichia*

coli. IV. Targets of selection and the specificity of adaptation. *Genetics*, 143: 15-26.

Umar M. H., and L. Van Griensven. 1997. Morphogenetic cell death in developing primordia of *Agaricus bisporus*. *Mycologia*, 89: 274-277.

Velicer G. J., and M. Vos. 2009. Sociobiology of the myxobacteria. *Annual Review of Microbiology*, 63: 599-623.

Yokota K., and R. W. Sterner. 2011. Trade-offs limiting the evolution of coloniality: ecological displacement rates used to measure small costs. *Proceedings of the Royal Society of London B*, 278: 458-463.

Chapter 6

GAMES OF LIFE AND DEATH: ANTIBIOTIC RESISTANCE AND PRODUCTION THROUGH THE LENS OF EVOLUTIONARY GAME THEORY

Peter L. Conlin[1] Josephine Chandler[2] Benjamin Kerr[1,*]

[1]Department of Biology and BEACON Center for the Study of Evolution in Action, University of Washington, Seattle, WA 98195, United States of America

[2]Department of Molecular Biosciences, University of Kansas, Lawrence, KS 66045, United States of America

∗ **corresponding author, email: kerrb@uw.edu**

Keywords: game theory | evolution | antibiotic resistance

Abstract

In this review, we demonstrate how game theory can be a useful first step in modeling and understanding interactions among bacteria that produce and resist antibiotics. We introduce the basic features of evolutionary game theory and explore model microbial systems that correspond to some classical games. Each game discussed defines a different category of social interaction with different resulting population dynamics (exclusion, coexistence, bistability, cycling). We then explore how the framework can be extended to incorporate some of the complexity of natural microbial communities. Overall, the game theoretical perspective helps to guide our expectations about the evolution of some forms of antibiotic resistance and production because it makes clear the precise nature of social interaction in this context.

Introduction

Although antibiotic resistance has been traditionally viewed as asocial, recent studies show that in some important cases antibiotic resistance is in fact the product of social interactions [1–5]. For example, an extracellular enzyme that inactivates an antibiotic can protect both the bacterium that produces it and its neighbors [6,7]. In such cases, drug susceptibility depends on social context. Social interactions are also important in the case of antibiotic production, where the density of producers can considerably impact the survival of sensitive competitors.

Here we demonstrate how evolutionary game theory [8,9], a mathematical framework focused on social interaction, is particularly helpful in understanding evolutionary outcomes in circumstances where antibiotic resistance and production involve a social dimension. Evolutionary game theory has been successfully applied to study topics including the evolution of cooperation [10,11], ritual fighting among animals [12], and more recently to the study of microbial interactions [13–18], but its usage in cases of antibiotic resistance and production is less common. In the following sections, we will review some basic features of game theory,

highlight microbial systems that exhibit classical game dynamics, discuss natural features that increase the complexity of the framework, and suggest some possible areas of interest for future study.

Game theory basics

In classical game theory [19], a game is a contest between individual players. Each player employs a strategy that yields some payoff. Generally the payoff to a player using a given strategy depends on the strategy employed by its partner(s). A simple illustration of this can be seen in the child's game Rock-Paper-Scissors, which is a two-player game with three strategies. This game is non-transitive: each strategy beats one other strategy and is beaten by the third. Specifically, Rock crushes Scissors, Scissors cuts Paper, and Paper covers Rock. Were you to play this game with a friend, your payoff would be given by the following table (or payoff matrix):

Table 6.1: **Payoff matrix for Rock-Paper-Scissors**

	Your partner's strategy		
	Rock	Paper	Scissors
Your strategy			
Rock	*Draw*	*Lose*	*Win*
Paper	*Win*	*Draw*	*Lose*
Scissors	*Lose*	*Win*	*Draw*

This game illustrates how the payoff of one player's strategy can be conditional on the strategy of another player. Playing Rock is exactly the right thing to do if your partner plays Scissors, but is precisely the wrong thing to do if your partner decides on Paper.

In evolutionary game theory, the focus shifts from the handful of players in a single game to a very large population of individuals playing many instances of a game in parallel[8]. The strategies are genetically determined and the payoffs are expressed in terms of fitness, which can be organized into a fitness matrix (similar to the payoff matrix above).The most successful genotype has the most offspring. Because offspring inherit the strategy of their parent, successful genotypes increase in proportion in the population. When a genotype that is very rare employs the most successful strategy, it is said to "invade" the population. Under certain conditions (see Supplement I), the fitness matrix contains all the information necessary to predict such evolutionary invasion [20,21].

To illustrate the idea, we consider a two-player game in which it is possible for an individual to produce a compound (termed a "public good") that benefits itself and its partner. There are two genotypes in this game: producers (**P**) and non-producers (**N**), and one possible fitness matrix is shown in Figure 1a. This fitness matrix assumes that the cost of production outweighs the benefit a producer receives from its own production. When **P** is common and **N** is rare, both genotypes tend to pair up with **P** partners when pairs form randomly. Because genotype **N** has a higher fitness than genotype **P** in such matches (i.e., $4 > 3$ in Fig. 1a), **N** can invade. Conversely, when **N** is common and **P** is rare, genotype **P** fails to invade because it has a lower fitness than **N** (i.e., $1 < 2$ in Fig. 1a). In this case, we say that **N** is stable to invasion, and genotype **N** is termed an Evolutionarily Stable Strategy (ESS). In this example, a pair of producers has higher collective fitness than a pair of non-producers (as in Fig. 1a). This is an instance of the famous Prisoner's Dilemma [10]. Despite initial proportions, **N** is predicted to drive **P** to extinction (Fig. 1b). Here, evolution is predicted to eliminate public good production, lowering average fitness in the process.

More generally, inequalities in the fitness matrix govern whether each genotype is an ESS. In a two-strategy two-player game (Fig. 1c) there are four possible ESS configurations (Figs. 1d-1g). Each configuration corresponds to a distinct evolutionary outcome. Specifically, the form of the fitness matrix determines whether a certain genotype dominates, whether

coexistence is predicted, or whether initial genotype proportions matter. That is, the nature of the game informs us about evolution of the population. In the next few sections we will illustrate this connection, where we discuss cases of antibiotic resistance and production as simple games, revisiting some of the evolutionary behavior shown in Figure 1.

Antibiotic resistance: the dilemma of being 'snowed in'

A common mechanism of antibiotic resistance in bacteria involves the production of an enzyme that deactivates the antibiotic [22,23]. For instance, β-lactamase hydrolyzes β-lactam antibiotics (e.g., ampicillin). This enzyme is costly to produce and can work outside the producing cell [24], and thus might be considered a public good. (Note, even if detoxification of the drug occurs exclusively within the cell it can still be considered a public good because it detoxifies the local environment [25,26].) We discussed costly public good production in the context of the Prisoner's Dilemma (Fig. 1a), which makes a clear evolutionary prediction: in a population of producers and non-producers, the producers are driven to extinction (Fig. 1b). Does the β-lactamase system conform to the predictions of the Prisoner's Dilemma?

Recent studies of β-lactamase production in *Escherichia coli* have shown that producer and non-producer cells can coexist in an environment containing ampicillin [1,3] Indeed, Yurtsev et al. [3] found that producer cells settled to a stable equilibrium regardless of initial proportions (Fig. 2a). This is not consistent with the predictions of the Prisoner's Dilemma, as producers have a relative growth advantage when rare [15]. This deviation can be explained by the finding that the antibiotic-degrading enzyme is primarily contained in the periplasmic space of the producing cell [6,24]; thus, there is partial "privatization" of the public good (Fig. 2b). When producers are rare, their private detoxification yields an advantage over the non-producers that depend solely on public detoxification.

The dynamics exhibited in the above experiments can be understood as a Snowdrift game [27,28]. In this game, two drivers are stuck behind a snowdrift. Each has the option of staying in their car or clearing a path. The payoff is always greater if you choose to do the opposite of

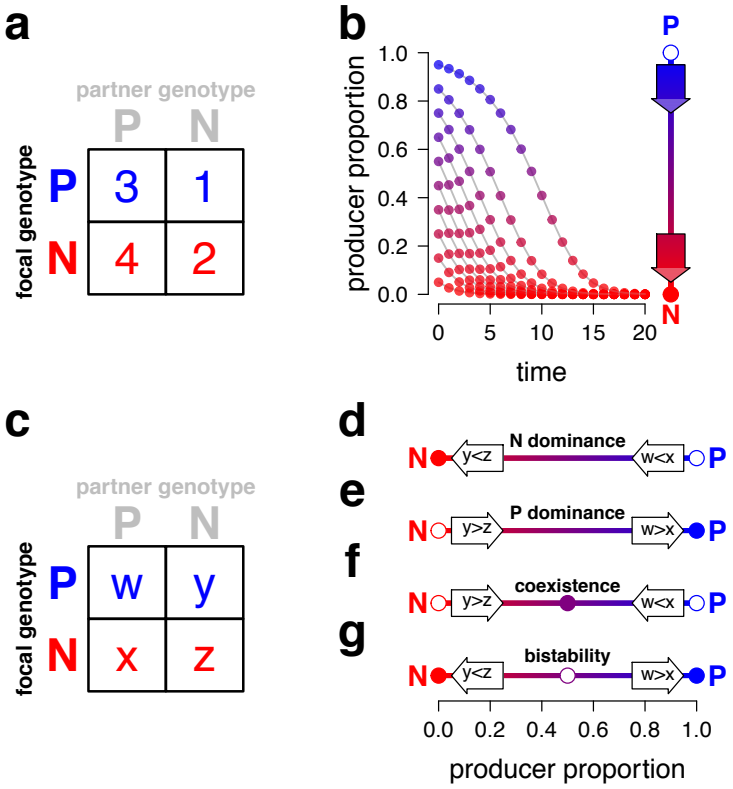

Figure 6.1: **Two-player two-strategy evolutionary games.** (a) The fitness matrix for a game between producers (**P**) and non-producers (**N**) of a public good (see Supplement for details). This matrix conforms to the Prisoner's Dilemma. Fitness of a focal player depends not only on its genotype (blue or red rows) but also the genotype of its partner (columns). (b) Predicted population dynamics of a simple game theoretical model, given the fitnesses in part a (see Supplement for details). Despite its initial proportion, the producer approaches extinction. The vertical line segment to the right is identical to the y-axis of the graph and large circles represent equilibria. Because **N** will invade a population of mostly **P** (top arrow), fixation for **P** is an unstable equilibrium (unfilled circle). Because **P** fails to invade a population of mostly **N** (bottom arrow), fixation for **N** is a stable equilibrium (filled circle) and **N** is an ESS. (c) A generic fitness matrix for a two-strategy two-player game. The fitness of a focal **P** individual (blue entries) is and when paired with a partner of genotype **P** and **N**, respectively. The fitness of a focal **N** individual (red entries) is and when paired with **P** and **N**, respectively. (d-g) Here we rotate the vertical line segment of part b clockwise by 90. If , **N** will invade a population of **P**. If , **P** will invade a population of **N**. On the other hand, if or , then **P** or **N**, respectively, is an ESS. (d) For the Prisoner's Dilemma, **P** fixation is unstable and N is stable to invasion (i.e., **N** the sole ESS). (e) When the fitness inequalities are reversed, **N** fixation is unstable and P is the sole ESS. (f) When both fixation states are unstable (i.e., no ESS), stable coexistence is achieved (purple filled circle). (g) When both fixation states are stable (i.e., two ESS's), either strategy can dominate depending on whether the initial proportion of **P** is above or below the unstable equilibrium (purple unfilled circle). Such dynamics are termed bistable.

your opponent. Analogously, when there are many producing cells in a population it pays to not produce, as the cost of production is avoided (compare entries in the first column of Fig. 2c). Conversely, when there are many non-producing cells in a population it pays to produce, as greater protection from the antibiotic is achieved (compare entries in the second column of Fig. 2c). If interactions occur randomly, then average fitnesses of the two strategies cross as the producer proportion increases (Fig. 2d) and a stable equilibrium is predicted (Fig. 2e and Fig. 1f). When moving from the Prisoner's Dilemma (Fig. 1d) to the Snowdrift game (Fig. 1f) the ordering of fitnesses of the two genotypes when paired with a non-producer has flipped (compare payoff matrices in Fig. 1a and Fig. 2c). Given that partial privatization is common among many public good systems [15,26,29], the Snowdrift game may be widely applicable in natural systems [28,30].

In the case of *E. coli* β-lactamase production, the experimentally described stable interior equilibrium is consistent with a snowdrift game (Fig. 2A). However it should also be noted that the results shown in Yurtsev et al. display dynamics that would not be predicted from a simple snowdrift game (for instance, when started at a low proportion, β-lactamase producers rise to a high proportion before decreasing to the interior equilibrium). This suggests the two player game framework is oversimplified; however, more detailed models (incorporating antibiotic deactivation dynamics and modeling the growth rate of the non-producer as a function of antibiotic concentration) can faithfully generate experimental results (see [3]).

Yurtsev et al. [3] also showed that the stable equilibrium shifts in response to changes in drug concentration. Specifically, the fitness of non-producers (red entries in Fig. 2c) decreases as drug concentration increases. Above a certain level of the drug, the fitness of the producer becomes higher than the non-producer across all possible scenarios (i.e., a shift from Fig. 1f to Fig. 1e). This would lead to the eventual fixation of the producer despite its starting proportion (an outcome predicted for the so-called Harmony game [31]).

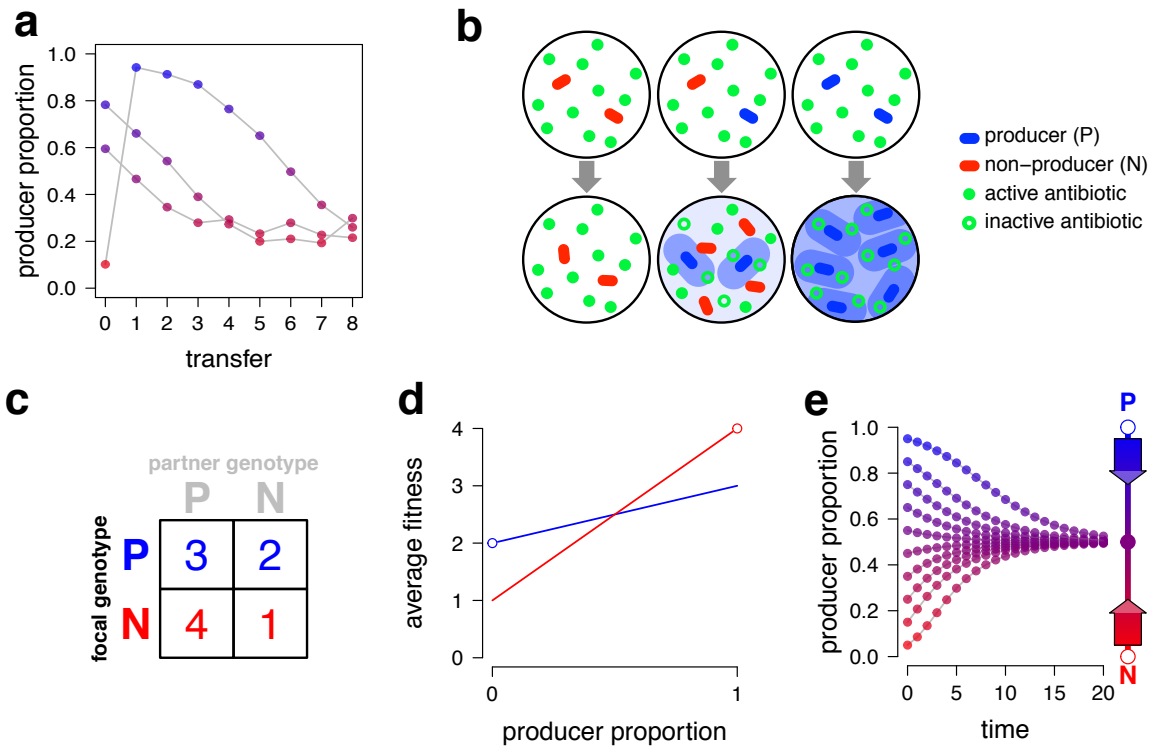

Figure 6.2: **Snowdrift game.** (a) Results of a laboratory experiment tracking the proportion of bacteria producing an antibiotic-inactivating enzyme β-lactamase). In the presence of the antibiotic (ampicillin), the producers and non-producers coexist, approaching the same final proportions despite their initial fractions (data reproduced with permission from Yurtsev *et al.* (2013)). (b) In this cartoon, we consider two genotypes: producers of an antibiotic-inactivating extracellular enzyme (blue cells) and non-producers (red cells). Shown are three possible pairwise interactions in the presence of an antibiotic (top) and the outcome of each interaction (bottom). A producer benefits neighboring cells by inactivating the antibiotic (purple shading represents enzyme concentration), but also receives greater private protection (indicated by the purple "halo"). (c) The fitness matrix for the cartoon in part b is shown. Compared with Fig. 1a, the producer now has a higher fitness when the partner is a non-producer because the enzyme (public good) is partially privatized. This arrangement of fitnesses is known as the Snowdrift game. (d) Predicted average fitnesses of each genotype given random interaction (note that the end points are the values in part c). The small empty circles correspond to points where the average fitness is not strictly defined (e.g., where producers or non-producers are absent). The point where the red and blue lines cross corresponds to a producer proportion where the fitness of each genotype is equal; thus, this point is an equilibrium. (e) Predicted population dynamics of a simple game theoretical model, given the average fitnesses in part d. The proportion of producers increases when producers are rare and decreases when producers are common. Thus, the producer proportion reaches a stable interior equilibrium, regardless of the initial fraction. There is no pure strategy ESS here (see also Fig. 1f).

Antibiotic production: choosing sides in a deadly game

In the previous section we considered a public good that can protect other cells from antibiotics, but many bacteria also produce their own proteinaceous antibiotics [32,33]. A strain that produces such a toxin (known as a bacteriocin) carries genes for both toxin production and immunity, while a non-producing strain has neither and consequently avoids associated costs [34]. In a mixed population of producers and non-producers the bacteriocin kills only non-producing types. Given that producers compete with non-producers for limited resources, producers can help one another by destroying mutual competitors. In this light, bacteriocins can be seen as an indirect "public good" [35,36]. However, as we shall see, this kind of public good game has very different dynamics than any we have previously considered.

In a study of bacteriocin production (colicin E3) in *E. coli*, Chao & Levin [37] found that the outcome of competition between the producer and a sensitive non-producer was dependent on initial genotype proportions. In contrast to the case of β-lactamase production where the producing strain has an advantage when rare, they found that the producer only had an advantage when fairly common (>2%). For a rare producer, the cost of production outweighs the diluted benefit of colicin production. For a common producer, the concentrated toxic benefit offsets the production costs. Thus, the fitness payoffs are such that each genotype does better when matched with its own type (Fig. 3a-b). If interactions occur randomly, each genotype is fitter than the other when common (Fig. 3c), which leads to a bistability (Fig. 3d and Fig. 1g).

The payoff structure here is roughly equivalent to the "coordination" game called Choosing Sides, which involves two drivers speeding toward each other on a dirt road [38]. Each driver must choose a direction to swerve (Left or Right) in order to avoid a crash. If both execute the same swerving maneuver they will manage to pass each other, but if they choose differing maneuvers they will collide. A rare non-producer in a population of colicin producers fares

poorly in the same way a Right Swerver fares poorly in a population of Left Swervers, and vice versa.

Complex games I: more strategies

The experiments presented above involve only two strategies, but new strategies can readily evolve in large populations of bacteria. The addition of new strategies to a game involves adding additional rows and columns to the payoff matrix (consider moving from a 2 x 2 to a 3 x 3 payoff matrix). For example, colicin resistance mutations occasionally arise in sensitive populations of *E. coli* [32,39,40]. When the resistant strain has a fitness intermediate between the sensitive and producer strain, the new strategy can lead to a cyclical dynamic [41,42]. Specifically, the sensitive strain outgrows the resistant strain, the resistant strain outgrows the producer, and a sufficiently common producer displaces the sensitive type through toxic killing in a relationship analogous to the game of rock–paper–scissors. The strategy set gets even larger still when further evolution of the three genotypes is considered [43–47].

Of course, natural microbial communities contain a diverse assortment of species with much richer strategy sets than we have considered [48]. This is beginning to be explored with pair-wise studies of antibiotic production and resistance in co-occurring species from natural communities [49–54]. By constructing large interaction matrices with this type of data, the nature of the multi-species game is elucidated. In particular, these enlarged payoff matrices provide critical information on the network structure of microbial communities (e.g., the symmetry and transitivity of killing interactions) [49,53,54].

Complex games II: non-random interaction

The experiments presented above were conducted under "well-mixed" conditions where extracellular products were uniformly distributed throughout the microbial community. However, microbes often live in complex biofilms where the distribution of extracellular products may

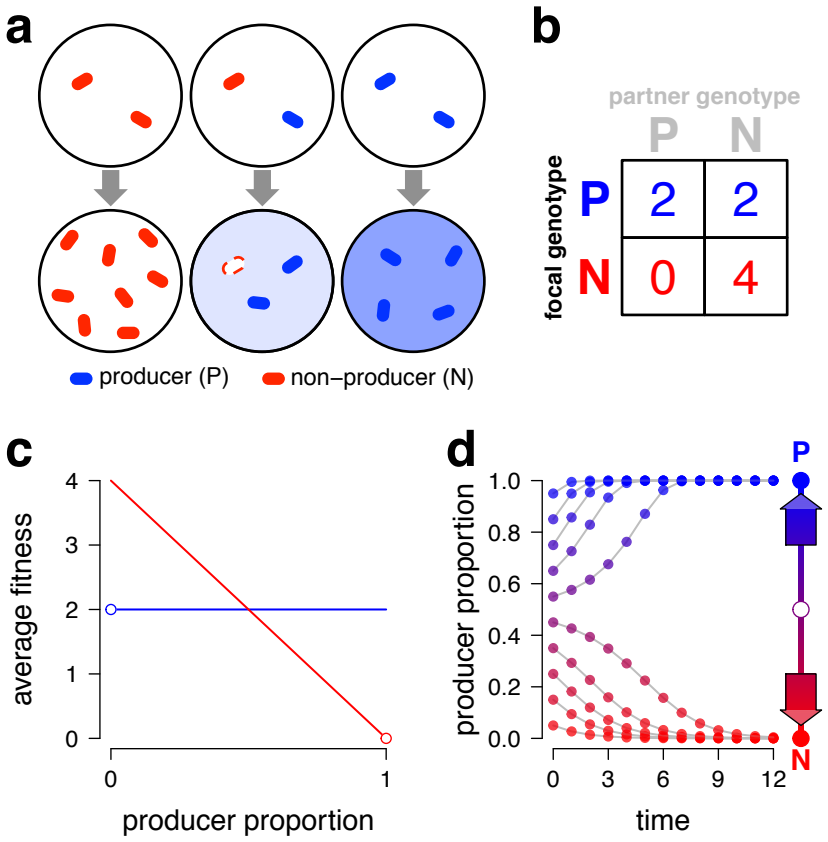

Figure 6.3: **Choosing Sides.** (a) In this cartoon, the two genotypes are producers of a toxin (blue cells) and sensitive non-producers (red cells). Three possible pairwise interactions (top) result in different outcomes (bottom). A non-producer is killed by the producer's toxin (where grey shading indicates toxin concentration), whereas the producer is immune to its own toxin. The producer does incur a growth cost for production; thus, the producer is less fit when paired with itself than the non-producer when paired with itself. (b) The fitness matrix for part a is shown. A producer has a higher fitness when the partner is a producer (first column), while the non-producer has a higher fitness when the partner is a non-producer (second column). This arrangement of fitnesses is similar to the Choosing Sides game. (c) Predicted average fitness of each genotype given random interaction. The point where the red and blue lines cross is an equilibrium. (d) Predicted population dynamics of a simple game theoretical model, given the average fitnesses in part c. The proportion of producers increases when producers are common and decreases when producers are rare. Thus, the producer proportion either approaches 0 or 1, depending on the initial fraction. The internal equilibrium is unstable and there are two ESS's: production and non-production (see also Fig. 1g).

be highly non-uniform [55–58]. Theoretically, limited diffusion and local interaction can completely transform the population dynamics of a system because a producer may disproportionately experience its own products (if diffusion is limited) and the products of its clone mates (if dispersal is limited) [59–63]. This effect of "spatial structure" has been illustrated experimentally in two of the examples we previously discussed (and elsewhere [64,65]).

Chao & Levin [37] showed that spatial structure can promote successful invasion by a colicin producer. In contrast to the bistability observed under well-mixed liquid culture conditions (Fig. 4a), the colicin-producing strain always displaced the non-producing sensitive strain in soft agar (Fig. 4b). Even if the producer was at a very low proportion globally, spatial structure gave colicin producers an advantage because the toxin became concentrated around producer microcolonies and killed neighboring non-producers; subsequently, the producer was able to capitalize on the local resources liberated.

Kerr et al. [41] demonstrated that spatial structure can promote the maintenance of diversity in a rock-paper-scissors community. In an unstructured habitat (a stirred flask), the distributed toxin rapidly killed the sensitive strain and the resistant strain then displaced the producer (Fig. 4c). Diversity was rapidly lost. However, in the structured habitat (the surface of an agar plate), local dispersal gave rise to patches of each cell type, and these patches 'chased' one another according to the rock-paper-scissors relationship (Fig. 4d-e). Given that such non-transitive relationships have been reported in natural microbial communities [49,50], it will be interesting to explore the role of spatial structure in the maintenance of diversity within natural systems (see [66–70]).

Complex games III: more players

In this review we have focused on games involving two players. However, interactions among bacteria rarely occur among discrete pairs. For this reason n-player games are often useful for modeling bacterial interactions (see Supplement III for the n-player case and Supplements II and IV for connections to dynamics in a single well-mixed population). Unlike increasing

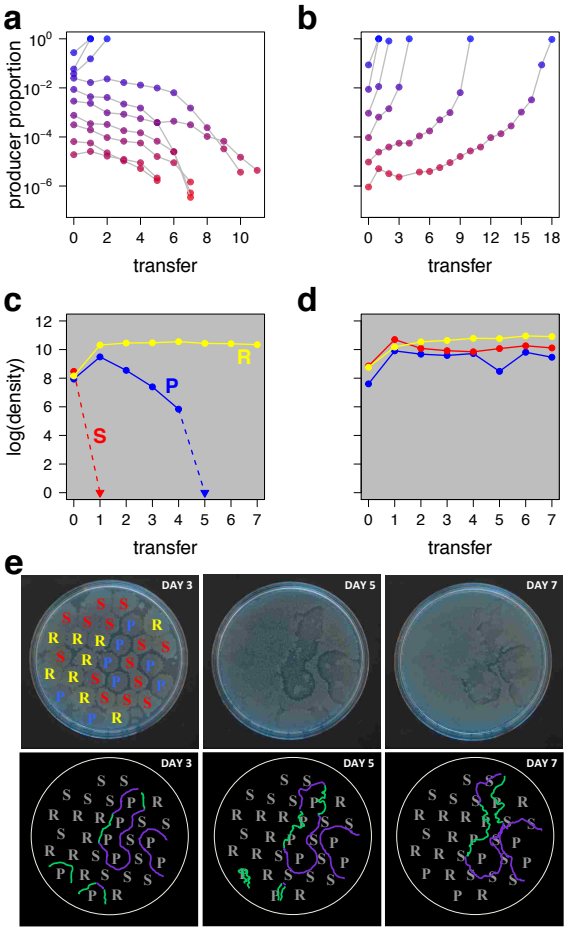

Figure 6.4: **Spatial games.** (a) An experiment tracking the proportion of colicin E3 producers in liquid culture. If the producers start above a critical fraction (0.02), then the producers drive the sensitive non-producers extinct. Otherwise, the producers go extinct (data reproduced with permission from Chao & Levin (1981)). (b) When the same community is propagated in a structured environment (soft agar), the producers increase despite initial proportion. (c) A second experiment tracking the density of three genotypes. In a well-mixed flask, the sensitive non-producer (**S**) quickly goes extinct (due to the ubiquitous toxin) and then the producer (**P**) is outcompeted by the resistant non-producer (**R**) (data reproduced with permission from Kerr et al. (2002)). (d) All three genotypes are maintained at high density when the community is propagated on the surface of an agar plate. (e) Time series photographs of a representative replicate of the RPS community propagated on agar. (Top row) The changing spatial configuration of the experimental community is shown in this first panel of photographs. Because borders could be identified where **P** interacted with **R** or **S**, the direction of clump movement over transfers could be inferred. (Bottom row) 'Chasing' between clumps is highlighted in this second panel. The borders where **P** chased **S** are colored in purple and the borders where **R** chased **P** are in green.

the number of strategies (which adds rows and columns to the payoff matrix), increasing the number of players requires that the dimensionality of the payoff matrix increase (for example, moving from a 2 x 2 to a 2 x 2 x 2 payoff matrix). Games involving an arbitrary number of players lead naturally to an explicit consideration of how fitness depends on the density of other players (density-dependent selection). Many bacteria have regulatory systems that can be activated at a specific cell density [71], some of which are known to control antibiotic production [72–74]. The relationship between cell density-dependent regulation and antibiotic production and resistance is an area that is just beginning to be explored, but one theoretical model suggests that linking antibiotic production to cell density may be important for competition because it can help to delay the cost of producing the antibiotic, thus improving the fitness of the producing cell ([75], but see [76,77]). Another area for future study related to density issues is the role of signaling in the production of antibiotic resistance phenotypes [4,5].

Conclusions

We demonstrate how evolutionary game theory can be a useful framework for understanding cases of antibiotic resistance and production that involve social interaction. We illustrated that the population dynamics found in microbial experiments are predicted by different two-strategy, two-player games. Certainly, the consideration of more strategies, more players and more complex interaction are promising directions for future research. Nonetheless, we feel that there is also value in the very simplest models. Specifically, these simple games define different categories of social interaction with different resulting dynamics. The game theoretical perspective focuses our attention on the precise nature of interaction, which can guide our expectations about the evolution of some forms of antibiotic resistance and production.

Acknowledgements

We thank B. Connelly, A. Dandekar, S. Estrela, S. Hammarlund, S. Hefty, H. Jordt, F. Meacham, C. O'Neil, and S. Singhal for comments on the manuscript. We acknowledge support from the National Science Foundation under Cooperative Agreement Number DBI-0939454, a University of Washington Royalty Research Fund Award (A74107), a National Science Foundation CAREER Award Grant to BK (DEB0952825), and a National Science Foundation Graduate Research Fellowship to PLC.

References

1. Dugatkin LA, Perlin M, Lucas JS, Atlas R: Group-beneficial traits, frequency-dependent selection and genotypic diversity: an antibiotic resistance paradigm. Proc. Biol. Sci. 2005, 272:79–83.

2. Perlin MH, Clark DR, McKenzie C, Patel H, Jackson N, Kormanik C, Powell C, Bajorek A, Myers DA, Dugatkin LA, et al.: Protection of Salmonella by ampicillin-resistant *Escherichia coli* in the presence of otherwise lethal drug concentrations. Proc. Biol. Sci. 2009, 276:3759–68.

3. Yurtsev EA, Chao HX, Datta MS, Artemova T, Gore J: Bacterial cheating drives the population dynamics of cooperative antibiotic resistance plasmids. Mol. Syst. Biol. 2013, 9:683.

4. Lee HH, Molla MN, Cantor CR, Collins JJ: Bacterial charity work leads to population-wide resistance. Nature 2010, 467:82–5.

5. Vega NM, Allison KR, Samuels AN, Klempner MS, Collins JJ: *Salmonella typhimurium* intercepts *Escherichia coli* signaling to enhance antibiotic tolerance. Proc. Natl. Acad. Sci. U. S. A. 2013, 110:14420–5.

6. Dugatkin LA, Perlin M, Atlas R: The Evolution of Group-beneficial Traits in the

Absence of Between-group Selection J. Theor. Biol. 2003, 220:67–74.

7. Brook I: Beta-lactamase-producing bacteria in mixed infections. Clin. Microbiol. Infect. 2004, 10:777–84.

8. Maynard Smith J: Evolution and the Theory of Games Cambridge University Press; 1982.

9. Nowak MA: Evolutionary Dynamics Harvard University Press; 2006.

10. Axelrod R, Hamilton W: The evolution of cooperation. Science 1981, 211:1390–1396.

11. Nowak MA, Sigmund K: Evolutionary dynamics of biological games. Science 2004, 303:793–9.

12. Maynard Smith J, Price GR: The logic of animal conflict Nature 1973, 246:15–18.

13. Turner P, Chao L: Prisoner's dilemma in an RNA virus Nature 1999, 398:441–443.

14. Turner PE, Chao L: Escape from Prisoner's Dilemma in RNA phage phi6. Am. Nat. 2003, 161:497–505.

15. Gore J, Youk H, van Oudenaarden A: Snowdrift game dynamics and facultative cheating in yeast. Nature 2009, 459:253–6.

16. Adami C, Schossau J, Hintze A: Evolution and stability of altruist strategies in microbial games Phys. Rev. E 2012, 85:011914.

17. Frey E: Evolutionary game theory: Theoretical concepts and applications to microbial communities Phys. A Stat. Mech. its Appl. 2010, 389:4265–4298.

18. Lenski RE, Velicer GJ, Ecology M, Lansing E, Smith M: Games microbes play. Selection 2000, 1:89–95.

19. Von Neumann J, Morgenstern O: Theory of Games and Economic Behavior 1944.

20. Hofbauer J, Sigmund K: Evolutionary Games and Population Dynamics Cambridge University Press; 1998.

21. Taylor PD, Jonker LB: Evolutionarily stable strategies and game dynamics. Math. Biosci. 1978, 40:145–156.

22. Walsh C: Molecular mechanisms that confer antibacterial drug resistance Nature 2000, 406:775–781.

23. Wright GD: Bacterial resistance to antibiotics: enzymatic degradation and modification. Adv. Drug Deliv. Rev. 2005, 57:1451–70.

24. Livermore DM: beta-Lactamases in laboratory and clinical resistance. Clin. Microbiol. Rev. 1995, 8:557–84.

25. Morris JJ, Papoulis SE, Lenski RE: Coexistence of Evolving Bacteria Stabilized By a Shared Black Queen Function. Evolution 2014, doi:10.1111/evo.12485.

26. Morris J, Lenski R, Zinser E: The Black Queen Hypothesis: evolution of dependencies through adaptive gene loss MBio 2012, 3:e00036–12.

27. Sugden R: The Economics of Rights, Cooperation and Welfare Palgrave Macmillan; 2004.

28. Doebeli M, Hauert C: Models of cooperation based on the Prisoner's Dilemma and the Snowdrift game Ecol. Lett. 2005, 8:748–766.

29. Ross-Gillespie A, Gardner A, West SA, Griffin AS: Frequency dependence and cooperation: theory and a test with bacteria. Am. Nat. 2007, 170:331–42.

30. Damore JA, Gore J: Understanding microbial cooperation. J. Theor. Biol. 2012, 299:31–41.

31. Licht AN: Games Commissions Play: 2x2 Games of International Securities Regulation. Yale J. Int. Law 1999, 24:61–125.

32. Riley MA, Gordon DM: The ecological role of bacteriocins in bacterial competition. Trends Microbiol. 1999, 7:129–33.

33. Riley MA: Bacteriocin-Mediated Competitive Interactions of Bacterial Populations and Communities In Prokaryotic Antimicrobial Peptides: From Genes to Applications. Edited by Drider D, Rebuffat S. Springer New York; 2011:13–27.

34. Cascales E, Buchanan SK, Duché D, Kleanthous C, Lloubès R, Postle K, Riley M, Slatin S, Cavard D: Colicin biology. Microbiol. Mol. Biol. Rev. 2007, 71:158–229.

35. Gardner A, West SA, Buckling A: Bacteriocins, spite and virulence. Proc. Biol. Sci. 2004, 271:1529–35.

36. West SA, Gardner A: Altruism, spite, and greenbeards. Science 2010, 327:1341–4.

37. Chao L, Levin BR: Structured habitats and the evolution of anticompetitor toxins in bacteria. Proc. Natl. Acad. Sci. U. S. A. 1981, 78:6324–8.

38. Young H: The economics of convention J. Econ. Perspect. 1996, 10:105–122.

39. James R, Kleanthous C, Moore GR: The biology of E colicins: paradigms and paradoxes. Microbiology 1996, 142:1569–80.

40. Feldgarden M, Riley M: The Phenotypic and Fitness Effects of Colicin Resistance in *Escherichia coli* K-12 Evolution 1999, 53:1019–1027.

41. Kerr B, Riley MA, Feldman MW, Bohannan BJM: Local dispersal promotes biodiversity in a real-life game of rock-paper-scissors. Nature 2002, 418:171–4.

42. Kirkup BC, Riley MA: Antibiotic-mediated antagonism leads to a bacterial game of rock-paper-scissors in vivo. Nature 2004, 428:412–4.

43. Frean M, Abraham ER: Rock-scissors-paper and the survival of the weakest. Proc. Biol. Sci. 2001, 268:1323–7.

44. Johnson CR, Seinen I: Selection for restraint in competitive ability in spatial competition systems. Proc. Biol. Sci. 2002, 269:655–63.

45. Prado F, Kerr B: The evolution of restraint in bacterial biofilms under nontransitive competition. Evolution 2008, 62:538–48.

46. Nahum JR, Harding BN, Kerr B: Evolution of restraint in a structured rock-paper-scissors community. Proc. Natl. Acad. Sci. U. S. A. 2011, 108:10831–8.

47. Biernaskie JM, Gardner a, West S a: Multicoloured greenbeards, bacteriocin diversity and the rock-paper-scissors game. J. Evol. Biol. 2013, 26:2081–94.

48. Foster K, Bell T: Competition, Not Cooperation, Dominates Interactions among Culturable Microbial Species Curr. Biol. 2012, 22:1845–1850.

49. Vetsigian K, Jajoo R, Kishony R: Structure and evolution of *Streptomyces* interaction networks in soil and in silico. PLoS Biol. 2011, 9:e1001184.

50. Cordero OX, Wildschutte H, Kirkup B, Proehl S, Ngo L, Hussain F, Le Roux F, Mincer T, Polz MF: Ecological populations of bacteria act as socially cohesive units of antibiotic production and resistance. Science 2012, 337:1228–31.

51. Hawlena H, Bashey F, Lively CM: Bacteriocin-mediated interactions within and between coexisting species. Ecol. Evol. 2012, 2:2521–6.

52. Bashey F, Hawlena H, Lively C: Alternative paths to success in a parasite community: within-host competition can favor higher virulence or direct interference Evolution 2013, 67:900–907.

53. Pérez-Gutiérrez R-A, López-Ramírez V, Islas Á, Alcaraz LD, Hernández-González I, Olivera BCL, Santillán M, Eguiarte LE, Souza V, Travisano M, et al.: Antagonism influences assembly of a *Bacillus* guild in a local community and is depicted as a food-chain network. ISME J. 2013, 7:487–97.

54. Aguirre-von-Wobeser E, Soberón-Chávez G, Eguiarte LE, Ponce-Soto GY, Vázquez-Rosas-Landa M, Souza V: Two-role model of an interaction network of free-living γ-proteobacteria from an oligotrophic environment. Environ. Microbiol. 2014, 16:1366–77.

55. Costerton J, Lewandowski Z, Caldwell D, Korber D, Lappin-Scott H: Microbial biofilms Annu. Rev. Microbiol. 1995, 49:711–45.

56. Hall-Stoodley L, Costerton JW, Stoodley P: Bacterial biofilms: from the natural environment to infectious diseases. Nat. Rev. Microbiol. 2004, 2:95–108.

57. Nadell CD, Xavier JB, Foster KR: The sociobiology of biofilms. FEMS Microbiol. Rev. 2009, 33:206–24.

58. Wintermute EH, Silver PA: Dynamics in the mixed microbial concourse. Genes Dev. 2010, 24:2603–14.

59. Nowak M, May R: Evolutionary games and spatial chaos Nature 1992, 359:826–829.

60. Hauert C: Effects of Space in 2 × 2 Games Int. J. Bifurc. Chaos 2002, 12:1531–1548.

61. Hauert C, Doebeli M: Spatial structure often inhibits the evolution of cooperation in the snowdrift game Nature 2004, 428:643–646.

62. Allen B, Gore J, Nowak MA: Spatial dilemmas of diffusible public goods. eLife 2013, 2:e01169.

63. Nadell C, Bucci V, Drescher K, Levin SA, Bassler BL, Xavier JB: Cutting through the complexity of cell collectives Proc. R. Soc. B Biol. Sci. 2013, 280:20122770.

64. Greig D, Travisano M: Density-dependent effects on allelopathic interactions in yeast. Evolution 2008, 62:521–7.

65. Inglis RF, Roberts PG, Gardner A, Buckling A: Spite and the scale of competition in *Pseudomonas aeruginosa*. Am. Nat. 2011, 178:276–85.

66. Pagie L, Hogeweg P: Colicin diversity: a result of eco-evolutionary dynamics. J. Theor. Biol. 1999, 196:251–61.

67. Durrett R, Levin S: Allelopathy in Spatially Distributed Populations J. Theor. Biol. 1997, 185:165–71.

68. Czárán TL, Hoekstra RF, Pagie L: Chemical warfare between microbes promotes biodiversity. Proc. Natl. Acad. Sci. U. S. A. 2002, 99:786–90.

69. Reichenbach T, Mobilia M, Frey E: Mobility promotes and jeopardizes biodiversity in rock-paper-scissors games. Nature 2007, 448:1046–9.

70. Weber MF, Poxleitner G, Hebisch E, Frey E, Opitz M: Chemical warfare and survival strategies in bacterial range expansions. J. Royal Soc. Interface 2014, 11:20140172.

71. Waters CM, Bassler BL: Quorum sensing: cell-to-cell communication in bacteria. Annu. Rev. Cell Dev. Biol. 2005, 21:319–46.

72. Duerkop BA, Varga J, Chandler JR, Peterson SB, Herman JP, Churchill MEA, Parsek MR, Nierman WC, Greenberg EP: Quorum-sensing control of antibiotic synthesis in *Burkholderia thailandensis*. J. Bacteriol. 2009, 191:3909–18.

73. Bainton N, Stead P, Chhabra S: N-(3-Oxohexanoyl)-L-homoserine lactone regulates carbapenem antibiotic production in *Erwinia carotovora* Biochem. J 1992, 288:997–1004.

74. Pierson LS, Keppenne VD, Wood DW: Phenazine antibiotic biosynthesis in *Pseudomonas aureofaciens* 30-84 is regulated by PhzR in response to cell density. J. Bacteriol. 1994, 176:3966–74.

75. Chandler JR, Heilmann S, Mittler JE, Greenberg EP: Acyl-homoserine lactone-dependent eavesdropping promotes competition in a laboratory co-culture model. ISME J. 2012, 6:2219–28.

76. Cornforth DM, Foster KR: Competition sensing: the social side of bacterial stress responses. Nat. Rev. Microbiol. 2013, 11:285–93.

77. Hibbing ME, Fuqua C, Parsek MR, Peterson SB: Bacterial competition: surviving and thriving in the microbial jungle. Nat. Rev. Microbiol. 2010, 8:15–25.

78. Rapoport A, Chammah AM: The Game of Chicken Am. Behav. Sci. 1966, 10:10–28.

79. Skyrms B: The Stag Hunt and the Evolution of Social Structure Cambridge University Press; 2004.

80. Queller DC, Ponte E, Bozzaro S, Strassmann JE: Single-gene greenbeard effects in the

social amoeba *Dictyostelium discoideum*. Science 2003, 299:105–6.

81. Smukalla S, Caldara M, Pochet N, Beauvais A, Guadagnini S, Yan C, Vinces MD, Jansen A, Prevost MC, Latgé J-P, et al.: FLO1 is a variable green beard gene that drives biofilm-like cooperation in budding yeast. Cell 2008, 135:726–37.

82. Frick IM, Mörgelin M, Björck L: Virulent aggregates of *Streptococcus pyogenes* are generated by homophilic protein-protein interactions. Mol. Microbiol. 2000, 37:1232–47.